

**Unclassified**

**NEA/CSNI/R(2008)6/VOL2**



Organisation de Coopération et de Développement Économiques  
Organisation for Economic Co-operation and Development

**26-Nov-2008**

**English text only**

**NUCLEAR ENERGY AGENCY  
COMMITTEE ON THE SAFETY OF NUCLEAR INSTALLATIONS**

**NEA/CSNI/R(2008)6/VOL2  
Unclassified**

**BEMUSE Phase IV Report:  
Simulation of a LB-LOCA in ZION Nuclear Power Plant**

**Appendices A to D**

**November 2008**

*The complete version is only available in pdf format.*

**JT03256245**

Document complet disponible sur OLIS dans son format d'origine  
Complete document available on OLIS in its original format

**English text only**

## Abbreviations

<b>0-D</b>	Zero Dimension or point
<b>1-D</b>	One Dimension
<b>2-D</b>	Two Dimension
<b>3-D</b>	Three Dimension
<b>AEKI</b>	Hungarian Academy of Sciences KFKI Atomic Energy Research Institute
<b>BAF</b>	Bottom of Active Fuel
<b>BE</b>	Best Estimate
<b>BEMUSE</b>	Best Estimate Methods Uncertainty and Sensitivity Evaluation
<b>CCFL</b>	Counter Current Flow Limitation
<b>CEA</b>	Commissariat à l'Energie Atomique (France)
<b>CL</b>	Cold Leg
<b>CSNI</b>	Committee on the Safety of Nuclear Installations
<b>DBA</b>	Design Basis Accident
<b>DNB</b>	Departure from Nucleate Boiling
<b>ECC</b>	Emergency Core Coolant
<b>ECCS</b>	Emergency Core Coolant System
<b>GAMA</b>	Group on Accident Management and Analysis
<b>GRS</b>	Gesellschaft für Anlagen und Reaktorsicherheit mbH (Germany)
<b>HL</b>	Hot Leg
<b>HPIS</b>	High Pressure Injection System
<b>IET</b>	Integral Effect Test
<b>IRSN</b>	Institut de Radioprotection et de Sûreté Nucléaire (France)
<b>ISP</b>	International Standard Problem
<b>JNES</b>	Japan Nuclear Energy Safety (Japan)
<b>KAERI</b>	Korea Atomic Energy Research Institute (South Korea)
<b>KINS</b>	Korean Institute of Nuclear Safety (South Korea)
<b>LB-LOCA</b>	Large Break Loss Of Coolant Accident
<b>LOCA</b>	Loss Of Coolant Accident
<b>LOFT</b>	Loss Of Fluid Test
<b>LOFW</b>	Loss Of Feed Water
<b>LP</b>	Lower Plenum
<b>LPIS</b>	Low Pressure Injection System
<b>LSTF</b>	Large-Scale Laboratory Facility
<b>LWR</b>	Light Water Reactor
<b>MATPRO</b>	Materials Properties correlations and computer subcodes
<b>NPP</b>	Nuclear Power Plant
<b>NRC</b>	U.S. Nuclear Regulatory Commission
<b>NRI</b>	Nuclear Research Institute (Czech Republic)
<b>PCT</b>	Peak Cladding Temperature
<b>PSI</b>	Paul Scherrer Institute (Switzerland)

<b>PWR</b>	Pressurized Water Reactor
<b>RTA</b>	Relevant Thermalhydraulic Aspects
<b>SB-LOCA</b>	Small Break Loss Of Coolant Accident
<b>SET</b>	Separate Effect Test
<b>SG</b>	Steam Generator
<b>TAF</b>	Top of Active Fuel
$T_{sat}$	Saturation Temperature
$t_{que}$	Time of complete quenching
<b>UNIPI</b>	University of Pisa (Italy)
<b>UP</b>	Upper Plenum
<b>UPC</b>	Universitat Politècnica de Catalunya (Spain)

# List of Figures

A.1 Zion NPP, aerial view . . . . .	2
A.2 Nodalization sketch . . . . .	5
A.3 Inconel-600 properties . . . . .	12
A.4 Stainless Steel: AISI 304 properties . . . . .	12
A.5 UO <sub>2</sub> properties . . . . .	18
A.6 Gap properties . . . . .	19
A.7 Zr-4 properties . . . . .	19
A.8 Core configuration . . . . .	25
A.9 Linear heat generation rate profiles . . . . .	26
A.10 Westinghouse pump homologous single phase head curves . . . . .	37
A.11 Westinghouse pump single phase homologous torque curves . . . . .	37
A.12 Head difference data . . . . .	38
A.13 Homologous torque difference curves . . . . .	38
A.14 LPIS . . . . .	41
A.15 Containment pressure . . . . .	41
A.16 Decay heat power factor . . . . .	43
A.17 RCPs velocity . . . . .	43
B.1 Sensitivity n°9: Containment pressure . . . . .	6
B.2 Sensitivity n°3: Power after scram . . . . .	6
C.1 Radial meshing of reactor pressure vessel with respect to the ZION vessel schematic. . . . .	11
C.2 PERICLES 2-D bundle test RE0064 quench fronts. . . . .	14
C.3 BETHSY 6.7c quench time. . . . .	15
C.4 Nodalization of fuel rod. . . . .	17
C.5 2.(Left) Gap thickness for the average channel (1) and hot rod in the hot FA (2) at level 1,647 m. 3. (Right) Gap heat conductance for the average channel (1) and hot rod in the hot FA (2) at level 1,647 m . . . . .	18
C.6 The heat conductance for the different channels in the steady-state condition. . . . .	19
C.7 1.Core nodalization. 2.Core axial linear heat flux variation . . . . .	20
C.8 Nodalization of reactor plant using the TECH-M-97code. . . . .	21
C.9 Loop 1 of primary system and reactor vessel . . . . .	26
C.10 Nodalization schema of secondary side of the cooling loop . . . . .	26

*BEMUSE Phase IV Report - Rev.1*

C.11 Sketch of CATHARE input deck: Primary Side. . . . .	36
C.12 Sketch of CATHARE input deck: Reactor Pressure Vessel. . . . .	37
C.13 3.Sketch of CATHARE input deck: Core. . . . .	38
C.14 Linear heat generation rate profiles. . . . .	39
C.15 Sketch of CATHARE input deck: intact loop 1. . . . .	40
C.16 Sketch of CATHARE input deck: broken loop 2. . . . .	41
C.17 7.Sketch of CATHARE input deck: secondary side of the steam generator. . . . .	42
C.18 Nodalization sketch for RV . . . . .	44
C.19 Nodalization of broken loop . . . . .	44
C.20 Nodalization of intact loops (Loops 2,3,4) . . . . .	45
C.21 Nodalization for core radial direction and FA layout . . . . .	46
C.22 Core configuration . . . . .	47
C.23 Heat structures on RPV . . . . .	48
C.24 Linear heat generation rate profile . . . . .	50
C.25 Nodalization diagram of Zion NPP for MULTID component . . . . .	53
C.26 Cross-sectional view of reactor vessel . . . . .	54
C.27 Nodalization sketch . . . . .	57
C.28 TRACE nodalization for Zion NPP . . . . .	61
C.29 Vessel nodalization . . . . .	62
C.30 General nodalization . . . . .	67
C.31 Vessel nodalization . . . . .	68
C.32 Vessel nodalization . . . . .	69
C.33 Vessel nodalization . . . . .	69
C.34 Vessel nodalization . . . . .	70
C.35 Vessel nodalization . . . . .	71
C.36 Vessel nodalization . . . . .	77
C.37 Loops nodalization . . . . .	78
C.38 Power generation. . . . .	79
C.39 Linear power generation. . . . .	79
C.40 UPC — Core nodalization . . . . .	82
C.41 UPC — Nodalization sketch . . . . .	83
D.1 AEKI — Normalized pressure distribution versus loop length . . . . .	86
D.2 CEA — Normalized pressure distribution versus loop length . . . . .	88
D.3 Relevant time trends. . . . .	91
D.4 EDO — Normalized pressure distribution versus loop length . . . . .	91
D.5 GRS — Normalized pressure distribution versus loop length . . . . .	93
D.6 IRSN — Normalized pressure distribution versus loop length . . . . .	95
D.7 JNES — Normalized pressure distribution versus loop length . . . . .	97
D.8 KAERI — Normalized pressure distribution versus loop length . . . . .	100
D.9 KINS — Normalized pressure distribution versus loop length . . . . .	103
D.10 NRI-1 — Normalized pressure distribution versus loop length . . . . .	105

*BEMUSE Phase IV Report - Rev.1*

---

D.11 PSI — Normalized pressure distribution versus loop length . . . . .	108
D.12 Simplified flow diagram of the UMAE. . . . .	111
D.13 UNIP1 — Normalized pressure distribution versus loop length . . . . .	113
D.14 UNIP1-2 — Normalized pressure distribution versus loop length . . . . .	116
D.15 UPC — Normalized pressure distribution versus loop length . . . . .	119

## List of Tables

A.1	Steady-state main parameters . . . . .	8
A.2	Pressure along the loop . . . . .	9
A.3	Mass flow per rod . . . . .	9
A.4	Core bypass mass flow . . . . .	9
A.5	Upper head bypass mass flow . . . . .	9
A.6	Upper head temperatures . . . . .	10
A.7	Thermal conductivity versus temperature for Stainless Steel: AISI 304 . . . . .	10
A.8	Volumetric heat capacity versus temperature for Stainless Steel: AISI 304 . . . . .	10
A.9	Thermal conductivity versus temperature for Inconel-600 . . . . .	11
A.10	Volumetric heat capacity versus temperature for Inconel-600 . . . . .	11
A.11	Thermal conductivity versus temperature for $UO_2$ . . . . .	13
A.12	Specific heat capacity versus temperature for $UO_2$ . . . . .	14
A.13	Thermal conductivity versus temperature for the gap . . . . .	15
A.14	Volumetric heat capacity versus temperature for the gap . . . . .	16
A.15	Thermal conductivity versus temperature for Zr-4 . . . . .	17
A.16	Specific heat capacity versus temperature for Zr-4 . . . . .	18
A.17	Fuel rods characteristics. Cold conditions . . . . .	20
A.18	Fuel rods characteristics. Hot conditions for the average rod . . . . .	20
A.19	Linear heat generation rate profiles for fuel . . . . .	21
A.20	Linear heat generation rate profiles for moderator . . . . .	22
A.21	Core heat structures features . . . . .	22
A.22	Fuel factor multiplier . . . . .	23
A.23	Moderator factor multiplier . . . . .	24
A.24	Heat structure 2041 . . . . .	27
A.25	Heat structure 1000 . . . . .	27
A.26	Heat structure 1001 . . . . .	28
A.27	Heat structure 3000 . . . . .	28
A.28	Heat structure 3150 . . . . .	28
A.29	Heat structure 3160 . . . . .	29
A.30	Heat structure 3200 . . . . .	29
A.31	Heat structure 3230 . . . . .	29
A.32	Heat structure 3220 . . . . .	30

*BEMUSE Phase IV Report - Rev.1*

A.33 Heat structure 3250	30
A.34 Heat structure 3270	30
A.35 Heat structure 3350	31
A.36 Heat structure 3500	31
A.37 Heat structure 3510	31
A.38 Heat structure 3550	32
A.39 Heat structure 3570	32
A.40 Heat structure 3560	32
A.41 Westinghouse pump homologous single phase head curves	33
A.42 Westinghouse pump single phase homologous torque curves	34
A.43 Head curves, difference curve data	35
A.44 Torque curves, difference curve data	36
A.45 Time sequence of imposed events	39
A.46 LPIS pressure-flow curve	40
A.47 Containment pressure	40
A.48 Decay heat power	42
A.49 Pump velocity for primary coolant pumps in intact loops	44
A.50 Pump velocity for primary coolant pumps in broken loop	45
A.51 Nodalization qualification at steady state level	46
A.52 Pressure along the loop	47
A.53 Resulting time sequence of main events	48
A.54 Time trends	49
A.55 Qualitative evaluation	50
B.1 Sensitivity parameters	2
B.2 Sensitivity n°3: Power after scram, lower case	3
B.3 Sensitivity n°3: Power after scram, upper case	4
B.4 Fuel rods characteristics. Cold conditions for the average rod	5
B.5 Sensitivity n°9: Containment pressure	5
C.1 Nodalization details.	11
C.2 Nodalization Code Resources.	19
C.3 Relative Power Peaking Factors for the Heated Channels.	19
C.4 Axial relative power distribution in the core.	20
C.5 - Maximum Linear Power.	20
C.6 Nodalisation Code Resources of the primary circuit	32
C.7 Core heat structures features	34
C.8 Nodalisation Code Resources of the primary circuit	35
C.9 Comparisons of the 1D and 3D modeling.	52
C.10 Maximum linear heat generation rates for Zones 2 and 5	60
C.11 ZION NPP power subdivision among the five RELAP5 group of heat structures.	65
C.12 Fuel rod characteristics (hot condition for the average rod).	65



*BEMUSE Phase IV Report - Rev.1*

---

C.13 RELAP5 nodalization code resources. . . . .	66
C.14 Maximum linear power and location. . . . .	66
C.15 Overview of Cathare2 code resources . . . . .	76
C.16 Maximum linear heat generation rates (kW/m) for zones 2 and 5 in the locations required for the submission results . . . . .	76
D.1 AEKI — Pressure distribution along the loop . . . . .	85
D.2 AEKI — Nodalization and steady state data table . . . . .	87
D.3 CEA — Pressure distribution along the loop . . . . .	88
D.4 CEA — Nodalization and steady state data table . . . . .	89
D.5 EDO — Pressure distribution along the loop . . . . .	90
D.6 EDO — Nodalization and steady state data table . . . . .	92
D.7 GRS — Pressure distribution along the loop . . . . .	93
D.8 GRS — Nodalization and steady state data table . . . . .	94
D.9 IRSN — Pressure distribution along the loop . . . . .	95
D.10 IRSN — Nodalization and steady state data table . . . . .	96
D.11 JNES — Pressure distribution along the loop . . . . .	97
D.12 JNES — Nodalization and steady state data table . . . . .	98
D.13 KAERI — Pressure distribution along the loop . . . . .	99
D.14 KAERI — Nodalization and steady state data table . . . . .	101
D.15 KINS — Pressure distribution along the loop . . . . .	102
D.16 KINS — Nodalization and steady state data table . . . . .	104
D.17 NRI-1 — Pressure distribution along the loop . . . . .	105
D.18 NRI-1 — Nodalization and steady state data table . . . . .	106
D.19 PSI — Pressure distribution along the loop . . . . .	107
D.20 PSI — Nodalization and steady state data table . . . . .	109
D.21 UNIPI1 — Pressure distribution along the loop . . . . .	112
D.22 UNIPI1 — Nodalization and steady state data table . . . . .	114
D.23 UNIPI-2 — Pressure distribution along the loop . . . . .	116
D.24 UNIPI-2 — Nodalization and steady state data table . . . . .	117
D.25 UPC — Pressure distribution along the loop . . . . .	118
D.26 UPC — Nodalization and steady state data table . . . . .	120

# Contents

<b>A</b>	<b>Input and Output specifications for simulation of a LB-LOCA in ZION-1 NPP</b>	
A.1	ZION Power Plant description . . . . .	2
A.2	Input deck description . . . . .	3
A.2.1	Description of the original input deck . . . . .	3
A.2.2	Description of the supplied input deck . . . . .	3
A.2.3	Additional information . . . . .	4
A.3	Common basis and requirements for simulation performance . . . . .	6
A.3.1	Core detail . . . . .	6
A.3.2	Downcomer / lower plenum . . . . .	6
A.3.3	Reflood options . . . . .	7
A.3.4	Break nodalization . . . . .	7
A.3.5	Gap / fuel . . . . .	7
A.3.6	CCFL / upper plate . . . . .	7
A.3.7	$\Delta P$ along the loops . . . . .	7
A.3.8	Upper header / bypass . . . . .	7
A.3.9	Core bypass . . . . .	7
A.4	Steady-state parameters description . . . . .	8
A.4.1	Material properties . . . . .	8
A.4.2	Core heat structures . . . . .	20
A.4.3	Steam generators heat structures . . . . .	27
A.4.4	Pressurizer heat structures . . . . .	27
A.4.5	Vessel heat structures . . . . .	27
A.4.6	Reactor coolant pumps curves . . . . .	33
A.5	Transient description . . . . .	39
A.5.1	Transient tables . . . . .	40
A.6	Output evaluation . . . . .	46
A.6.1	Steady State . . . . .	46
A.6.2	Transient . . . . .	48
A.7	references . . . . .	52
<b>B</b>	<b>Sensitivity calculations specifications</b>	<b>53</b>
B.1	Introduction . . . . .	2
B.2	List of sensitivity parameters . . . . .	2
B.3	Output . . . . .	7

B.4	References . . . . .	8
<b>C</b>	<b>Codes and input decks</b>	<b>9</b>
C.1	CEA, France . . . . .	10
C.1.1	Description of the code: CATHARE . . . . .	10
C.1.2	Description of the input deck . . . . .	10
C.1.3	Comments on the CATHARE calculations for the phase IV of BEMUSE . . . . .	12
C.2	EDO GUIDROPRESS, Russia . . . . .	16
C.2.1	Description of the code: TECH-M-97 . . . . .	16
C.2.2	References . . . . .	22
C.3	GRS, Germany . . . . .	23
C.3.1	Description of the code: ATHLET . . . . .	23
C.3.2	Description of the input deck . . . . .	24
C.4	IRSN, France . . . . .	27
C.4.1	Description of the code: CATHARE2.5 . . . . .	27
C.4.2	Description of the IRSN CATHARE Input Deck . . . . .	31
C.5	JNES, Japan . . . . .	43
C.5.1	Description of the code: TRACE v4.05 . . . . .	43
C.5.2	Description of the input deck . . . . .	43
C.6	KAERI, South Korea . . . . .	51
C.6.1	Description of the Code: MARS 3.1 . . . . .	51
C.6.2	Description of the Input Deck . . . . .	51
C.6.3	References . . . . .	55
C.7	KINS, South Korea . . . . .	56
C.7.1	Description of the code: RELAP5/MOD3.3 . . . . .	56
C.7.2	Description of the input deck . . . . .	56
C.7.3	Nodalization sketch . . . . .	56
C.7.4	Maximum linear heat generation rates . . . . .	56
C.8	NRI-1, Czech Republic . . . . .	58
C.8.1	Description of the code: RELAP5/MOD3.3 . . . . .	58
C.8.2	Description of the input deck . . . . .	58
C.9	PSI, Switzerland . . . . .	59
C.9.1	Description of the code: TRACEv5.0rc3 . . . . .	59
C.10	UNIPI1 Italy . . . . .	63
C.10.1	CODES AND INPUTS . . . . .	63
C.11	UNIPI-2, Italy . . . . .	73
C.11.1	Description of the code: Cathare2 v2.5.1 . . . . .	73
C.11.2	Description of the input deck . . . . .	74
C.12	UPC, Spain . . . . .	80
C.12.1	Description of the code: RELAP5/MOD3.3 . . . . .	80
C.12.2	Description of the input deck . . . . .	80

<b>D Steady state achievement</b>	<b>84</b>
D.1 AEKI, Hungary . . . . .	85
D.2 CEA, France . . . . .	88
D.3 EDO, Russia . . . . .	90
D.3.1 References . . . . .	92
D.4 GRS, Germany . . . . .	93
D.5 IRSN, France . . . . .	95
D.6 JNES, Japan . . . . .	97
D.7 KAERI, South Korea . . . . .	99
D.8 KINS, South Korea . . . . .	102
D.9 NRI-1, Czech Republic . . . . .	105
D.10 PSI, Switzerland . . . . .	107
D.11 UNIPI1, Italy . . . . .	110
D.11.1 NODALIZATION QUALIFICATION PROCESS AND RESULTS . . . . .	110
D.12 UNIPI-2, Italy . . . . .	116
D.13 UPC, Spain . . . . .	118

APPENDIX A

# Input and Output specifications for simulation of a LB-LOCA in ZION-1 NPP

**Coordinators:** F.Reventós (UPC), M. Pérez (UPC), L. Batet (UPC), R. Pericas (UPC)

**Participating Organizations and Authors**

AEKI, Hungary	I. Trosztel, I. Tóth
CEA, France	P. Bazin, A. de Crécy, P. Germain
FSUE EDO GUIDROPPRESS, Russia	S. Borisov
GRS, Germany	H. Glaeser, T. Skorek
IRSN, France	J. Joucla, P. Probst
JNES, Japan	A. Ui
KAERI, South Korea	B. D. Chung
KINS, South Korea	D.Y. Oh
NRI-1, Czech Republic	M. Kyncl, R. Pernica
PSI, Switzerland	A. Manera
UNIPI-1, Italy	F. D'Auria, A. Petruzzi
UNIPI-2, Italy	F. D'Auria, A. Del Nevo
UPC, Spain	M. Pérez, F. Reventós, L. Batet



## A.1 ZION Power Plant description

Zion Station (Reference [5]) was a dual-reactor nuclear power plant operated and owned by the Commonwealth Edison network. This power generating station is located in the extreme eastern portion of the city of Zion, Lake County, Illinois. It is approximately 40 direct-line miles north of Chicago, Illinois and 42 miles south of Milwaukee, Wisconsin.



Figure A.1: Zion NPP, aerial view

The two-unit Zion Nuclear Power Station (see Figure A.1, Reference [4]) was retired in February, 1998. The 25-year old plant had not been in operation since February, 1997. In 1998 Commonwealth Edison, owner of the plant, concluded that Zion could not produce competitively priced power. At this time plans were started to keep the facility in long-term safe storage and to begin dismantlement after 2010. All nuclear fuel has been removed permanently from the reactor vessel, and the fuel has been placed in the plant's onsite spent fuel pool.

Zion 1 main features (References [4] and [5]):

- Zion, Illinois, United States
- 4 loops
- Pressurized water reactor
- Westinghouse design
- Net Output: 1040 MWe
- Thermal power 3250 MWth
- Permanently shut down.

- Date started: June 1973
- Date closed: January 1998

## A.2 Input deck description

Zion RELAP5 input deck supplied with this specification has been built by modifying a general input deck for PWR simulating a SB-LOCA received from NRC.

### A.2.1 Description of the original input deck

The original input deck (file typpwr.inp) has only 2 loops: 1 triple loop simulating the 3 intact loops and 1 single loop simulating the broken one. Pressurizer is connected to the intact loop. Accumulators are in both loops and the one in the intact loop is re-scaled, according to the triple volume condition. Nominal power is set to 3600 MWth.

Point kinetics is used.

There are heat structures for reactor pressure vessel, core and steam generators. A set of tables covers the materials properties for core fuel, core fuel gap, core fuel cladding, inconel and stainless steel. All these tables are implemented in the deck.

Safety components simulate safety injection and charging systems (primary side, both loops), relief valves and auxiliary feed water (secondary side, both loops) and PORV (pressurizer) . No control is implemented and steady-state is reached by activating a time dependent volume and a single junction connected to core inlet annulus.

Break is located in cold leg of the single loop.

Input units are British, while output units are SI.

### A.2.2 Description of the supplied input deck

In order to run BEMUSE phase 4 exercise which is a Large Break LOCA different changes are proposed. This proposal comes after analyzing some available information (References [2] and [3]) and after making some decisions when needed.

The changes from the original input deck are listed below, classified in two different groups: those related to plant description and those to transient features.

Changes related to plant description:

1. Power set to 3250 MWth
2. Point kinetics has been removed. Decay heat is given by means of a power factor in input table 900. The curve implemented is suitable for a Nuclear Power Plant. In figure 16 there is a comparison between the curve used in BEMUSE phase 2 for LOFT facility and the curve proposed for BEMUSE phase 4.
3. More detail nodalization has been implemented for the hydrodynamic components simulating the core and the core bypass, which are now subdivided in 18 nodes.
4. The downcomer bypass has been converted in the core bypass.
5. Stainless steel heat structures have been added for pressurizer and surge line.
6. New heat structures for the fuel and moderator have been implemented with the aim of having the same degree of detail used in phase 2. Five zones are distinguished (see Figure A.8):



- Peripheral channel
  - Average channel
  - Hot channel
  - Hot fuel assembly in hot channel
  - Hot rod in hot fuel assembly
7. Triple intact loop has been split into three intact loops.
  8. Material properties are those used in phase 2 (revised and accepted by all participants of BEMUSE project)
  9. Fuel rods characteristics have been modified according to Reference [3].

Changes related to transient features:

1. Safety injection has been rearranged. Original safety injection seems to simulate both high and low pressure systems. In the new model, only the low pressure injection is simulated, and 3 LPIS are provided, one per intact loop (no LP injection is simulated in the broken loop). A flow-pressure table has been implemented (see Table A.46 on page 40)
2. Following the split of the original intact loop, single accumulators have been connected to each intact loop. Regarding the features of a LB-LOCA the accumulator of the broken loop has been removed.
3. Charging system has been removed.
4. Large break has been input by means of 2 motor valves connected to time dependent volumes simulating containment conditions and a trip valve connecting the cold leg volumes where the break takes place.
5. In addition to LPIS flow table other tables for transient conditions have been implemented, including containment pressure and pump's velocity (Tables A.47, A.49 and A.50 on pages 40, 44 and 45).

### A.2.3 Additional information

Two pieces of information are supplied additionally: an EXCEL file and a nodalization diagram (see Figure A.2).

Although information needed for phase 4 exercise is contained in the supplied RELAP5 input deck, an EXCEL file has been prepared summarizing the most relevant input parameters, which are basically geometrical features. The aim of this file together with the nodalization diagram is to help non RELAP5 users to follow the contents of this specification.

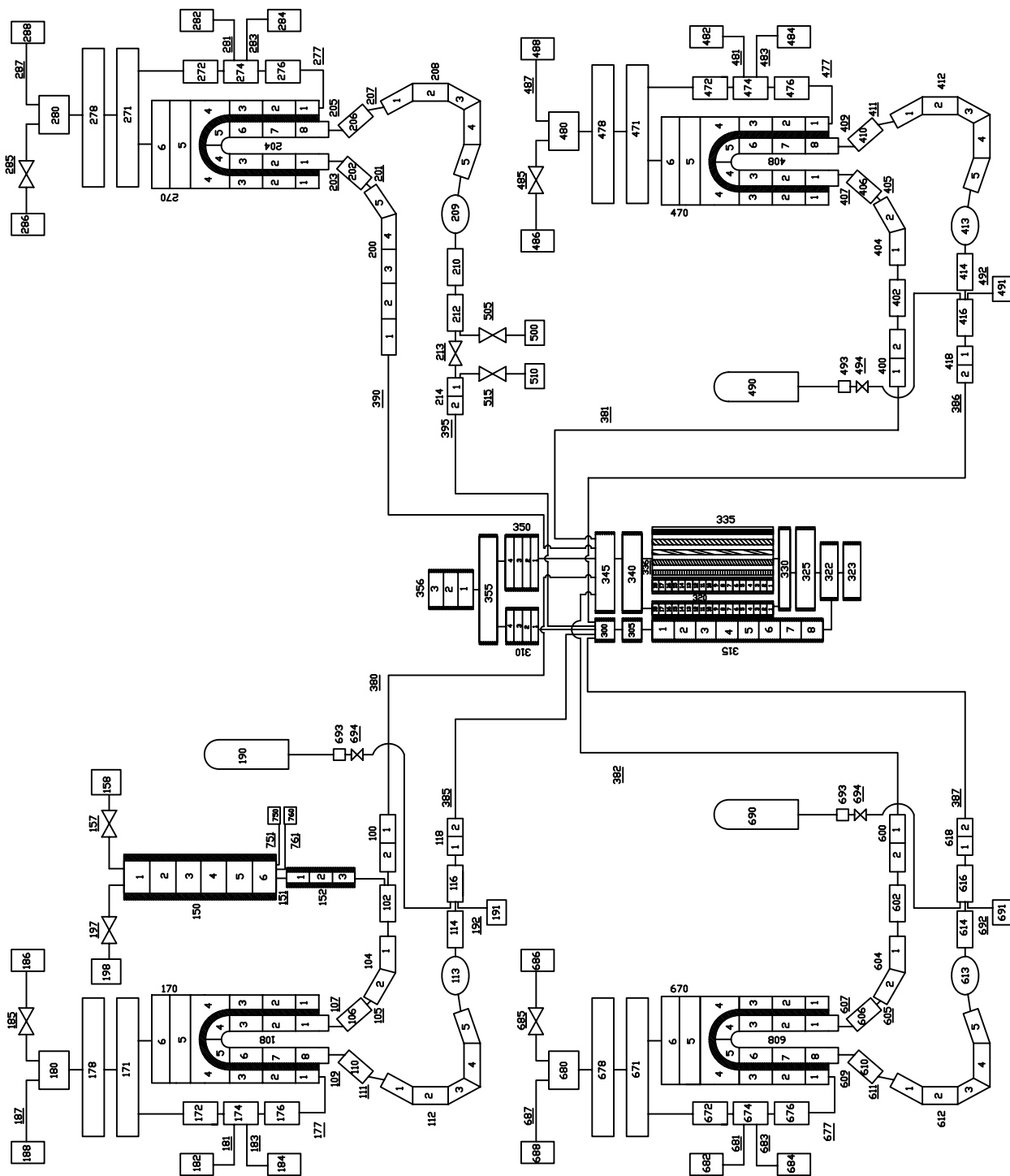


Figure A.2: Nodalization sketch

### A.3 Common basis and requirements for simulation performance

With the aim to have a common basis for comparison a number of nodalization requirements and recommendations were stated by BEMUSE phase IV participants in the 5th meeting of BEMUSE, held on 26 - 28 June 2007 at the NEA Headquarters.

It was also agreed to supply further steady state data for the transient simulation:

- Mass flow per FA, for different channels and types of FA.
- Cold and hot gap dimensions for the average rod.
- RELAP5 parameters required for Wallis correlation.
- Pressure values along the loop.
- Upper header bypass mass flow.
- Upper header temperature.
- Core bypass mass flow.

This information can be found in Section A.4.

#### A.3.1 Core detail

At least two core channels of cylindrical geometry with crossflow junctions (if that is possible) have to be considered.

One channel should contain the hot channel, the hot fuel assembly and the hot rod (corresponding to heat structure zones number 3, 4 and 5), being the central one, while the other one should contain average and peripheral channels (corresponding to heat structure zones number 1 and 2).

For 3D code users, in addition, 4 azimuthal sectors (or 8), and 4 (8) hot fuel pins (one per sector) could be used.

For 1D code users it is *recommended* not to use a channel only devoted to hot FA, in order to avoid having an overheated water channel in the core.

#### A.3.2 Downcomer / lower plenum

At least two downcomers (1 for broken loop and the other for the 3 intact loops) with crossflow junctions (if that is possible) and no form loss coefficients. Perfect cylinder can be assumed.

Lower plenum should be modelled in consistency with downcomer option. Users should provide details on this issue.

For example, UPC has divided lower plenum (volumes 322 and 325 in Figure A.2) into 4 sectors. Crossflow areas are calculated assuming perfect cylinder geometry.

### A.3.3 Reflood options

It will be used bottom-up and top-down reflood.

For RELAP5 users it is *recommended* to use option 1 (the average pressure in the connected hydrodynamic volumes is less than 1.2 MPa , and the average void fraction in the interconnected hydrodynamic volumes is greater than 0.9)

### A.3.4 Break nodalization

Trip valves will be used (RELAP5 users) or equivalent (other codes) without form loss coefficients. Default code values, will be used in discharge models.

### A.3.5 Gap / fuel

No use of advanced models.

### A.3.6 CCFL / upper plate

CCFL option will be activated for the upper tie plate junction. Data are provided in Section A.4.

Each code should apply the best model available.

### A.3.7 $\Delta P$ along the loops

The provided pressure curve along the circuit (see Table A.2) is to be considered as an objective and the participants should try to approach to it.

### A.3.8 Upper header / bypass

Tables A.5 and A.6 contain the mass flow and the temperatures during steady state for upper header.

### A.3.9 Core bypass

Table A.4 has the core bypass mass flow.

## A.4 Steady-state parameters description

The main steady state features of the plant are summarized in Table A.1.

Parameter	Steady-state value
Power (MW)	3250.0
Pressure in cold leg (MPa)	15.8
Pressure in hot leg (MPa)	15.5
Pressurizer level (m)	8.8
Core outlet temperature (K)	603.0
Primary coolant flow (kg/s)	17357.
Secondary pressure (MPa)	6.7
SG downcomer level (m)	12.2
Feed water flow per loop (kg/s)	439.
Accumulator pressure (MPa)	4.14
Accumulator gas volume (m <sup>3</sup> ) (only tank)	15.1
Accumulator liquid volume (m <sup>3</sup> ) (only tank)	23.8
RCP's velocity (rad/s)	120.06

Table A.1: Steady-state main parameters

- Counter current flow limitation:

NRI-1 group submitted the following information for CCFL related data: Hydraulic diameter for core exit junctions = 0.04341667 ft

RELAP5 users will use Wallis correlation with the following parameters (Reference[6])

- Gas intercept,  $c = 0.8625$
- Slope,  $m = 1.0$

- Pressure along the loop

### A.4.1 Material properties

Material properties are those used in BEMUSE phase 2 (Ref.5)

N°	Position along the loop		Volume <sup>(1)</sup>	Pressure (MPa)
1	Hot leg inlet	HL IN	100-01	15.53
2	Hot leg outlet	HL OUT	104-02	15.51
3	Steam generator inlet plenum	SG IN	106	15.50
4	U-tube top	UT Top	108-05	15.33
5	Steam generator outlet plenum	SG OUT	110	15.33
6	Downstream SG outlet nozzle	OUT SG NOZZLE	112-01	15.27
7	Bottom of loop seal	LOOP SEAL	112-04	15.28
8	Pump inlet	PUPM IN	112-05	15.27
9	Pump outlet	PUMP OUT	114	15.77
10	Cold leg in	CL IN	116	15.75
11	Cold leg out	CL OUT	118-02	15.77
12	Lower plenum (0.2 m from bottom of vessel)	LP	323	15.81
13	Bottom of active core	BAF	435-01	15.75
14	Top of active core	TAF	435-18	15.65

Table A.2: Pressure along the loop

<sup>(1)</sup> See RELAP5 nodalization sketch in Figure A.2

- Mass flow per rod.

Mass flow per rod
0.441 kg/s

Table A.3: Mass flow per rod

It can be considered (1D codes) that all the fuel assemblies have quite the same mass flow rate at the entrance. If 3D code users find big dispersion in the flow rates, they should report them to UPC as soon as possible.

- Core bypass

Core bypass mass flow
220.7 kg/s

Table A.4: Core bypass mass flow

- Upper head

UH mass flow <sup>(2)</sup>
22.2 kg/s

Table A.5: Upper head bypass mass flow

<sup>(2)</sup> Mass flow from volume 300 to 310 (see RELAP5 nodalization sketch in Figure A.2)

- Temperatures

Temperature volumes 310, 350, 355 <sup>(3)</sup>	Temperature volume 356 <sup>(3)</sup>
571 K	590 K

Table A.6: Upper head temperatures

<sup>(3)</sup> See RELAP5 nodalization sketch in Figure A.2.

Table A.6 is intended for 1D users. 3D users should reasonably approach this situation.

Temperature (K)	Thermal conductivity (W/m/K)
373.00	15.50
700.00	21.00
1000.00	26.30

Table A.7: Thermal conductivity versus temperature for Stainless Steel: AISI 304

Temperature (K)	Volumetric heat capacity (J/cm <sup>3</sup> /K)
273.15	3.474
366.50	3.870
477.59	4.114
588.59	4.224
699.82	4.290
810.93	4.366
922.04	4.474
1144.26	4.721

Table A.8: Volumetric heat capacity versus temperature for Stainless Steel: AISI 304

Temperature (K)	Thermal conductivity (W/m/K)
366.5	15.55
477.6	17.29
588.7	19.02
700.0	20.79
810.9	22.65
922.0	24.65
1033.2	26.72
1144.3	28.64

Table A.9: Thermal conductivity versus temperature for Inconel-600

Temperature (K)	Volumetric heat capacity (J/cm <sup>3</sup> /K)
293	3.761
373	3.926
473	4.086
573	4.201
673	4.323
773	4.443
873	4.765
973	4.877
1073	4.980
1173	5.089
1373	5.304

Table A.10: Volumetric heat capacity versus temperature for Inconel-600



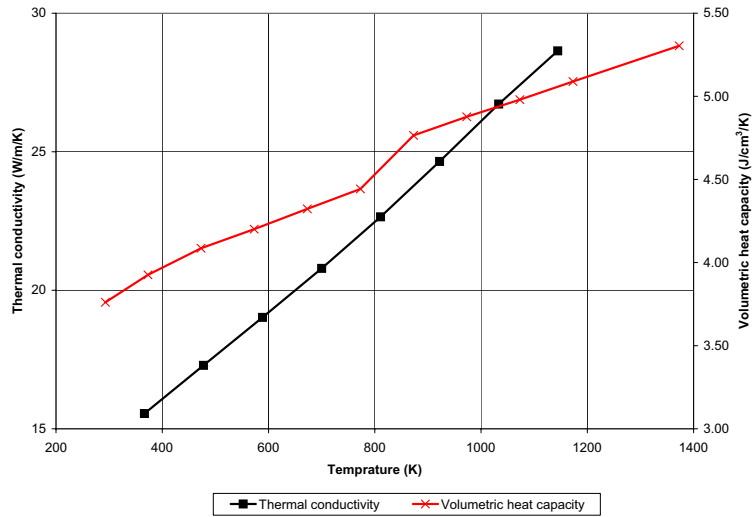


Figure A.3: Inconel-600 properties

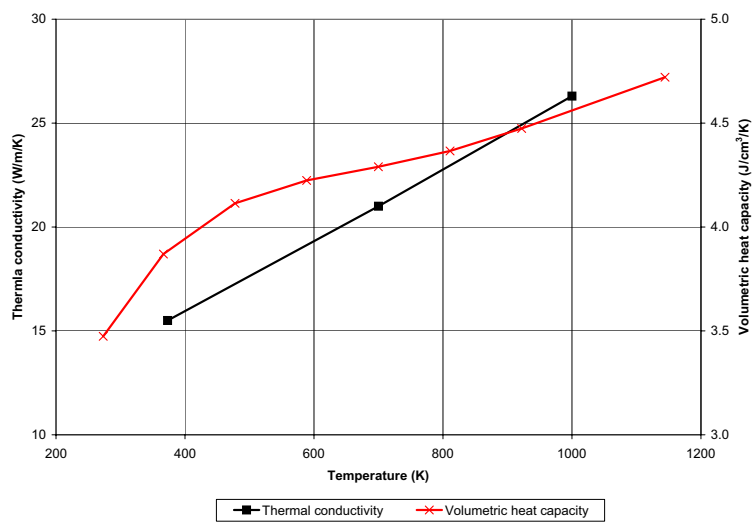


Figure A.4: Stainless Steel: AISI 304 properties

Temperature(K)	Thermal conductivity (W/m/K)
300	7.167
400	6.222
500	5.476
600	4.872
700	4.375
800	3.959
900	3.607
1000	3.304
1100	3.043
1200	2.817
1300	2.622
1400	2.454
1500	2.314
1600	2.199
1700	2.110
1800	2.045
1900	2.006
2000	1.990
2100	1.996
2200	2.024
2300	2.070
2400	2.135
2500	2.214
2600	2.307
2700	2.411
2800	2.525
2900	2.645
3000	2.771
3120	2.928
3121	2.500
3400	2.500

Table A.11: Thermal conductivity versus temperature for UO<sub>2</sub>

Temperature (K)	Specific heat capacity (J/kg/K)
300	236.6
350	252.3
450	273.8
550	287.8
650	297.2
750	303.5
850	307.7
950	310.4
1050	312.3
1150	313.8
1250	315.6
1350	317.9
1450	321.3
1550	326.2
1650	332.8
1750	341.5
1850	352.7
1950	366.5
2050	383.3
2150	403.4
2250	426.8
2350	453.8
2450	484.6
2550	519.3
2650	558.0
2750	600.8
2850	647.8
2950	699.1
3050	754.5
3120	795.9
3120	506.5
3200	481.5
3300	452.9
3400	426.7

Table A.12: Specific heat capacity versus temperature for UO<sub>2</sub>

Temperature (K)	Thermal conductivity (W/m/K)
273	0.1440
373	0.1796
573	0.2435
773	0.3010
973	0.3543
1273	0.4287
1573	0.4980
2073	0.6056
2573	0.7057

Table A.13: Thermal conductivity versus temperature for the gap

Temperature (K)	Volumetric heat capacity(W/cm <sup>3</sup> /K)
273	0.021978
400	0.015000
500	0.012000
600	0.010000
700	0.008571
800	0.007500
900	0.006667
1000	0.006000
1100	0.005455
1200	0.005000
1300	0.004615
1400	0.004286
1500	0.004000
1600	0.003750
1700	0.003529
1800	0.003333
1900	0.003158
2000	0.003000
2100	0.002857
2200	0.002727
2300	0.002609
2400	0.002500
2500	0.002400
2600	0.002308
2700	0.002222
2800	0.002143
2900	0.002069
3000	0.002000
3100	0.001935
3260	0.001840

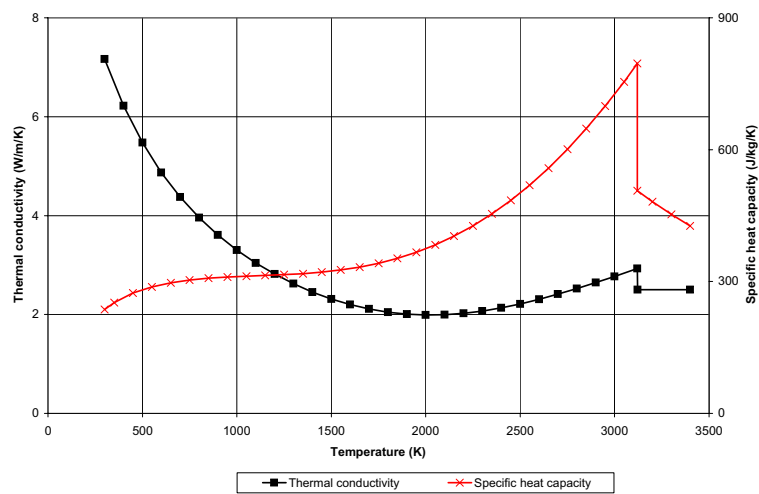
Table A.14: Volumetric heat capacity versus temperature for the gap

Temperature (K)	Thermal conductivity (W/m/K)
300	12.682
400	14.041
500	15.294
600	16.487
700	17.666
800	18.877
900	20.166
1000	21.580
1100	23.164
1200	24.964
1300	27.026
1400	29.396
1500	32.121
1600	35.246
1700	38.818
1800	42.881
1900	47.484
2000	52.670
2098	58.364
2099	36.000
2400	36.000

Table A.15: Thermal conductivity versus temperature for Zr-4

Temperature (K)	Specific heat capacity (J/kg/K)
300	281
400	302
640	331
1090	375
1093	502
1113	590
1133	615
1153	719
1173	816
1193	770
1213	619
1233	469
1248	356
1300	356

Table A.16: Specific heat capacity versus temperature for Zr-4

Figure A.5: UO<sub>2</sub> properties

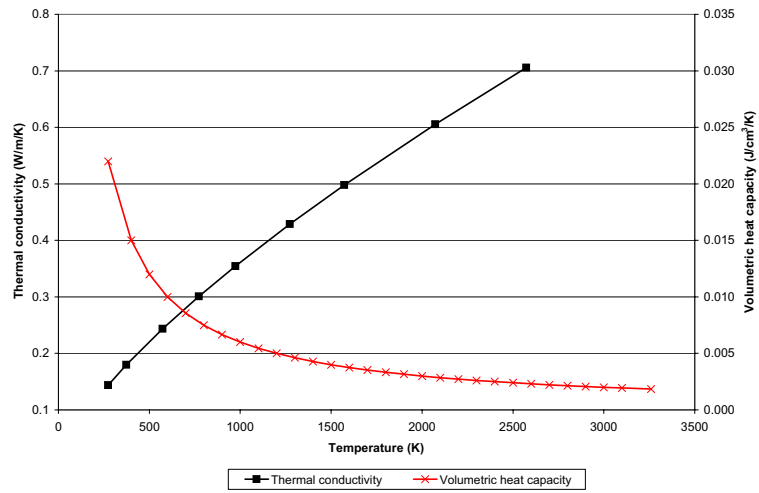


Figure A.6: Gap properties

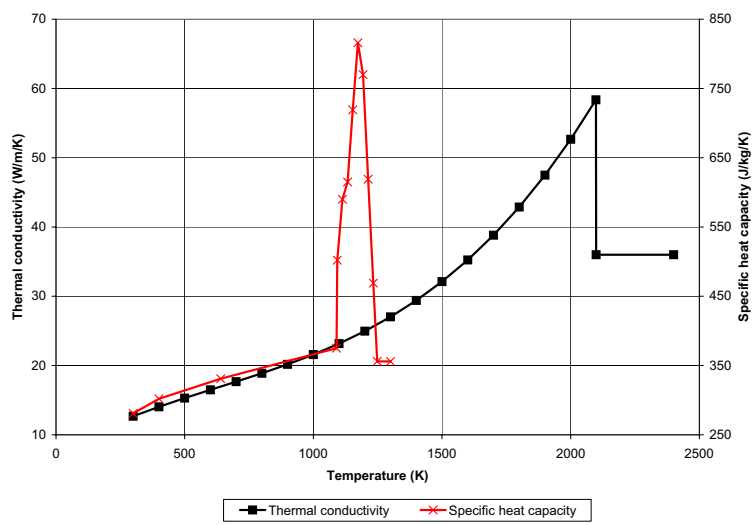


Figure A.7: Zr-4 properties



#### A.4.2 Core heat structures

Parameter	Unit	Value	Reference
<b>Fuel pin</b>			
Outside diameter	mm	10.7	Reference[3]
Cladding thickness	mm	0.61	Standard value
Active fuel length	m	3.66	-
Gap thickness	mm	0.09	Derived from Reference[3]
Internal pressure	MPa	2.17	-
Free volume	mm <sup>3</sup>	20369	-
Rod pitch	cm	1.43	Reference[3]
Assembly pitch	cm	21.5	Reference[3]
Rods per FA	-	204	Reference[3]
<b>Fuel pellet</b>			
Diameter	mm	9.3	Reference[3]
Length	mm	11.2	Reference[3]
Radial profile of heat generation	-	assumed constant	-
Number of fuel rods	-	39372	Derived from Reference[3]

Table A.17: Fuel rods characteristics. Cold conditions

Parameter	Unit	Value
<b>Fuel pin</b>		
Outside diameter	mm	10.71
Cladding thickness	mm	0.61
Gap thickness	mm	0.054
<b>Fuel pellet</b>		
Diameter	mm	9.38

Table A.18: Fuel rods characteristics. Hot conditions for the average rod

Values in Table A.18 should be used for all simulated rods.

Linear power for FUEL (kW/m)						
Node	Height(m)	Peripheral channel	Average channel	Hot channel	Hot FA	Hot rod
1	0.203	8.57	10.71	12.85	15.00	16.07
2	0.407	13.02	16.28	19.54	22.79	24.42
3	0.610	15.79	19.74	23.69	27.63	29.61
4	0.813	17.96	22.45	26.94	31.43	33.67
5	1.017	19.35	24.19	29.02	33.86	36.28
6	1.220	20.41	25.51	30.62	35.72	38.27
7	1.423	20.97	26.22	31.46	36.71	39.33
8	1.627	21.43	26.78	32.14	37.50	40.17
9	1.830	21.56	26.94	32.33	37.72	40.42
10	2.033	21.52	26.89	32.27	37.65	40.34
11	2.237	21.26	26.57	31.88	37.20	39.86
12	2.440	20.83	26.04	31.25	36.46	39.06
13	2.643	20.03	25.04	30.05	35.05	37.56
14	2.847	19.07	23.84	28.61	33.38	35.76
15	3.050	17.79	22.23	26.68	31.13	33.35
16	3.253	15.63	19.54	23.45	27.36	29.31
17	3.457	12.44	15.55	18.66	21.77	23.32
18	3.660	8.37	10.46	12.56	14.65	15.70

Table A.19: Linear heat generation rate profiles for fuel

Linear power for MODERATOR (kW/m)						
Node	Height(m)	Peripheral channel	Average channel	Hot channel	Hot FA	Hot rod
1	0.203	0.220	0.275	0.330	0.384	0.412
2	0.407	0.334	0.417	0.501	0.584	0.626
3	0.610	0.405	0.506	0.607	0.709	0.759
4	0.813	0.460	0.576	0.691	0.806	0.863
5	1.017	0.496	0.620	0.744	0.868	0.930
6	1.220	0.523	0.654	0.785	0.916	0.981
7	1.423	0.538	0.672	0.807	0.941	1.008
8	1.627	0.549	0.687	0.824	0.961	1.030
9	1.830	0.553	0.691	0.829	0.967	1.036
10	2.033	0.552	0.690	0.828	0.965	1.034
11	2.237	0.545	0.681	0.818	0.954	1.022
12	2.440	0.534	0.668	0.801	0.935	1.002
13	2.643	0.514	0.642	0.770	0.899	0.963
14	2.847	0.489	0.611	0.734	0.856	0.917
15	3.050	0.456	0.570	0.684	0.798	0.855
16	3.253	0.401	0.501	0.601	0.701	0.752
17	3.457	0.319	0.399	0.478	0.558	0.598
18	3.660	0.215	0.268	0.322	0.376	0.402

Table A.20: Linear heat generation rate profiles for moderator

Core zone	Rod average linear power (kW/m)	Power per rod (kW)	Maximum linear power (kW/m)	Number of rods	Fuel power (kW)	Moderator power (kW)	Total power (MW)
1	17.56	64.25	21.56	13056	838881.02	21509.77	860.39
2	21.94	80.32	26.94	13056	1048601.27	26887.21	1075.49
3	26.33	96.38	32.33	13056	1258321.53	32264.65	1290.59
4	30.72	112.44	37.72	203	22825.71	585.27	23.41
5	32.92	120.47	40.42	1	120.47	3.09	0.12
Total	-	-	-	39372	3168750	81250	3250

Table A.21: Core heat structures features

Multiplier is the fraction of the total power provided by the node.

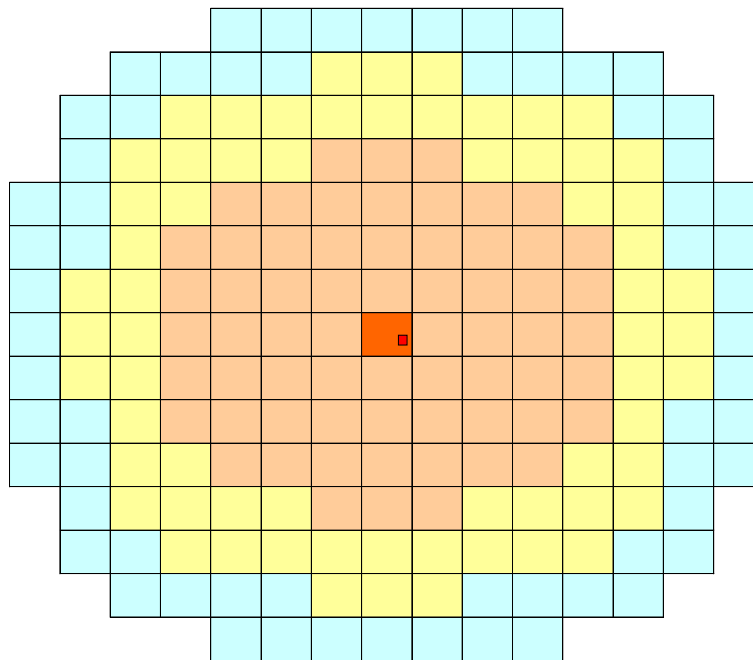
<b>Fuel Factor Multiplier</b>					
<b>Node</b>	<b>Peripheral channel</b>	<b>Average channel</b>	<b>Hot channel</b>	<b>Hot FA</b>	<b>Hot rod</b>
1	6.9991E-03	8.7489E-03	1.0499E-02	1.9044E-04	1.0052E-06
2	1.0638E-02	1.3298E-02	1.5957E-02	2.8946E-04	1.5278E-06
3	1.2898E-02	1.6123E-02	1.9348E-02	3.5096E-04	1.8524E-06
4	1.4669E-02	1.8337E-02	2.2004E-02	3.9915E-04	2.1067E-06
5	1.5805E-02	1.9756E-02	2.3708E-02	4.3005E-04	2.2698E-06
6	1.6673E-02	2.0841E-02	2.5009E-02	4.5366E-04	2.3944E-06
7	1.7133E-02	2.1416E-02	2.5699E-02	4.6617E-04	2.4604E-06
8	1.7502E-02	2.1877E-02	2.6253E-02	4.7622E-04	2.5135E-06
9	1.7608E-02	2.2010E-02	2.6411E-02	4.7910E-04	2.5287E-06
10	1.7574E-02	2.1968E-02	2.6362E-02	4.7819E-04	2.5239E-06
11	1.7363E-02	2.1704E-02	2.6045E-02	4.7244E-04	2.4935E-06
12	1.7016E-02	2.1270E-02	2.5524E-02	4.6300E-04	2.4437E-06
13	1.6361E-02	2.0452E-02	2.4542E-02	4.4519E-04	2.3497E-06
14	1.5580E-02	1.9475E-02	2.3370E-02	4.2393E-04	2.2375E-06
15	1.4529E-02	1.8162E-02	2.1794E-02	3.9534E-04	2.0866E-06
16	1.2769E-02	1.5961E-02	1.9154E-02	3.4744E-04	1.8338E-06
17	1.0161E-02	1.2701E-02	1.5241E-02	2.7647E-04	1.4592E-06
18	6.8379E-03	8.5474E-03	1.0257E-02	1.8606E-04	9.8201E-07

Table A.22: Fuel factor multiplier

Multiplier is the fraction of the total power provided by the node.

<b>Moderator Factor Multiplier</b>					
<b>Node</b>	<b>Peripheral channel</b>	<b>Average channel</b>	<b>Hot channel</b>	<b>Hot FA</b>	<b>Hot rod</b>
1	1.7946E-04	2.2433E-04	2.6920E-04	4.8832E-06	2.5773E-08
2	2.7277E-04	3.4097E-04	4.0916E-04	7.4221E-06	3.9174E-08
3	3.3073E-04	4.1341E-04	4.9609E-04	8.9990E-06	4.7496E-08
4	3.7614E-04	4.7018E-04	5.6421E-04	1.0235E-05	5.4018E-08
5	4.0526E-04	5.0657E-04	6.0789E-04	1.1027E-05	5.8200E-08
6	4.2751E-04	5.3439E-04	6.4126E-04	1.1632E-05	6.1395E-08
7	4.3930E-04	5.4912E-04	6.5895E-04	1.1953E-05	6.3088E-08
8	4.4877E-04	5.6096E-04	6.7315E-04	1.2211E-05	6.4448E-08
9	4.5148E-04	5.6435E-04	6.7722E-04	1.2285E-05	6.4838E-08
10	4.5062E-04	5.6328E-04	6.7594E-04	1.2261E-05	6.4715E-08
11	4.4521E-04	5.5651E-04	6.6781E-04	1.2114E-05	6.3937E-08
12	4.3631E-04	5.4539E-04	6.5446E-04	1.1872E-05	6.2659E-08
13	4.1952E-04	5.2440E-04	6.2928E-04	1.1415E-05	6.0248E-08
14	3.9949E-04	4.9936E-04	5.9923E-04	1.0870E-05	5.7371E-08
15	3.7255E-04	4.6569E-04	5.5883E-04	1.0137E-05	5.3503E-08
16	3.2741E-04	4.0926E-04	4.9112E-04	8.9087E-06	4.7020E-08
17	2.6053E-04	3.2567E-04	3.9080E-04	7.0891E-06	3.7416E-08
18	1.7533E-04	2.1916E-04	2.6300E-04	4.7707E-06	2.5180E-08

Table A.23: Moderator factor multiplier



# FA	# rods per FA = 204	# fuel rods
64	peripheral channel	13056
64	average channel	13056
64	hot channel	13056
1	hot FA in hot channel	203
1 rod	hot rod in hot FA	1
193	TOTAL	39372

Figure A.8: Core configuration

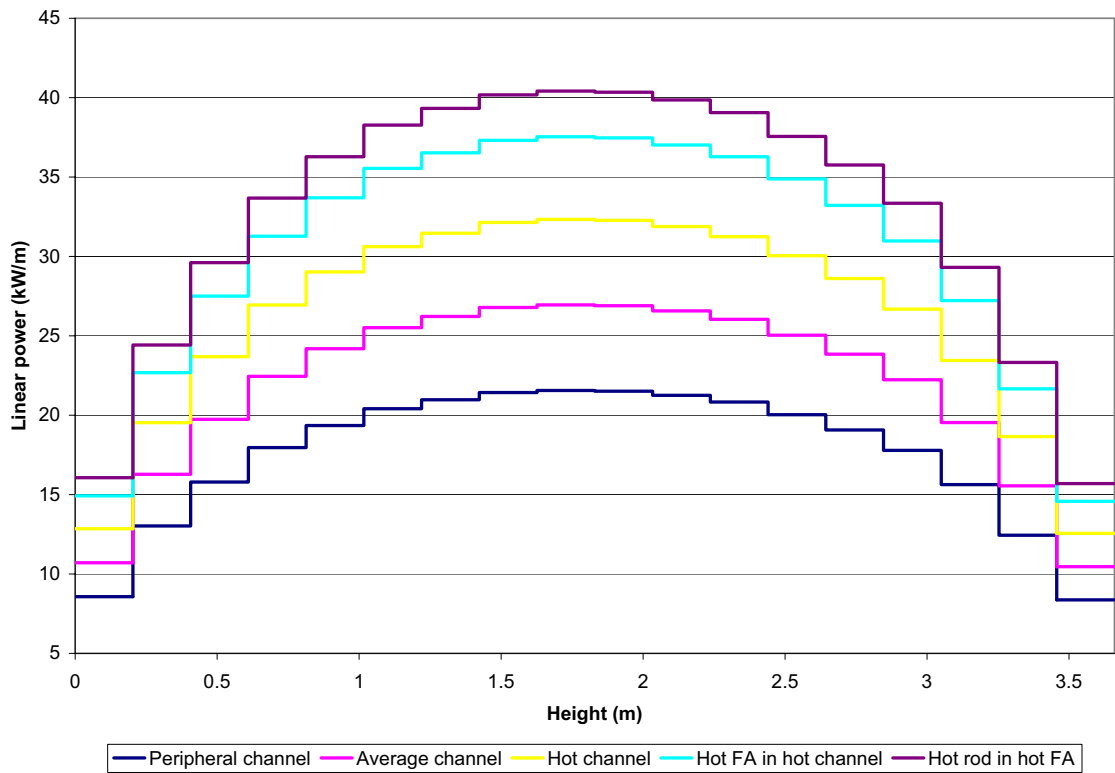


Figure A.9: Linear heat generation rate profiles

### A.4.3 Steam generators heat structures

Heat structure number	2041
Geometry	cylindrical
Material	Inconel-600
Inner radius (m)	0.010
Outer radius (m)	0.011
Hydrodynamic volume associated to the left surface area	pipe 108 (01-08 nodes), pipe 204 (nodes 01-08), pipe 408 (01-08 nodes), pipe 608 (nodes 01-08)
Hydrodynamic volume associated to the right surface area	pipe 170 (01-04 nodes), pipe 270 (nodes 01-04), pipe 470 (01-04 nodes), pipe 670 ( nodes01-04)
Left area (m <sup>2</sup> )	16948.00
Right area (m <sup>2</sup> )	19134.82
Number of U-tubes per SG	3388

Table A.24: Heat structure 2041

### A.4.4 Pressurizer heat structures

Heat structure number	1000
Geometry	Cylindrical
Material	Stainless Steel
Inner radius (m)	1.042
Outer radius (m)	1.274
Hydrodynamic volume associated to the left surface area	pipe 150(nodes 01-06)
Hydrodynamic volume associated to the right surface area	none
Left area (m <sup>2</sup> )	97.74
Right area (m <sup>2</sup> )	119.46

Table A.25: Heat structure 1000

### A.4.5 Vessel heat structures



Heat structure number	1001
Geometry	Cylindrical
Material	Stainless Steel
Inner radius (m)	0.146
Outer radius (m)	0.222
Hydrodynamic volume associated to the left surface area	pipe 152 (nodes 01-03)
Hydrodynamic volume associated to the right surface area	none
Left area (m <sup>2</sup> )	18.53
Right area (m <sup>2</sup> )	28.18

Table A.26: Heat structure 1001

Heat structure number	3000
Geometry	Cylindrical
Material	Stainless Steel
Inner radius (m)	2.172
Outer radius (m)	2.445
Hydrodynamic volume associated to the left surface area	branch300, branch305, pipe 310 (nodes 01-04)
Hydrodynamic volume associated to the right surface area	none
Left area (m <sup>2</sup> )	53.37
Right area (m <sup>2</sup> )	60.08

Table A.27: Heat structure 3000

Heat structure number	3150
Geometry	Cylindrical
Material	Stainless Steel
Inner radius (m)	2.013
Outer radius (m)	2.083
Hydrodynamic volume associated to the left surface area	pipe 315 (nodes 01-08)
Hydrodynamic volume associated to the right surface area	pipe 315 (nodes 01-08)
Left area (m <sup>2</sup> )	70.03
Right area (m <sup>2</sup> )	72.46

Table A.28: Heat structure 3150

Heat structure number	3160
Geometry	Cylindrical
Material	Stainless Steel
Inner radius (m)	2.197
Outer radius (m)	2.416
Hydrodynamic volume associated to the left surface area	pipe 315(nodes 01-08)
Hydrodynamic volume associated to the right surface area	none
Left area (m <sup>2</sup> )	76.44
Right area (m <sup>2</sup> )	84.06

Table A.29: Heat structure 3160

Heat structure number	3200
Geometry	Cylindrical
Material	Stainless Steel
Inner radius (m)	1.880
Outer radius (m)	1.937
Hydrodynamic volume associated to the left surface area	pipe 320 (nodes 01-18)
Hydrodynamic volume associated to the right surface area	pipe 320 (nodes 01-18)
Left area (m <sup>2</sup> )	48.14
Right area (m <sup>2</sup> )	49.61

Table A.30: Heat structure 3200

Heat structure number	3230
Geometry	Spherical, hemisphere
Material	Stainless Steel
Inner radius (m)	2.240
Outer radius (m)	2.382
Hydrodynamic volume associated to the left surface area	single volume 323
Hydrodynamic volume associated to the right surface area	none

Table A.31: Heat structure 3230

Heat structure number	3220
Geometry	Cylindrical
Material	Stainless Steel
Inner radius (m)	2.240
Outer radius (m)	2.382
Hydrodynamic volume associated to the left surface area	Branch 322
Hydrodynamic volume associated to the right surface area	none
Left area (m <sup>2</sup> )	7.79
Right area (m <sup>2</sup> )	8.28

Table A.32: Heat structure 3220

Heat structure number	3250
Geometry	Cylindrical
Material	Stainless Steel
Inner radius (m)	1.880
Outer radius (m)	1.937
Hydrodynamic volume associated to the left surface area	single volume 325, branch 330
Hydrodynamic volume associated to the right surface area	pipe 315 (nodes 07-08)
Left area (m <sup>2</sup> )	17.25
Right area (m <sup>2</sup> )	17.78

Table A.33: Heat structure 3250

Heat structure number	3270
Geometry	Rectangular
Material	Stainless Steel
Left boundary coordinate (m)	0.000
Right boundary coordinate (m)	0.076
Hydrodynamic volume associated to the left surface area	none
Hydrodynamic volume associated to the right surface area	single volume 323, branch 322, snglvol325, branch330
Surface area (m <sup>2</sup> )	117.69

Table A.34: Heat structure 3270

Heat structure number	3350
Geometry	Cylindrical
Material	Stainless Steel
Inner radius (m)	2.044
Outer radius (m)	2.072
Hydrodynamic volume associated to the left surface area	pipe 335 (nodes 01-18)
Hydrodynamic volume associated to the right surface area	pipe 320 (nodes 01-18)
Left area (m <sup>2</sup> )	47.00
Right area (m <sup>2</sup> )	47.66

Table A.35: Heat structure 3350

Heat structure number	3500
Geometry	Cylindrical
Material	Stainless Steel
Inner radius (m)	1.880
Outer radius (m)	1.937
Hydrodynamic volume associated to the left surface area	branch 340, branch 345, pipe 350 (nodes 01-04)
Hydrodynamic volume associated to the right surface area	branch300, branch305, pipe 310 (nodes 01-04)
Left area (m <sup>2</sup> )	46.20
Right area (m <sup>2</sup> )	47.60

Table A.36: Heat structure 3500

Heat structure number	3510
Geometry	Rectangular
Material	Stainless Steel
Left boundary coordinate (m)	0.000
Right boundary coordinate (m)	0.015
Hydrodynamic volume associated to the left surface area	none
Hydrodynamic volume associated to the right surface area	branch340, branch 345, pipe 350 (node 01)
Surface area (m <sup>2</sup> )	354.81

Table A.37: Heat structure 3510

Heat structure number	3550
Geometry	Spherical, hemisphere
Material	Stainless Steel
Inner radius (m)	2.178
Outer radius (m)	2.367
Hydrodynamic volume associated to the left surface area	pipe 356 (node 01)
Hydrodynamic volume associated to the right surface area	none

Table A.38: Heat structure 3550

Heat structure number	3570
Geometry	Cylindrical
Material	Stainless Steel
Inner radius (m)	2.178
Outer radius (m)	2.367
Hydrodynamic volume associated to the left surface area	pipe 356(nodes 02-03)
Hydrodynamic volume associated to the right surface area	none
Left area (m <sup>2</sup> )	11.25
Right area (m <sup>2</sup> )	12.23

Table A.39: Heat structure 3570

Heat structure number	3560
Geometry	Rectangular
Material	Stainless Steel
Left boundary coordinate (m)	0.000
Right boundary coordinate (m)	0.144
Hydrodynamic volume associated to the left surface area	none
Hydrodynamic volume associated to the right surface area	branch 355, pipe 356(nodes 01-03)
Surface area (m <sup>2</sup> )	46.57

Table A.40: Heat structure 3560

### A.4.6 Reactor coolant pumps curves

Data from the built-in pump curves of RELAP5, (Reference[6])

Octant	w/q or q/w	h/w <sup>2</sup> or h/q <sup>2</sup>	Octant	w/q or q/w	h/w <sup>2</sup> or h/q <sup>2</sup>	
#1	0.00	1.73	#5	0.00	-0.16	
	0.20	1.50		0.10	-0.12	
	0.46	1.24		0.20	-0.06	
	0.52	1.23		0.28	0.00	
	0.60	1.24		0.40	0.09	
	0.66	1.24		0.60	0.31	
	0.80	1.17		0.70	0.42	
	0.90	1.10		0.80	0.50	
	1.00	1.00		0.88	0.54	
#2	0.00	-0.96	#6	1.00	0.59	
	0.10	-0.90		0.00	1.40	
	0.20	-0.81		0.37	0.80	
	0.30	-0.70		0.43	0.74	
	0.40	-0.54		0.50	0.68	
	0.53	-0.30		0.58	0.64	
	0.65	0.00		0.64	0.62	
	0.80	0.37		0.70	0.61	
	1.00	1.00		1.00	0.59	
#3	-1.00	3.55	#7	-1.00	0.00	
	-0.60	2.73		0.00	-0.16	
	#4	-0.32	2.20	#8	-1.00	0.00
		-0.18	2.00		0.00	-0.96
		0.00	1.73			
-1.00	3.55					
-0.89	3.20					
-0.74	2.80					
-0.60	2.47					
-0.46	2.20					
-0.20	1.73					
0.00	1.40					

Table A.41: Westinghouse pump homologous single phase head curves

Octant	w/q or q/w	t/w <sup>2</sup> or t/q <sup>2</sup>	Octant	w/q or q/w	t/w <sup>2</sup> or t/q <sup>2</sup>
#1	0.00	1.01	#5	0.00	-1.00
	0.10	0.96		0.25	-0.60
	0.20	0.92		0.40	-0.37
	0.30	0.90		0.50	-0.25
	0.40	0.89		0.60	-0.16
	0.50	0.91		0.80	-0.01
	0.70	0.99		1.00	0.11
	0.80	1.02	#6	0.00	1.42
	0.90	1.02		0.60	0.61
	1.00	1.00		0.80	0.35
#2	0.00	-0.87	1.00	0.11	
	0.10	-0.76	#7	-1.00	0.00
	0.20	-0.63		0.00	-0.87
	0.30	-0.48	#8	-1.00	0.00
	0.40	-0.31		0.00	-1.00
	0.74	0.40			
	1.00	1.00			
#3	-1.00	2.98			
	-0.82	2.40			
	-0.60	1.87			
	-0.46	1.60			
	-0.34	1.40			
	-0.20	1.21			
	-0.10	1.10			
	0.00	1.01			
#4	-1.00	2.98			
	-0.91	2.80			
	-0.80	2.60			
	-0.70	2.42			
	-0.60	2.25			
	-0.42	2.00			
	0.00	1.42			

Table A.42: Westinghouse pump single phase homologous torque curves

Octant	w/q or q/w	h/w <sup>2</sup> or h/q <sup>2</sup>	Octant	w/q or q/w	h/w <sup>2</sup> or h/q <sup>2</sup>
#1	0.00	0.00	#5	0.00	0.00
	0.10	0.83		0.20	-0.34
	0.20	1.09		0.40	-0.65
	0.50	1.02		0.60	-0.93
	0.70	1.01		0.80	-1.19
	0.90	0.94		1.00	-1.47
#2	0.00	0.00	#6	0.00	0.11
	0.10	-0.04		0.10	0.13
	0.20	0.00		0.25	0.15
	0.30	0.10		0.40	0.13
	0.40	0.21		0.50	0.07
	0.80	0.67		-0.60	-0.04
	0.90	0.80		0.70	-0.23
	1.00	1.00		-0.80	-0.51
#3	-1.00	-1.16		0.90	-0.91
	-0.90	-1.24		1.00	-1.47
	-0.80	-1.77	#7	-1.00	0.00
	-0.70	-2.36		0.00	0.00
	-0.60	-2.79	#8	-1.00	0.00
	-0.50	-2.91		0.00	0.00
	-0.40	-2.67			
	-0.25	-1.69			
	-0.10	-0.50			
0.00	0.00				
#4	-1.00	-1.16			
	-0.90	-0.78			
	-0.80	-0.50			
	-0.70	-0.31			
	-0.60	-0.17			
	-0.50	-0.08			
	-0.35	0.00			
	-0.20	0.05			
	-0.10	0.08			
	0.00	0.11			

Table A.43: Head curves, difference curve data



Octant	w/q or q/w	h/w <sup>2</sup> or h/q <sup>2</sup>	Octant	w/q or q/w	h/w <sup>2</sup> or h/q <sup>2</sup>
#1	0.00	0.54	#5	0.00	-0.63
	0.20	0.59		0.20	-0.51
	0.40	0.65		0.40	-0.39
	0.60	0.77		0.60	-0.29
	0.80	0.95		0.80	-0.20
	0.90	0.98		0.90	-0.16
	0.95	0.96		1.00	-0.13
	1.00	0.87			
#2	0.00	-0.15	#6	0.00	0.36
	0.20	0.02		0.20	0.32
	0.40	0.22		0.40	0.27
	0.60	0.46		0.60	0.18
	0.80	0.71		0.80	0.05
	0.90	0.81	1.00	-0.13	
	0.95	0.85	#7	-1.00	-1.44
	1.00	0.87		-0.80	-1.25
		-0.60		-1.08	
#3	-1.00	0.62		-0.40	-0.92
	-0.80	0.68		-0.20	-0.77
	-0.60	0.53		0.00	-0.63
	-0.40	0.46	#8	-1.00	-1.44
	-0.20	0.49		-0.80	-1.12
	0.00	0.54		-0.60	-0.79
		-0.40		-0.52	
#4	-1.00	0.62		-0.20	-0.31
	-0.80	0.53		0.00	-0.15
	-0.60	0.46			
	-0.40	0.42			
	-0.20	0.39			
	0.00	0.36			

Table A.44: Torque curves, difference curve data

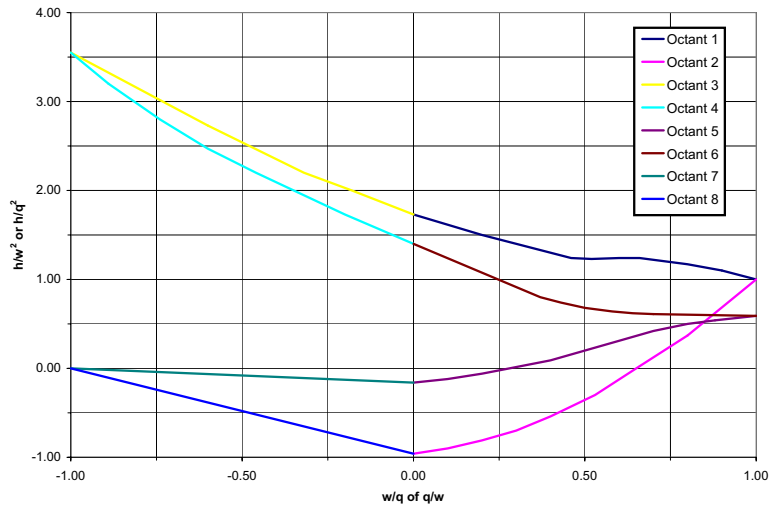


Figure A.10: Westinghouse pump homologous single phase head curves

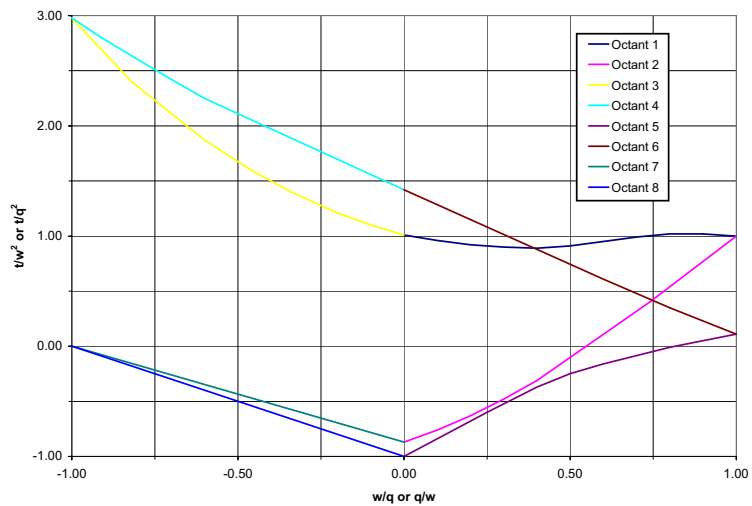


Figure A.11: Westinghouse pump single phase homologous torque curves

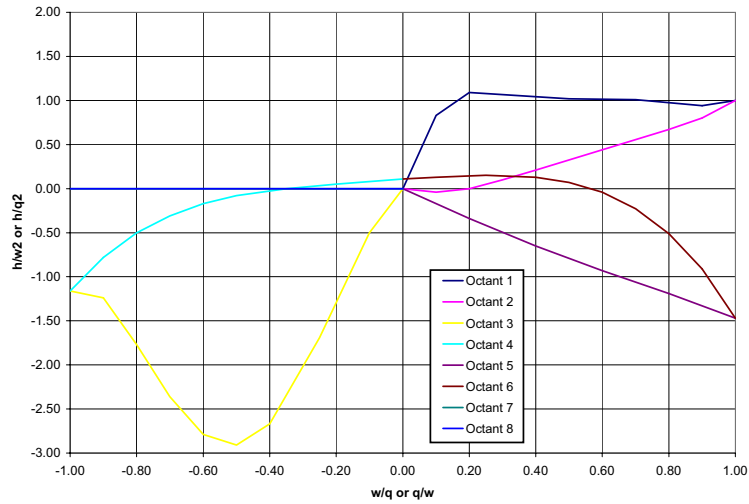


Figure A.12: Head difference data

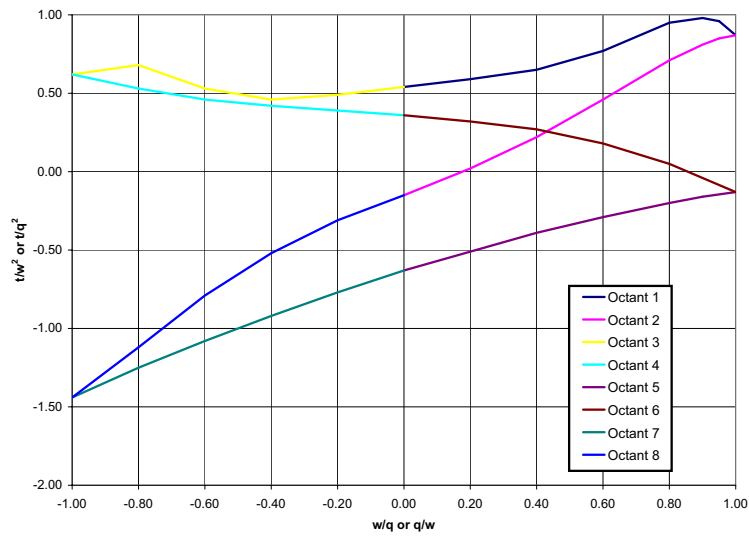


Figure A.13: Homologous torque difference curves

## A.5 Transient description

Event	Time(s)
Break	0.0
SCRAM	0.0
Reactor coolant pumps trip	0.0
Steam line isolation	10.0
Feed water isolation	20.0
HPIS	NO

Table A.45: Time sequence of imposed events

LPIS injection: 1.42 MPa pressure set point. Driven by a flow-pressure table (see Table A.46)

Accumulators injection: 4.14 MPa pressure set point.

Containment pressure imposed as a function of time after the break (see Table A.47)

Reactor coolant pumps velocity imposed as a function of time after the break (see tables A.49, A.50)

Decay power imposed by means of a reactor power multiplier as a function of time after break (see Table A.48)

### A.5.1 Transient tables

<b>Pressure (MPa)</b>	<b>Flow (kg/s)</b>
0.1	88.0
1.0	88.0
1.4	0.0

Table A.46: LPIS pressure-flow curve

<b>Time after SCRAM (s)</b>	<b>Pressure (MPa)</b>
0.0	0.10
12.5	0.35
50.0	0.25
200.	0.20
1.e5	0.20

Table A.47: Containment pressure

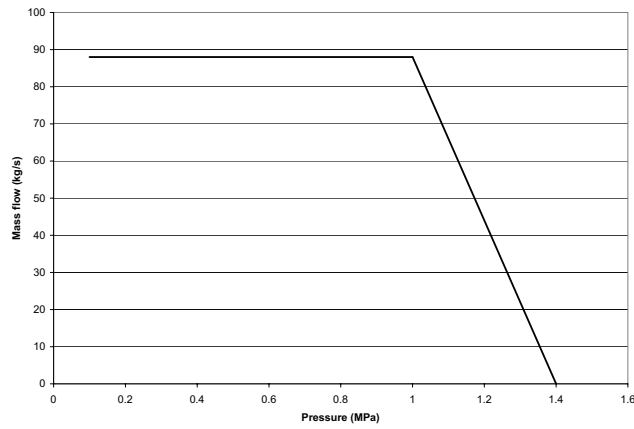


Figure A.14: LPIS

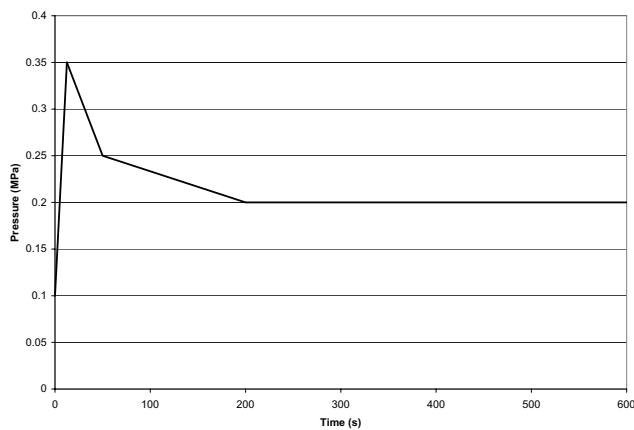


Figure A.15: Containment pressure

Time after SCRAM (s)	Reactor power (multiplier)
0.0	1.000000000
0.1	1.000000000
0.2	1.000000000
0.3	0.988404399
0.4	0.933006063
0.5	0.864047288
0.6	0.798640798
0.7	0.719875559
0.8	0.625345987
0.9	0.494420309
1.0	0.342882587
2.0	0.118618375
3.0	0.106901571
4.0	0.098596180
5.0	0.092207526
6.0	0.087099523
7.0	0.082918506
8.0	0.079434403
9.0	0.076485583
10.0	0.073954346
15.0	0.065148526
20.0	0.059670900
30.0	0.052719618
40.0	0.048209285
50.0	0.044933723
60.0	0.042418700
100.0	0.036122462
200.0	0.030459138
300.0	0.028022673
400.0	0.026470518
500.0	0.025300162
600.0	0.024340455
1.e+5	0.001460000

Table A.48: Decay heat power

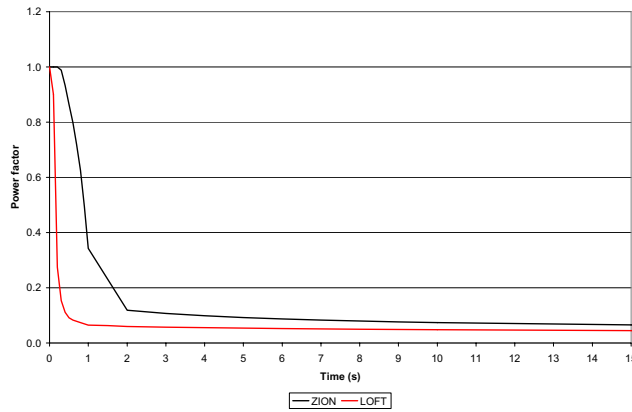


Figure A.16: Decay heat power factor

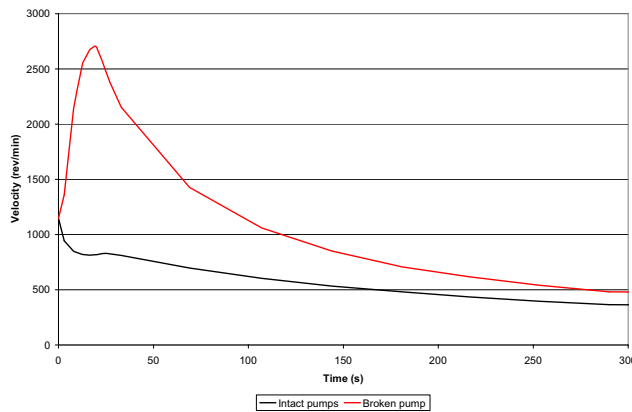


Figure A.17: RCPs velocity



<b>Time after SCRAM (s)</b>	<b>Pump velocity (rev/min)</b>
0.0	1146.5
3.0	944.5
8.0	849.6
9.5	838.0
12.3	822.2
12.8	819.8
16.5	812.7
19.2	816.8
20.0	817.7
23.1	828.3
25.0	829.0
27.0	826.6
33.0	812.2
69.0	697.7
107.0	602.8
144.0	533.1
181.0	480.5
216.0	435.8
253.0	396.8
290.0	364.9
1.e5	0.0

Table A.49: Pump velocity for primary coolant pumps in intact loops

<b>Time after SCRAM (s)</b>	<b>Pump velocity (rev/min)</b>
0.0	1146.5
3.0	1358.3
8.0	2140.8
9.5	2286.8
12.3	2517.5
12.8	2555.3
16.5	2676.8
19.2	2707.6
20.0	2699.2
23.1	2571.1
25.0	2478.0
27.0	2382.0
33.0	2154.0
69.0	1426.4
107.0	1060.4
144.0	850.0
181.0	708.4
216.0	618.8
253.0	541.0
290.0	480.9
1.e5	0.0

Table A.50: Pump velocity for primary coolant pumps in broken loop

## A.6 Output evaluation

### A.6.1 Steady State

N°	Quantity	Unit	Calculated value
<b>Nodalization development</b>			
1	Primary circuit volume (with pressurizer, without accumulators) - volume of the pipes	m <sup>3</sup> m <sup>3</sup>	
2	Secondary circuit volume - volume of the pipes	m <sup>3</sup>	
3	Non active heat structures area	m <sup>2</sup>	
4	Core HS area	m <sup>2</sup>	
5	SG U-tubes HS external surface area (w/o tube sheet)	m <sup>2</sup>	
6	Core heat transfer volume (volume surrounding active core)	m <sup>3</sup>	
7	SG U-tubes heat transfer volume (without tube sheet)	m <sup>3</sup>	
8	Maximum linear power for zone 2 (average channel)	kW/m	
9	Maximum linear power for zone 5 (hot rod in hot channel)	kW/m	
<b>Steady State</b>			
1	Core power	MW	
2	Heat transfer in the SGs (4 loops)	MW	
3	Primary system hot leg pressure	MPa	
4	Pressurizer pressure (top volume)	MPa	
5	Steam generator 1 exit pressure	MPa	
6	Accumulator 1 pressure	MPa	
7	Intact HL 1 temperature (near vessel)	K	
8	Intact CL 1 temperature (near vessel)	K	
9	Reactor vessel downcomer temperature	K	
10	Broken loop HL temperature (near vessel)	K	
11	Broken loop CL temperature (near vessel)	K	
12	Pressurizer temperature (lower volume)	K	
13	Rod surface temperature (hot rod in hot channel, at height 1.6 - 1.8 m)	K	
14	Upper head temperature	K	
15	Reactor coolant pump of loop 1 velocity	rev/min	
16	Reactor pressure vessel pressure loss	kPa	
17	Core pressure loss	kPa	
18	Primary system total loop pressure loss	kPa	

Table A.51: Nodalization qualification at steady state level

N°	Quantity	Unit	Calculated value
19	Steam generator 1 pressure loss	kPa	
20	Primary system total mass inventory (with pressurizer, without accumulators)	kg	
21	Steam generator total mass inventory	kg	
22	Primary system total loop coolant mass flow	kg/s	
23	Steam generator 1 feedwater mass flow	kg/s	
24	Core coolant mass flow	kg/s	
25	Core bypass mass flow (LP-UP)	kg/s	
26	Pressurizer level (collapsed)	m	
27	Secondary side downcomer level	m	

Table A.51: *continued*

N°	Position along the loop		Calculated (MPa)
1	Hot leg inlet	HL IN	
2	Hot leg outlet	HL OUT	
3	Steam generator inlet plenum	SG IN	
4	U-tube top	UT Top	
5	Steam generator outlet plenum	SG OUT	
6	Downstream SG outlet nozzle	OUT SG NOZZLE	
7	Bottom of loop seal	LOOP SEAL	
8	Pump inlet	PUPM IN	
9	Pump outlet	PUMP OUT	
10	Cold leg in	CL IN	
11	Cold leg out	CL OUT	
12	Lower plenum (0.2 m from bottom of vessel)	LP	
13	Bottom of active core	BAF	
14	Top of active core	TAF	

Table A.52: Pressure along the loop

### A.6.2 Transient

<b>Events</b>	<b>Calculated time after transient initiation</b>
LB-LOCA initiated	
Reactor scrammed	
DNB in core	
Primary coolant pumps tripped	
Partial top-down rewet initiated <sup>(4)</sup>	
Pressurizer emptied	
Accumulator in loop 1 injection initiated	
Partial top-down rewet ended <sup>(4)</sup>	
Maximum cladding temperature reached	
LPIS in loop 1 injection initiated	
Accumulator in loop 1 emptied	
Core cladding fully quenched	

Table A.53: Resulting time sequence of main events

<sup>(4)</sup> Partial top-down rewet is understood as significant (about 60 K) clad temperature decrease in the inner channel of the active core.

N°	Parameter
1	Intact loop pressure in hot leg
2	Broken loop RCP side pressure
3	Broken loop vessel side in cold leg
4	SG pressure - secondary side
5	Accumulator 1 pressure
6	Lower plenum liquid temperature mean value (if that is possible)
7	Lower plenum steam temperature mean value (if that is possible)
8	Intact loop hot leg liquid temperature mean value (if that is possible)
9	Intact loop hot leg steam temperature mean value (if that is possible)
10	Upper head liquid temperature
11	Broken loop RCP side break flow
12	Broken loop vessel side break flow
13	Integral break flow
14	Total ECCS integral flow
15	Primary side total mass (with pressurizer, without accumulators)
16	Steam generator 1 pressure drop
17	Primary pumps pressure drop
18	Cladding temperature in hot rod in hot channel -(0.4 - 0.6m) (*)
19	Cladding temperature in hot rod in hot channel -(1.6 - 1.8m) (*)
20	Cladding temperature in hot rod in hot channel -(2.8 - 3.0m) (*)
21	Cladding temperature in avg rod in avg channel -(0.4 - 0.6m) (*)
22	Cladding temperature in avg rod in avg channel -(1.6 - 1.8m) (*)
23	Cladding temperature in avg rod in avg channel -(2.8 - 3.0m) (*)
24	Maximum cladding temperature
25	Hot rod fuel centerline temperature at 1.6 - 1.8m

Table A.54: Time trends

(\*) For 3D codes maximum radial temperature of fixed elevation should be supplied.

Event	Unit	Calculated time after break
<b>Break flowrate behaviour</b>		
Integral break flowrate at dryout time	kg	
Integral break flowrate at ACC injection time	kg	
Integral break flowrate at core quench time	kg	
Integral break flowrate at 500s	kg	
<b>Pressurizer behaviour</b>		
Time of emptying (level below 0.1m)	s	
PZR pressure/primary pressure at 5s	-	
PZR pressure/primary pressure at 10s	-	
PZR pressure/primary pressure at emptying time	-	
Time of PZR primary pressure equalization	-	
<b>Dryout occurrence</b>		
DNB in core	s	
Time of maximum cladding temperature	s	
Peak cladding temperature	K	
Time of core fully quenched	s	
<b>Upper plenum pressure behaviour</b>		
Pressure at dryout time	MPa	
Pressure at 10s	MPa	
Pressure at 20s	MPa	
Pressure at fully core quench time	MPa	
Pressure at 500s	MPa	
<b>Accumulator behaviour</b>		
ACC1 injection time	s	
ACC1 pressure 10s after injection initiation	MPa	
ACC1 pressure 20s after injection initiation	MPa	
ACC1 pressure at core quench time	MPa	
Integral ACC1 flowrate at core quench time	kg	
Integral ACC1 flowrate at 500s	kg	
ACC1 emptied	s	
<b>LPIS behaviour</b>		
LPIS injection time	s	
LPIS flowrate at core quench	kg/s	

Table A.55: Qualitative evaluation

Event	Unit	Calculated time after break
LPIS flowrate at 500s	kg/s	
Integral LPIS flowrate at core quench time	kg	
Integral LPIS flowrate at 100s	s	
<b>Accumulator + LPIS behaviour</b>		
Total integral ECC flowrate at core quench time	kg	
Total integral ECC flowrate at 100s	kg	
Total integral ECC flowrate at 500s	kg	
<b>Primary system mass behaviour</b>		
Minimum mass/ initial mass	-	
Primary mass at core quench time/ initial mass	-	
Primary mass at 500s/ initial mass	-	

Table A.55: *continued*

Core is considered to be fully quenched when temperatures for all rods satisfy:  $T_{clad} < T_{sat} + 30K$



## **A.7 references**

- [1]. "Input and Output Specifications for the LOFT L2-5 Experiment. Phase 2 of BEMUSE Programme" A.Petruzzi, F.d'Auria. DIMNP NT 517(05).
- [2]. Severe Accident Risks: An Assessment for Five U.S Nuclear Power Plants. Final Summary Report NUREG-1150. Vol.1.
- [3]. 2005 World Nuclear Industry handbook. Nuclear Engineering International.
- [4]. Net source: [http://en.wikipedia.org/wiki/Zion\\_Nuclear\\_Power\\_Station](http://en.wikipedia.org/wiki/Zion_Nuclear_Power_Station)
- [5]. Net source: <http://earth.google.com/>
- [6]. RELAP5/MOD3.3 CODE MANUAL. VOLUME I: CODE STRUCTURE, SYSTEM MODELS, AND SOLUTION METHODS.



APPENDIX B

# Sensitivity calculations specifications

**Coordinators:** F.Reventós (UPC), M. Pérez (UPC), L. Batet (UPC), R. Pericas (UPC)

**Participating Organizations and Authors**

AEKI, Hungary	I. Trosztel, I. Tóth
CEA, France	P. Bazin, A. de Crécy, P. Germain
FSUE EDO GUIDROPPRESS, Russia	S. Borisov
GRS, Germany	H. Glaeser, T. Skorek
IRSN, France	J. Joucla, P. Probst
JNES, Japan	A. Ui
KAERI, South Korea	B. D. Chung
KINS, South Korea	D.Y. Oh
NRI-1, Czech Republic	M. Kyncl, R. Pernica
PSI, Switzerland	A. Manera
UNIPI-1, Italy	F. D'Auria, A. Petruzzi
UNIPI-2, Italy	F. D'Auria, A. Del Nevo
UPC, Spain	M. Pérez, F. Reventós, L. Batet



## B.1 Introduction

With the aim to proceed in the same way as in previous phase II of BEMUSE programme, a list of sensitivity calculations is proposed in this document.

Base case calculation and the analysis of sensitivity results is known to be a good tool to prepare uncertainty analysis of next phase.

The selection of the sensitivity parameters takes into account conclusions written in reports of previous phases II and III, together with what was agreed in the 4<sup>th</sup> BEMUSE meeting held in Barcelona May 2006. According to the last point, the proposed list (see Table B.1) considers only **initial** and **boundary conditions** and the **ranges** pretend to be **realistic**. Only sensitivities specified in Table B.1 are mandatory and participants can also add other sensitivity calculations according to their own interest. This second kind of sensitivity calculations has to be a limited number and participants should provide enough information for comparison sake.

## B.2 List of sensitivity parameters

Participants are requested to perform both maximum and minimum values calculations for each sensitivity parameter listed below.

N	Parameter	Range	
		Minimum	Maximum
1	Fuel conductivity (for all fuel rods)	value <sub>BC</sub> - 0.4 W/m-K	value <sub>BC</sub> + 0.4 W/m-K
2	Gap conductivity (for all fuel rods)	value <sub>BC</sub> * 0.8	value <sub>BC</sub> * 1.2
3	Power after scram	value <sub>BC</sub> - 8% see Table B.2	value <sub>BC</sub> + 8% see Table B.3
4	Power before scram	value <sub>BC</sub> - 3.3%	value <sub>BC</sub> + 3.3%
5	Hot rod power (whole rod, same axial shape)	value <sub>BC</sub> - 7.6%	value <sub>BC</sub> + 7.6%
6	LPIS delay (3/3)	-	value <sub>BC</sub> + 30 sec
7	Accumulator liquid volume (3/3)	value <sub>BC</sub> - 33 ft <sup>3</sup>	value <sub>BC</sub> + 33 ft <sup>3</sup>
8	Accumulator pressure (3/3)	value <sub>BC</sub> - 100 psig	value <sub>BC</sub> + 100 psig
9	Containment pressure	see Table B.5	-
10	Hot/cold conditions for pellet radius (for all fuel rods)	see Table B.4	-

Table B.1: Sensitivity parameters

where BC stands for Base Case, and (3/3) means the 3 safety injection systems

Participants should use Tables B.2 and B.3 for Sensitivity N°3 (see Figure B.2), and Table A.47 for Sensitivity N°9 (see Figure B.1).

<b>Time after SCRAM (s)</b>	<b>Power after scram multiplier</b>
0.0	1.
0.1	1.
0.2	1.
0.3	0.909332047
0.4	0.858365578
0.5	0.794923505
0.6	0.734749534
0.7	0.662285514
0.8	0.575318308
0.9	0.454866684
1.0	0.31545198
2.0	0.109128905
3.0	0.098349445
4.0	0.090708486
5.0	0.084830924
6.0	0.080131561
7.0	0.076285026
8.0	0.073079651
9.0	0.070366736
10.0	0.068037998
15.0	0.059936644
20.0	0.054897228
30.0	0.048502049
40.0	0.044352542
50.0	0.041339025
60.0	0.039025204
100.0	0.033232665
200.0	0.028022407
300.0	0.025780859
400.0	0.024352877
500.0	0.023276149
600.0	0.022393219
1.e5	0.0013432

Table B.2: Sensitivity n°3: Power after scram, lower case

Time after SCRAM (s)	Power after scram multiplier
0.0	1.
0.1	1.
0.2	1.
0.3	1.
0.4	1.
0.5	0.933171071
0.6	0.862532062
0.7	0.777465604
0.8	0.675373666
0.9	0.533973934
1.0	0.370313194
2.0	0.128107845
3.0	0.115453697
4.0	0.106483874
5.0	0.099584128
6.0	0.094067485
7.0	0.089551986
8.0	0.085789155
9.0	0.08260443
10.0	0.079870694
15.0	0.070360408
20.0	0.064444572
30.0	0.056937187
40.0	0.052066028
50.0	0.048528421
60.0	0.045812196
100.0	0.039012259
200.0	0.032895869
300.0	0.030264487
400.0	0.028588159
500.0	0.027324175
600.0	0.026287691
1.e5	0.0015768

Table B.3: Sensitivity n°3: Power after scram, upper case

Parameter	Unit	Value
<b>Fuel pin</b>		
Outisde diameter	mm	10.7
Cladding thickness	mm	0.61
Gap thickness	mm	0.09
<b>Fuel pellet</b>		
Diameter	mm	9.3

Table B.4: Fuel rods characteristics. Cold conditions for the average rod

Values in Table B.4 should be used for all simulated rods

Time after SCRAM (s)	Pressure (MPa)
0.0	0.10
12.5	0.25
50.0	0.18
200.	0.10
1.e5	0.10

Table B.5: Sensitivity n°9: Containment pressure



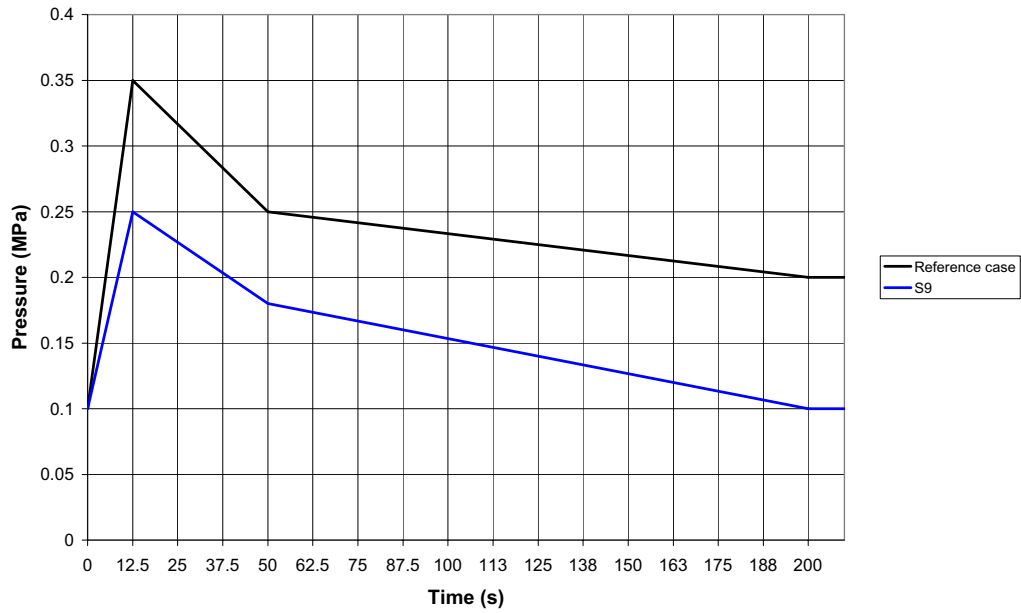


Figure B.1: Sensitivity n°9: Containment pressure

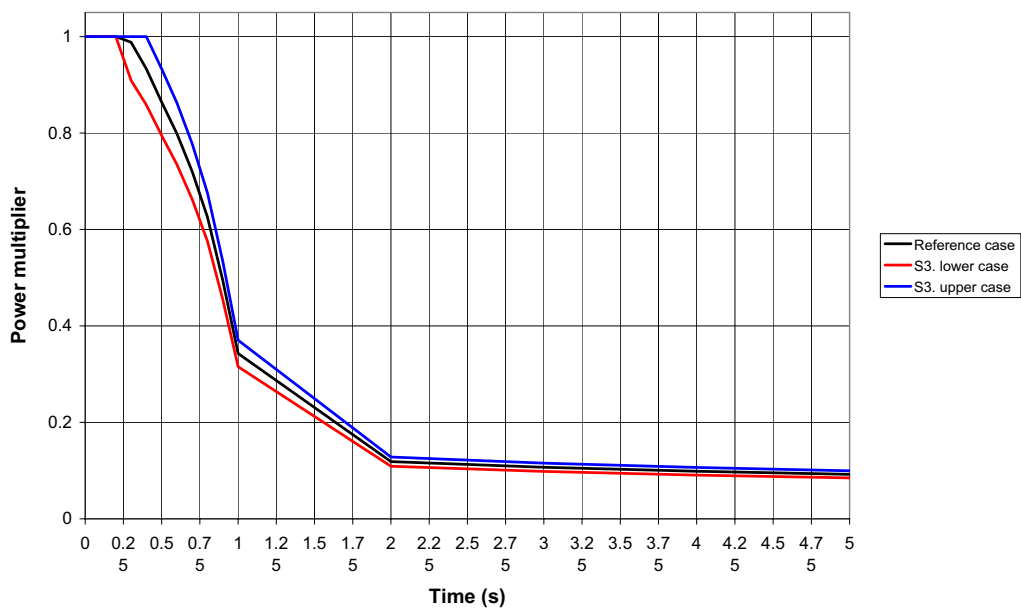


Figure B.2: Sensitivity n°3: Power after scram

## B.3 Output

For each sensitivity calculation the following output parameters should be submitted:

- Time dependent parameters
  - Upper plenum pressure
  - Rod surface temperature in hot rod in hot channel - 2/3 core height (between 1.6 - 1.8m)
  - Mass inventory
- Point parameters
  - $\Delta PCT$ , defined as the difference between the PCT of the base case calculation and the PCT obtained from the sensitivity run, making reference to the hot rod in the hot fuel assembly at 2/3 core height.
  - $\Delta T_{REFLOOD}$ , defined as the difference between the reflood times predicted in the base case and in the sensitivity run, making reference to the hot rod in the hot fuel assembly at 2/3 core height. 'Reflood time' is the time when the rod surface temperature achieves a value close to the local fluid temperature. (about  $T_{SAT} + 30$  K)

by filling up excel file 'SensitivitiesRev3.xls'.

## **B.4 References**

6. "Bemuse Phase II Report. Re-analysis of the ISP-13 Exercise, Post Test Analysis of the LOFT L2-5 Test Calculation. November 2006." Nuclear Safety NEA/CSNI/R(2006)2 May 2006.
7. "BEMUSE phase III Report. Uncertainty and Sensitivity Analysis of the LOFTL25-5 Test." NEA/CSNI/R(2007)4. May 2007.



APPENDIX C

## Codes and input decks

**Coordinators:** F.Reventós (UPC), M. Pérez (UPC), L. Batet (UPC), R. Pericas (UPC)

**Participating Organizations and Authors**

AEKI, Hungary	I. Trosztel, I. Tóth
CEA, France	P. Bazin, A. de Crécy, P. Germain
FSUE EDO GUIDROPRESS, Russia	S. Borisov
GRS, Germany	H. Glaeser, T. Skorek
IRSN, France	J. Joucla, P. Probst
JNES, Japan	A. Ui
KAERI, South Korea	B. D. Chung
KINS, South Korea	D.Y. Oh
NRI-1, Czech Republic	M. Kyncl, R. Pernica
PSI, Switzerland	A. Manera
UNIPI-1, Italy	F. D'Auria, A. Petruzzi
UNIPI-2, Italy	F. D'Auria, A. Del Nevo
UPC, Spain	M. Pérez, F. Reventós, L. Batet



## C.1 CEA, France

### C.1.1 Description of the code: CATHARE

The development of the CATHARE code has been initiated in 1979. It is a joint effort of CEA (Atomic Energy Research Center), IRSN (Nuclear Safety Institute), EDF (the French utility) and FRAMATOME-ANP (the French vendor). The code is able to perform safety analysis with best estimate calculations of thermohydraulic transients in Pressurized Water Reactors for postulated accidents or other incidents, such as LBLOCAs, SBLOCAS, SGTR, Loss of RHR, Secondary breaks, Loss of Feed-water,

The code is based on a 2-fluid 6-equation model. The presence of non condensable gases such as nitrogen, hydrogen, air, can be modeled by one to four additive transport equations. The code is able to model any kind of experimental facility or PWR (Western type and WWER), and is usable for other reactors (Fusion reactor, RBMK reactors, BWRs, research reactors).

CATHARE has a modular structure. Several modules can be assembled to represent the primary and secondary circuits of any Reactor and of any separate-effect test or integral effect test facility. The modules are:

- the 1-D module to describe pipe flow,
- the volume module
- the 3-D module to describe multidimensional effects in the vessel
- wall heat transfer,
- boundary conditions

To complete the modelling of the circuits, sub-modules can be connected to the main modules.

All modules use the 2-fluid model to describe steam-water flow and four non condensable gases may be transported. Both thermal and mechanical non-equilibrium of the two phases are described. The range of parameters is rather large: pressure from 0.1 to 25 MPa, gas temperature from 20°C to 2000°C, fluid velocities up to supersonic conditions, duct hydraulic diameters from 0.01 to 0.75 m.

Mass, momentum, and energy equations are established for any CATHARE module. They are written for each phase. They are derived from exact local instantaneous equations, using some simplification through physical assumptions and using time and space averaging procedures. One up to four transport equations can be added when non condensable gases are present.

The numerical method in the CATHARE code uses a first order finite volume - finite difference scheme with a staggered mesh and the donor cell principle. The time discretization varies from the fully implicit discretization used in the 0-D and 1-D modules to the semi-implicit scheme used in the 3-D module. These methods are known for their robustness in a wide range of flow configurations. Mass and energy equations use a conservative form and are discretized in order to keep a very good mass and energy conservation. The wall conduction is implicitly coupled to hydraulic calculations.

### C.1.2 Description of the input deck

The CATHARE input deck used to describe the Zion reactor is composed of 50 components: 22 pipe modules, 17 volume modules, one 3-D module and 9 boundary condition modules.

Details on the components of the input deck for the primary and secondary side are given in the following table:

	Primary	Secondary	Total
Number of Pipes	14	8	22
Number of Volumes	9	8	17
Number of Boundary Conditions (BC)	1	8	9
Number of double ended breaks	1	0	1
Number of 3D modules	1	0	1
Total number of hydraulic modules	26	24	50
Number of Tee Sub-Modules	1	4	5
Number of 3D ports	8	0	8
Number of volume ports	18	20	38
Number of pipe meshes	593	360	954
Number of 3D meshes	480	0	480
Total accounted scalar meshes	1112	404	1516

Table C.1: Nodalization details.

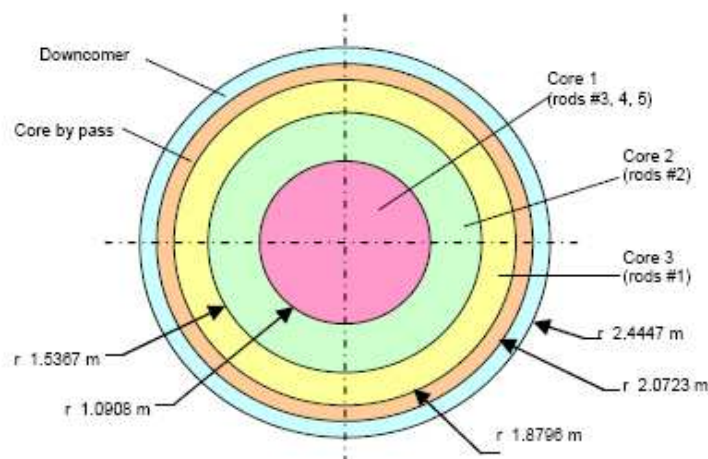


Figure C.1: Radial meshing of reactor pressure vessel with respect to the ZION vessel schematic.

- Total number of meshes for fuel: 2200
- Total number of meshes for passive heat structures: 2892
- Total number of meshes for structures: 5092

The RPV is represented by a 3-D module (VESSEL). The meshing uses a cylindrical coordinate representation divided into: 5 rings (r), 4 angular sectors and 24 meshes in elevation (z) then there are 480 3D meshes. The geometry represents the annular downcomer (external ring) connected to the cold leg nozzles, the lower plenum, the active core (3 internal rings, elevation 6 to 15), the core by pass (ring 4) and the upper-plenum connected to the 4 hot leg nozzles (at elevation 18) (cf. figure 1 below). So there are 12 channels for the core, 4 channels for the by-pass and 4 channels for the downcomer.

Several kinds of fuel rods are represented inside the core.

The first kind composes the peripheral channel (13056 rods) which is represented by the third ring of the core. The second kind composes the average channel (13056 rods) which is represented by



the second ring of the core. The first ring of the core is composed of the three other kinds of rods: the hot channel (13056 rods), the hot fuel assembly (203 rods) and the hot rod (1 rod). In the input deck, in order to have a perfect symmetry between the four sectors of the meshing, we put 1 hot rod, 51 rods from the hot fuel assembly and 3263 rods from the hot channel in each sector of the first ring. So we have in fact 4 hot rods, 204 rods of the hot fuel assembly and 13052 rods of the hot channel, which is a bit different from the specifications but this has a very little impact on the total power.

Models used:

- Fuel model: applied for the 5 types of rods in the active part of the core with power distribution between fuel and moderator.
- Reflood model: bottom-up reflooding applied in the 12 channels of the core, top-down reflooding is not applied.
- CCFL model: applied at the top of the core.
- Double ended break model: sonic blocking conditions are calculated on both side of the break.
- Fouling factor applied on the SG U-tubes to reach the specified hot leg temperature.
- Upper head temperature imposed at the specified value (576 K) during the steady state.

### C.1.3 Comments on the CATHARE calculations for the phase IV of BEMUSE

#### Comments on the comparison of the 13 participations.

The overall behaviour of all the computations is rather similar as long as the pressure and the mass inventory is regarded. Concerning the core thermal behaviour, the spread of results for the first peak (before reflooding) and for the second (or third) one (during reflood) is not so high (roughly 200 K for each peak). The major differences between the computations come with the reflooding behaviour and mainly its duration.

The comparison made on figure 5.19 (hot rod cladding temperature at the mid-core elevations, from 1.6 to 1.8 m) shows a rewetting of the mid-core obtained at time ranging within 90 and 220 s. This difference between minimum and maximum values (obtained in the 3 CATHARE computations) seems to be rather high. Concerning the CATHARE computations, this behaviour is rather similar to what is observed in the other large break studies.

Concerning the comparison made on figure 5.20 (hot rod cladding temperature at the top core), an even more pronounced difference between different computations on the quenching occurrence can be observed. But, concerning CATHARE, this late quenching of the top core is less significant than this observed in the core middle, due to some troubles using the top-down reflooding model (model not used or not really efficient).

In order to explain these differences, each code should justify its behaviour during the reflooding phase.

Here after is the "justification" of the CATHARE behaviour during reflood.

CATHARE has a consistent validation against its "reflood" test matrix (cf. next paragraph). This latter is composed of both separate effect test experiments and integral tests facilities. The validation results are rather satisfactory and in particular do not show any systematic trend (for instance

computed reflood longer than the experimental one). In addition the behaviour of the CATHARE contributions to BEMUSE phase IV are very similar to usual studies on the large break LOCA performed on real plant configurations (both 3 loop and 4 loop configurations). The actual question is whether or not the reflood duration in unsteady inlet flowrate conditions is realistic or not. For this aspect no experiment can directly answer to this question due to the lack of representative integral test experiments. For the large break system effect, only LOFT experiment has initial conditions representative of a large break LOCA, but unfortunately, due to its half core length, this experiment gives a very short reflooding phase. So, there is no experiment giving the real plant reflood behaviour.

In addition, all the CATHARE contributions show similar trends even with a rather different input deck (0D/1D and 3D RPV description). Among the 3 participations, a lot of sensitivity studies have been performed (official ones S01 to S10, but also a lot of others) and none of these sensitivities shows a drastic reduction in the reflood duration.

### **CATHARE validation against Reflooding experiments.**

The CATHARE validation test matrix dealing with large break LOCA and Reflood includes both separate effect experiments and integral test facilities.

#### **On Separate effect tests (SET)**

The SET for Reflood validation is based on the following experiments:

- PERICLES (1D 368 rod bundle and 2D 3x7x17 rod bundle)
- ROSCO (4x4 bundle with 2 kinds of rods + constant and oscillating flowrate)
- ERSEC (tube geometry and 36 rod bundle)
- REWET II (19 rod bundle and including top down reflooding)

The overall trends are the following:

Good prediction of the rod temperature, at least in the 2/3 of the core height. For constant flowrate inlet conditions, the reflooding durations lie between 250 to 400 s both in the experiments and in the computations (see an example on figure 3). For the oscillating flowrate conditions (some ROSCO tests), the oscillations are so strong that the total quenching time are rather short ( 50 s).

#### **On Integral test facility (IET)**

The integral test validation is based on

LOFT L2-5, LOFT LP02-6 LB-LOCA experiments BETHSY 6.7c (LB-LOCA: end of refill phase + reflooding phase)

The overall behaviour of CATHARE computations against LOFT experiments is rather good. The full quenching of the core is obtained rather early in the computations as in the experiments:

- For test L2-5: experiment: 65 s, CATHARE: 60 s
- For test LP02-6: experiment: 60 s, CATHARE: 65 s

For the BETHSY test, the overall behaviour of the computation is rather good although oscillations seem to be greater in the computation than in the experiment. The computed quench time is 270 s for 220 s in the experiment C.3.

Fig. 15: test RE0064

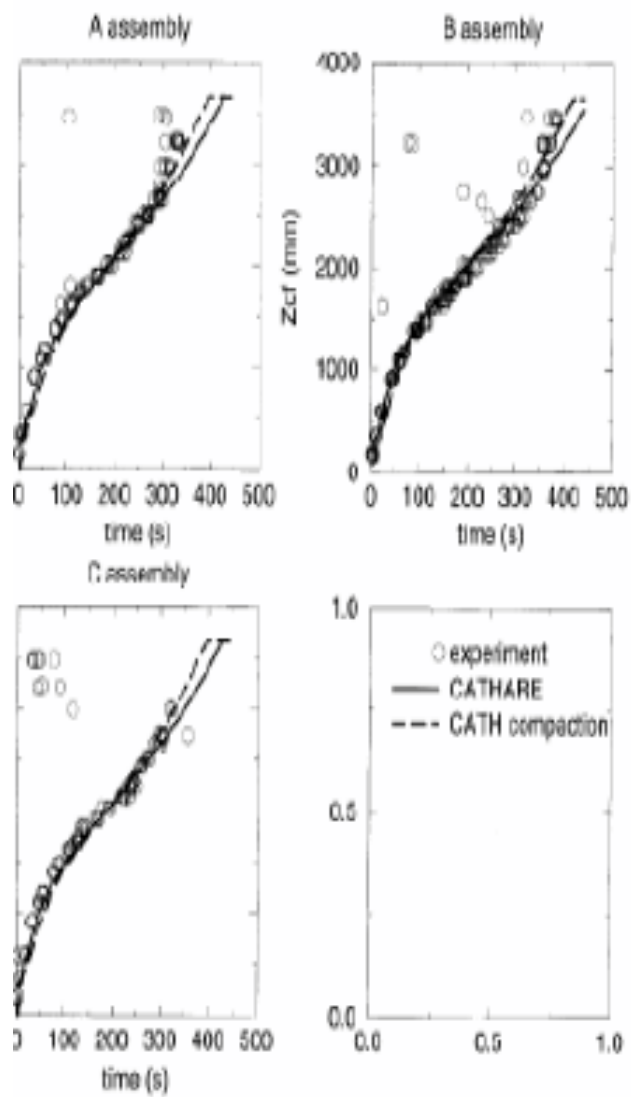


Figure C.2: PERICLES 2-D bundle test RE0064 quench fronts.

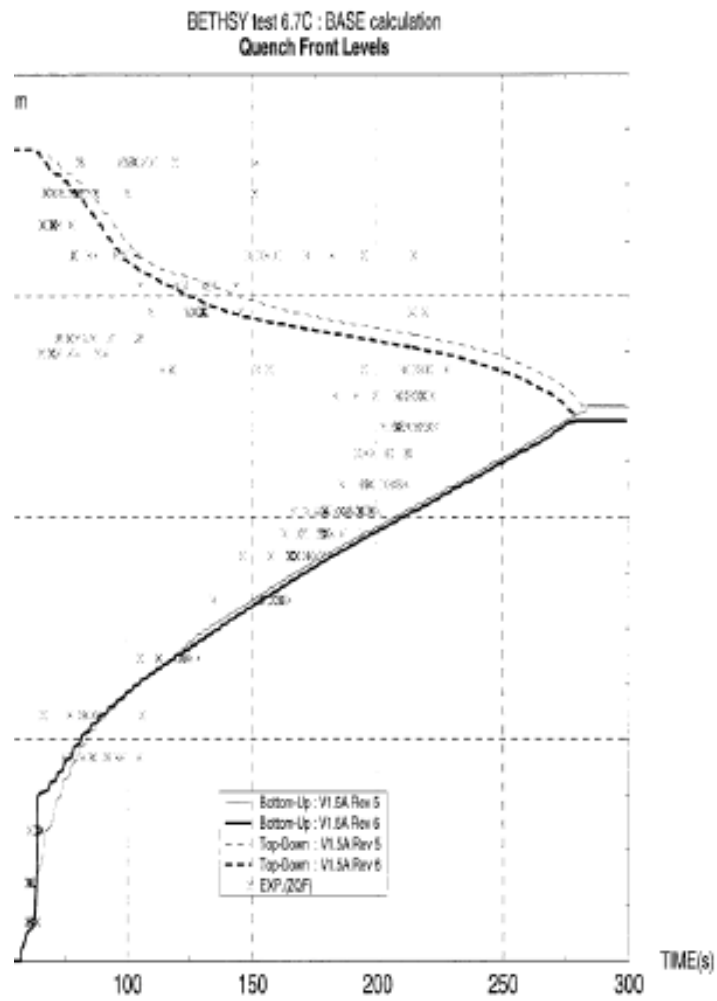


Figure C.3: BETHSY 6.7c quench time.

## C.2 EDO GUIDROPRESS, Russia

### C.2.1 Description of the code: TECH-M-97

#### Applied computer code

Calculations of LBLOCA were performed using the TRAP-97 code package, whose constituent part is the computer code TECH-M-97 /1-4/. The TECH-M-97 computer code is used during safety assessment of WWER power plants for analysis of changes of coolant parameters in the primary circuit and temperature conditions in the core during accidents caused by loss of integrity of the primary circuit including guillotine break of the main coolant pipeline. The program verified on a plenty of domestic and foreign experiments, including international standard problems IAEA and Nuclear Energy Agency of Organization for Economic Co-operation and Development (OECD/NEA) /4-7/. The code TECH-M-97 is certificated Gosatomnadzor of Russia in 1999. The discontinuity, energy and momentum equations written down in one-dimensional approximation and the equation of state are used for calculation of coolant parameters. One-dimensional equation of thermal conductivity is used for determination of temperature field in the fuel rod and metalworks. Neutron kinetics equation written down in point approximation with account for six groups of delayed neutrons is used in calculation of reactor power. The computer code makes provision for possible application of different procedures and correlations intended to determine the heat exchange conditions, pressure loss coefficients, modeling of coolant phase-separation processes in the reactor chambers and critical discharge of water, steam and steam-water mixture. Structure of the TECH-M-97 computer code represents a set of the interconnected modules and computer codes 4, 7.

#### Fuel rod model

As it was mentioned in 7, for determination of temperature field in the fuel rod in the computer code TECH-M-97 is used program TVEL. Unsteady-state temperature field in a fuel rod is determined by solving one-dimensional thermal conductivity equation by difference method with a known variation of thermal-and-physical parameters of coolant, coolant flow rate and heat rate in the fuel. The procedure involves calculation of a factor of thermal conductivity between fuel core and cladding and calculation of heat generated during reaction between the cladding material and coolant. Possibility of deformation of fuel rod cladding under the action of difference between pressure of gaseous medium inside the fuel rod and external pressure is taken into account.

Time histories of the total heat rate in the fuel rod and axial power distribution are considered to be known for the whole unsteady conditions under consideration. Power distribution over the fuel core cross-section is supposed to be uniform. The thermal-and-physical parameters of the coolant (pressure, enthalpy, temperature) and coolant flow rate at each moment are supposed to be known. At the initial moment of the considered unsteady conditions the temperature field in fuel rod is a stable one. The central hole surface, fuel core external surface, cladding internal and external surfaces are supposed to be presented in any fuel rod cross-section as the concentric circumferences (Figure C.4). The temperature values in the equidistant points from the center of these circumferences are equal.

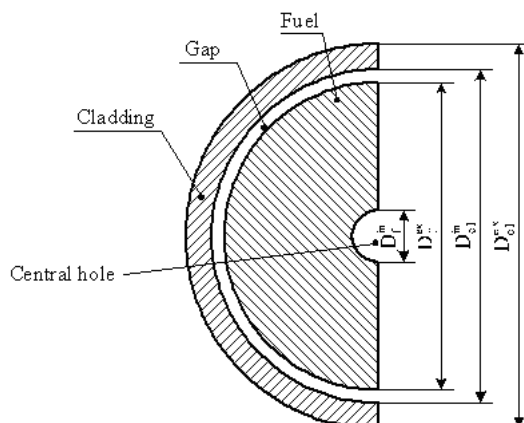


Figure C.4: Nodalization of fuel rod.

Dimensions of the fuel rod and its cladding (the central hole diameter, pellet external diameter, the internal and external diameters fuel rod cladding), gap pressure are used in the input file. All indicated parameters correspond to a "cold" condition (20 °C). In the future the program automatically defines the geometrical sizes of pellet and its cladding and gap pressure taking into account their thermal expansion. It is supposed that the gaseous medium inside the fuel rod follows the equation of state for ideal gas. In calculating its pressure the gaseous medium filling the central hole, the gap between the fuel core and cladding, and gas plenum is taken into account.

The cladding can be deformed under the action of pressure of the gaseous medium inside the fuel rod. It is supposed that during deformation of the cladding its instantaneous flaking off from the fuel core occurs on the section whereof length is known beforehand. After the moment of deformation the pressure of the gaseous medium inside the fuel rod is considered to be equal to the external pressure. In case the temperature of the fuel rod cladding surface exceeds 700 °C, the reaction between the material of the fuel rod cladding (zirconium alloy or zirconium-base alloy) and coolant (steam) takes place on this surface.

Fuel, cladding and gaseous medium inside the fuel rod properties are considered to be the known functions of the temperature. To determine the temperature field, the fuel rod is conventionally broken down into several sections in axial and radial directions. The thermal-and-physical parameters of the coolant and heat rate and, consequently, the radial temperature distribution are assumed to be the same in all cross-sections within one axial section except for the deformed cladding section, which is considered separately.

Variation of the gap thickness and a heat conductance during the LB LOCA is presented in Figures 2 and 3. It is seen in Figure 2, the gap thickness in the steady-state condition ( $t = 0$  s) is essentially smaller than in the "cold" condition (0,055 mm for the average channel and 0,04 mm for the hot rod in hot FA). The gap thickness tends to the value, which corresponds to the "cold" condition (0,09 mm) after scram and the fuel and cladding temperatures decreasing.

Variation of the fuel and cladding temperatures, gap thickness, pressure and temperature of the gaseous medium results in its heat conductance during the accident (Figure 3). The dependence of heat conductance from linear heat generation rate for the different channels in the steady-state condition is presented in figure C.5.

## Nodalization of reactor plant

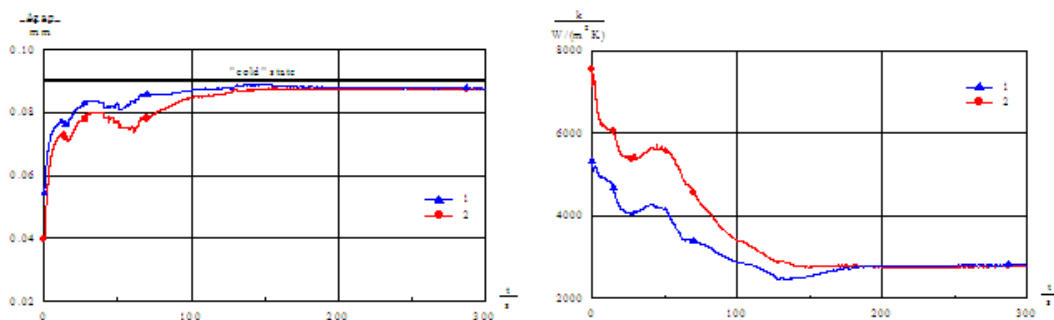


Figure C.5: 2.(Left) Gap thickness for the average channel (1) and hot rod in the hot FA (2) at level 1,647 m. 3. (Right) Gap heat conductance for the average channel (1) and hot rod in the hot FA (2) at level 1,647 m

Nodalization of reactor plant using the TECH-M-97 code is shown in Figure C.8 and Table 1 summarized the nodalization code resources used. Nodalization includes the following main components:

- reactor;
- circulation loops;
- pressurizer;
- emergency core cooling system.

Three components are singled out to describe the reactor such as the reactor core, pressure chamber and collection chamber. The pressure and collection chambers are presented by 7 and 4 control volumes respectively. The core is simulated with a system of parallel channels (six parallel channels) (Figure C.7.1) combining the fuel rods with close power level and differing in power: five channels are the heated ones and one channel is non-heated one to simulate core bypass flow. The core channels along the height are divided into 12 sections, 10 of which simulate the fuel part, and two others simulate the core inlet and outlet. Power of the heated channels is determined as a product of power of the medium-powered channel by the factor considering the core radial power peaking. The code makes the automatic comparison of the sum of power of the heated channels and the total core thermal power that is also assigned in the code. In case of disagreement of these powers the code makes a uniform distribution of this difference among all channels

In determining the core radial power peaking factors the used data are the ones presented in Tables 13, 14 and Figure 9 of Ref. 8. Table 2 gives the relative power peaking factors for the heated channels. Axial power distribution in the core is assumed similar for all channels and is given in Table 3. Core axial linear heat flux variation obtained during simulation using TECH-M-97 code is given in Figure C.7.2 Table 4 contains the maximum linear powers considered in the axial discretization of the linear power profiles for the six temperature zones.

Each of the circulation loops consists of the hot leg, steam generator, cold leg and RCP. Each intact loop is divided into 16 calculated volumes, whereas the damaged loop is divided into 20 calculated volumes. The steam generator is described by seven calculated volumes. Five of them are the SG tubing, two others are the SG input and output collectors. Pressurizer and connecting pipeline are represented by one and two volumes, respectively. Coolant discharge is simulated on the cold leg of

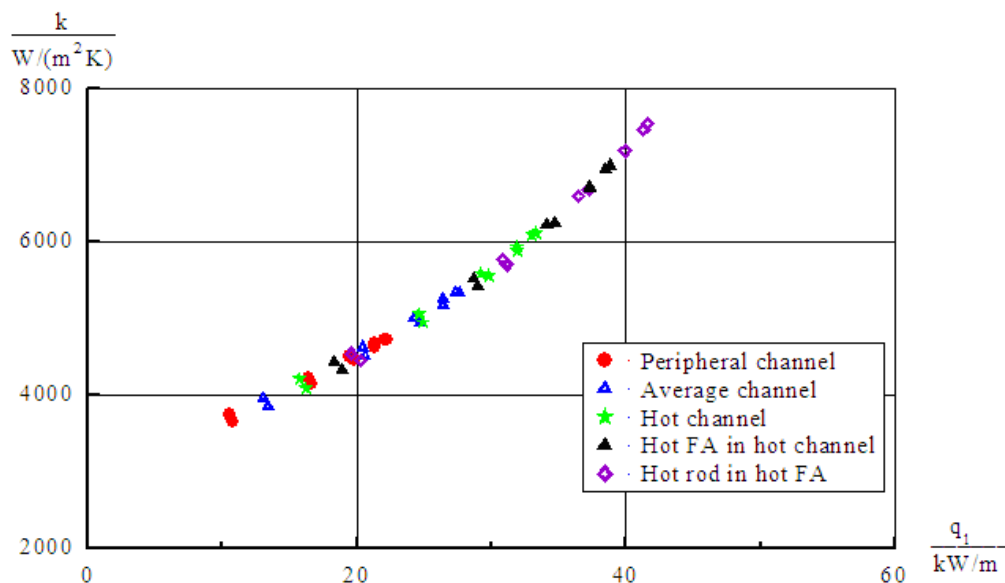


Figure C.6: The heat conductance for the different channels in the steady-state condition.

TOTAL NUMBER OF HYDRAULIC NODES	87
TOTAL NUMBER OF MESH POINTS (Heat Structures)	811
NUMBER OF CORE CHANNELS (without bypass)	5
NUMBER OF AXIAL CORE NODES PER CHANNEL	12

Table C.2: Nodalization Code Resources.

Channel	Number fuel rod in the channel	Power peaking factor
Peripheral channel	13056	0,80
Average channel	13056	1,0
Hot channel	13056	1,20
Hot FA in hot channel	203	1,40
Hot rod in hot FA	1	1,50

Table C.3: Relative Power Peaking Factors for the Heated Channels.

calculated loop 4 out of volumes 67 and 68. The emergency core cooling system (low-pressure pumps, accumulator) is connected to elements 2, 18, 34.



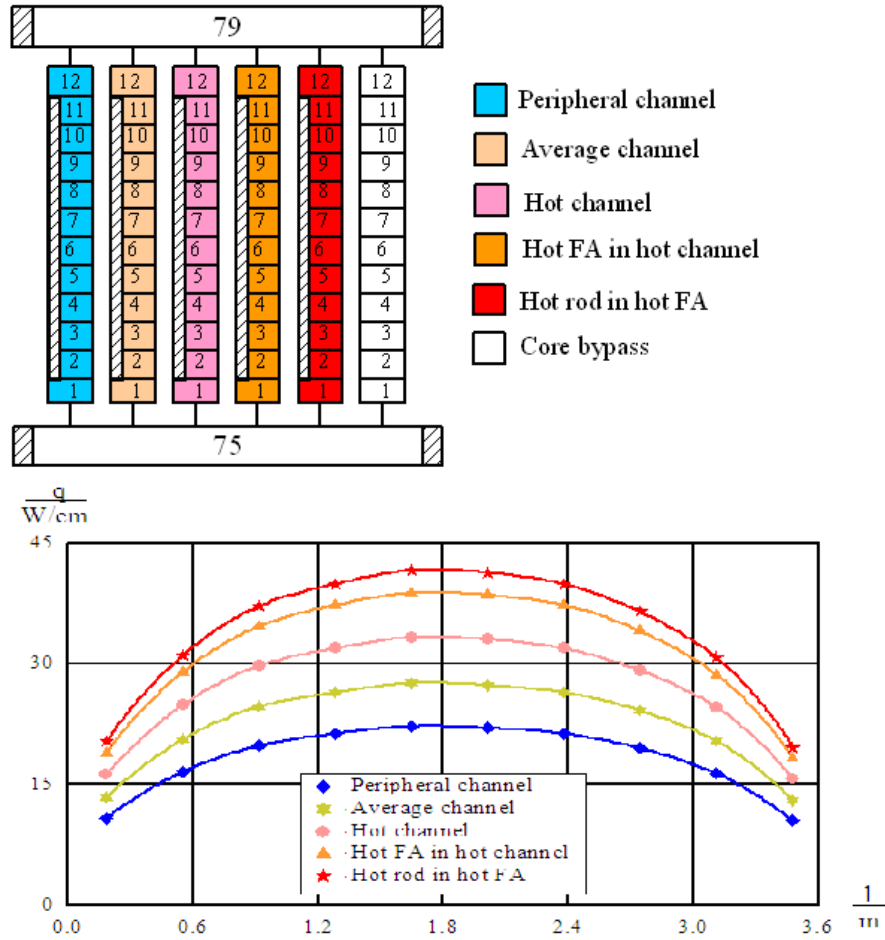


Figure C.7: 1.Core nodalization. 2.Core axial linear heat flux variation

Parameter	Value									
Hcore, %	5	15	25	35	45	55	65	75	85	95
Power, rel.units	0,6	0,92	1,1	1,18	1,23	1,22	1,18	1,08	0,91	0,58

Table C.4: Axial relative power distribution in the core.

	Hot rod in hot FA (Zone 5)			Average rod in average channel (Zone 2)		
	Bottom Level (below 1,22 m)	2/3 Core Height (between 1,22 - 2,44 m)	Top Level (above 2,44 m)	Bottom Level (below 1,22 m)	2/3 Core Height (between 1,22 - 2,44 m)	Top Level (above 2,44 m)
Maximum Linear Power (KW/m)	37,2	41,6	36,5	24,7	27,6	24,2
Elevation (m)	0,915	1,647	1,745	0,915	1,647	1,745

Table C.5: - Maximum Linear Power.

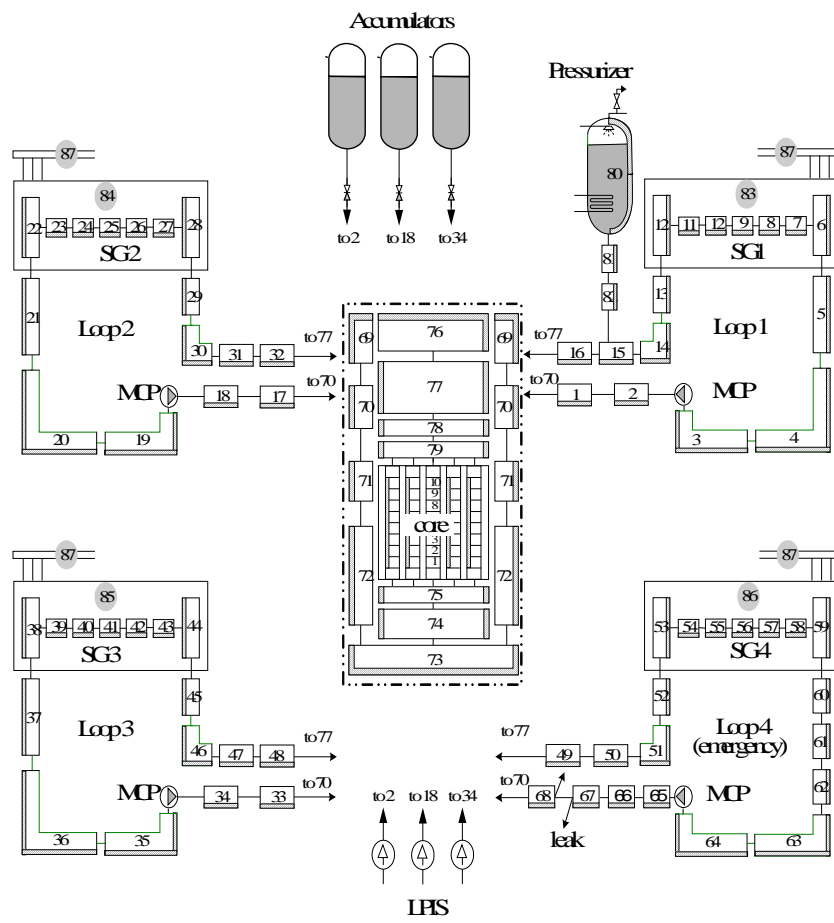


Figure C.8: Nodalization of reactor plant using the TECH-M-97code.

### C.2.2 References

1. A. D. Efanov, V. V. Lozhkin, V. V. Sergeev, O. A. Sudnitsyn, S. I. Zaitsev, "Analysis of Reflooding Tests and Verification of Computer Codes", Proceedings of International Conference "Thermophysics'98" on "Thermophysical Aspects of WWER-Type Reactor Safety", Obninsk, Russia, 26-29 May, 1998.
2. V. P. Spaskov, Yu. G. Dragunov et al., "Calculation Assessment of Reactor and WWER Reactor Plant Thermal-Hydraulic Characteristics", Moscow, Akademkniga, 2004. (in Russian)
3. IAEA-EBP-WWER-01, "Guidelines for Accident Analysis of WWER Nuclear Power Plants", IAEA, Vienna, 1995.
4. Dragunov Yu. G., Fil N. S., Borisov S. L., Borisov L. N., Zajtsev S.I "Validation of the Program TECH-M-97 by the Results of the Experiment with LB LOCA on the Large-Scale Facility with Nuclear Heating", Nuclear Energy, 2005, vol. 99, pub. 6, p. 444-453. (in Russian)
5. IAEA-TECDOC-477, "Simulation of a loss of coolant accident with hydroaccumulator injection", IAEA, Vienna, 1988.
6. ISP33 OECD/NEA/CSNI International Standard Problem No.33, "PACTEL Natural Circulation Stepwise Coolant Inventory Reduction Experiment" Comparison Report. V.I. VTT, Nuclear Energy, December 1994.
7. BEMUSE Phase II Report. Re-analysis of the ISP-13 Exercise, Post Test Analysis of the LOFT L2-5Test Calculation. NEA/CSNI/R(2006)2, 2006
8. M. Pérez, F. Reventós, Ll. Batet, "Phase 4 of BEMUSE Programme: Simulation of a LB-LOCA in ZION Nuclear Power Plant. Input and Output Specifications" rev. 3, Universitat Politècnica de Catalunya, Spain, 2007

## C.3 GRS, Germany

### C.3.1 Description of the code: ATHLET

ATHLET is a one dimensional two fluid code.

#### **Balance equations.**

The physical model of the code is based on the system of five or six integral balance equations. The system of five governing equations consists of:

- separate balance equations of liquid and vapour mass,
- separated balance equation of liquid and gas phase energy, and
- mixture momentum balance equation.

In the system of six governing equations separate momentum equations for gas and liquid phase are applied.

Application of finite volume method for spatial discretization allows a rather coarse nodalization of modelled objects.

The system of governing equations is closed by state equations, interfacial transfer conditions and constitutive equations.

Non-condensable gas as well as boron dilution can be simulated by ATHLET.

#### **Constitutive equations**

The constitutive equations comprise correlations dealing with:

- phase relative velocity,
- wall shear,
- interfacial heat and mass transfer,
- wall heat transfer,
- rewetting velocity/quenching.

In the five equations version the relative velocity is determined using drift flux models. In ATHLET, the full-range flooding based drift flux model applicable for co-current and counter-current flow is used. The code version with separate momentum balance equations uses a flow pattern dependent interfacial friction model, which is partially based on drift flux correlations. The mass transfer rate is computed by a model based on correlations for heat transfer controlled growth or shrinkage of vapour bubbles and liquid droplets. The wall shear is calculated using a two-phase flow multiplier. Martinelli-Nelson and Chisholm models are optionally available.

Heat conduction in fuel rods, walls and other structures can be simulated using a heat transfer model based on the Fourier equation.

Circulating pumps are modelled by means of pump characteristics and calculation of rotor rotation speed.

### Numerical methods

The numerical time integration method in ATHLET is a fully implicit method with time step management and convergence control of time step integration. The numerical method enables time discretization control. A special stationary state option is available, where steady-state iterations are performed to obtain accurate initial conditions for transient calculations.

### C.3.2 Description of the input deck

#### Modelling of the Zion reactor

##### Spatial discretization

The complete primary circuit has been modelled. From the secondary circuit steam generator and main steam line are modelled. The remaining part of the circuit is simulated by proper boundary conditions:

- mass flow and inlet enthalpy ( $G, h$ ) for feed-water flow,
- outside pressure and outlet enthalpy ( $p, h$ ) for steam flow into turbine.

At the primary circuit all four loops are modelled. The reactor downcomer is divided into 4 channels, each one joined to a cold leg of one loop.

The reactor core is divided into 2 channels and core bypass. The outer channel consists of peripheral channel and average channel, in nomenclature of BEMUSE 4 specification. The inner channel is equivalent with hot channel including hot fuel assembly and hot rod. For downcomer channels as well as for core channels cross flows are simulated. The remaining parts of the vessel are modelled as single channels:

- one upper plenum,
- one lower plenum,
- one upper head.

The statistic of the applied nodalization is summarized in the following table.

<u>Thermo-fluid objects</u>	
Loops	4
Channels in reactor core	2
Volumes/branches	26
Axial volumes/pipes	94
Control volumes/total	392
Junctions	486
<u>Heat conduction objects</u>	
Heat objects	88
Heat slabs/volumes	523

The heat slabs are divided into radial layers. The usual number of layers in a heat slab is 3. In the fuel element there are 3 layers in the fuel pellet, 1 layer for the gap and 2 layers in the clad. The fuel rods are divided into 18 axial volumes equivalent to thermo-fluid channel nodalization.

Parameters of the rods used by core modelling are described in the following table:

Outer channel	13056 rods of 64250 W (zone 1)
	13056 rods of 80320 W (zone 2)
Inner channel	13056 rods of 96380 W (zone3)
	203 rods of 112440 W (zone 4)
	1 hot rod of 120470 W (zone 5)

The maximum linear power in zones 2 and 5 is:

	Zone 2	Zone 5
Lower part of the rod (nodes 1–6)	25.11 kW/m	37.67 kW/m
Middle part of the rod (nodes 7–12)	26.92 kW/m	40.38 kW/m
Upper part of the rod (nodes 13–18)	24.73 kW/m	37.09 kW/m

The nodalization scheme of the reactor and one of the primary loops is shown in the figure ref:GRS1. The nodalization scheme of the simulated part of a secondary loop is presented in figure ref:GRS2.

### Physical models

For the simulation of 2F Large Break LOCA at the Zion reactor the six balance equation model has been applied. The critical discharge (CRD) is simulated using CRD tables obtained by determination of the critical discharge rates for various conditions. The critical discharge rates are calculated with a steady state model based on four balance equations.

For determination of two-phase pressure losses Martineli–Nelson multiplier is used.

The counter-current flow limitation (CCFL) is in ATHLET implemented in the interfacial friction model and therefore always considered.

The fuel gap is simulated as a heat slab with heat conduction and heat capacity taken from the BEMUSE 4 specification.

For simulation of the core rewetting a special quench model is applied.

### Nodalization sketch

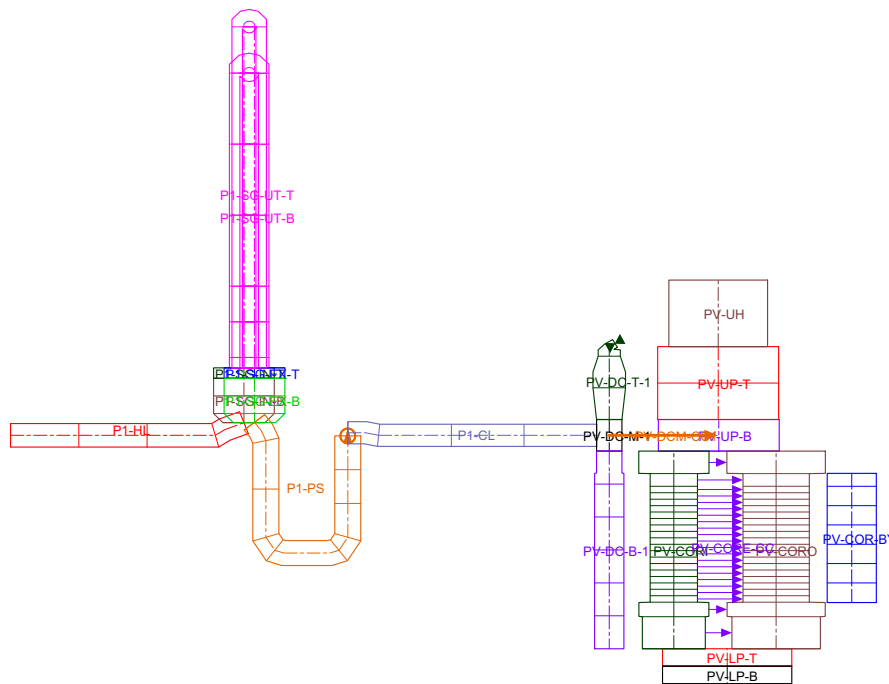


Figure C.9: Loop 1 of primary system and reactor vessel

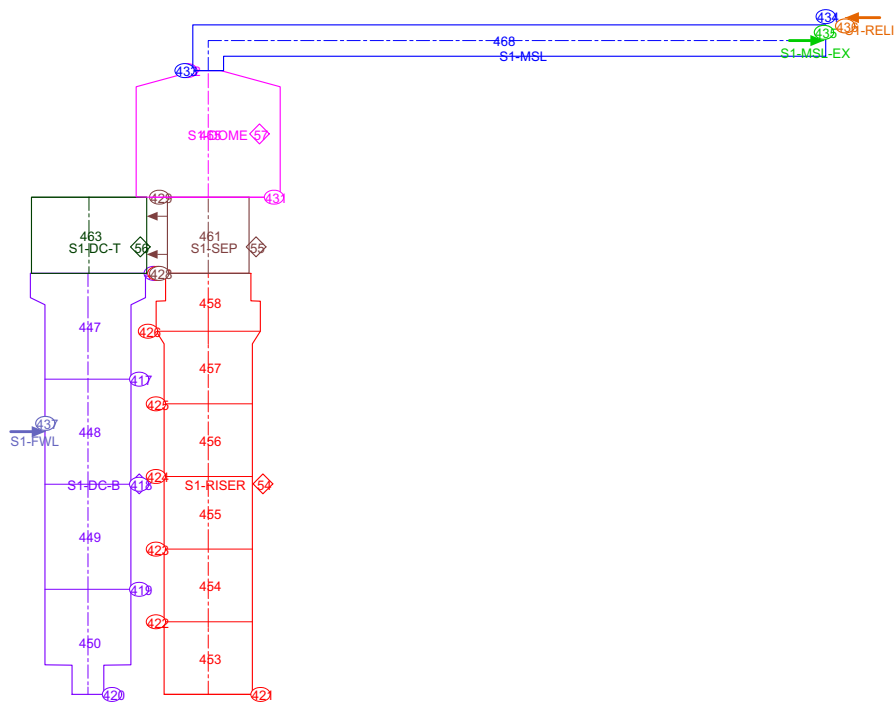


Figure C.10: Nodalization schema of secondary side of the cooling loop

## C.4 IRSN, France

### C.4.1 Description of the code: CATHARE2.5

The CATHARE2 V2.5.1 mod6.1 code is the outcome of more than 20 years of joint development effort by CEA, IRSN, EDF and AREVA NP. CATHARE is a system code devoted to nuclear reactor safety analysis. Two-phase flows are described using two-fluid six-equation model and the presence of non-condensable gases can be taken into account by one to four additive transport equations. The code allows a three-dimensional modeling of the pressure vessel. It comes with a complete physical assessment.

#### Range of application

CATHARE includes several independent modules that take into account any two-phase flow behavior:

- Mechanical non-equilibrium,
- Vertical: co-or counter current flow, flooding counter current flow limitation (CCFL), etc...
- Horizontal: stratified flow, critical or not critical flow co- or counter current flow, etc...
- Thermal non-equilibrium: critical flow, cold water injection, super-heated steam, reflooding, etc...
- All flow regime and all heat transfer regimes.

Various modules offer space discretization adapted to volumes (0D), pipes (1D) or vessels (3D) ready to assemble for any reactor design. CATHARE is limited to transients during which no severe damage occurs to fuel rods; more precisely, fuel ballooning and clad rupture are supposed to have no major effect on fluid flow in the primary circuit.

Time discretization is fully implicit (semi-implicit for 3D) and allows to achieve solution stability over a broad range of time step values. Maximum time step is of user's responsibility according to the problem being solved.

#### Main characteristics

The code is based on a 2-fluid 6-equation model including 4 non-condensable gas equations and additional equations for radio-chemical components transport:

- energy balance equations,
- momentum balance equations,
- 2 mass balance equations,
- 0, 1, 2, 3 or 4 mass balance equations for 0, 1, 2, 3 or 4 non-condensable gases.

The 6 principal variables are pressure (P), liquid enthalpy (Hl), gas enthalpy (Hg), void fraction (a), liquid velocity (vl) and gas velocity (vg). And, if it exists, xi (i=1, 4) the non condensable mass



fraction (with related transport equations).

Remark: The system has always 6 equations: even in single-phase case, a residual phase treatment is used:

- $a_{min}= 10^{-5}$ ,  $a_{max}= 1-10^{-5}$  ;
- $a= a_{min}$  ,  $T_g=T_{sat}$ ,  $V_g=V_l$  for single phase liquid ;
- $a= a_{max}$  ,  $T_l=T_{sat}$ ,  $V_l=V_g$  for single phase gas ;

Other calculations are also available:

- Radio chemical elements transport;
- Mass and energy balances per zone;
- Radial heat conduction (for multi-layer wall and fuel structures);
- 2D conduction for rewetting (for multi-layer wall and fuel structures);
- Fuel thermo-mechanics (clad deformation, clad rupture, clad oxidation);
- Point kinetics model.

Successive sets of closure laws or " Revisions " have been developed in an iterative methodology of improvement. The revision 6.1 of the closure laws is implemented in the version 2.5.

### Numerical features

The discretization is of the first order in space and time.

Spatially CATHARE uses:

- Finite Volumes (mass, energy) and finite differences (momentum) discretizations,
- Structured and staggered meshing,
- First order upwind scheme for convective terms (donor cell principle).

Timely CATHARE uses:

- Fully implicit (0 and 1D) and semi-implicit (3D) discretizations,
- Implicit wall conduction (+ implicit coupling with hydraulic).

The resulting non-linear system is solved by a Newton-Raphson iterative method.

### Modelling features

Any kind of hydraulic circuit is represented by elements, which are connected through junctions. These elements are modeled with CATHARE modules, such as:

- 0-D volume module,
- 1-D pipe basic module,
- 3-D module,
- Boundary condition module,
- Double-ended break module.

It is possible to calculate heat exchange between one primary and several secondary circuits through heat exchangers. Other types of objects are available to represent:

- Specific models related to the other calculations made by CATHARE: these are the main sub-modules (reflood, multi-layer wall, point kinetics model)
- Punctual modifications of the standard thermal hydraulic equations : these are the gadgets sub-modules which are used to represent valves, injections, break, pump
- Others sub-modules refer to specific aspects of particular PWR transients (modeling steam generator feed water overflow, mixing effects in the vessel bottom).

### **Validation process**

The set of physical laws is subjected to an extensive assessment on two different kinds of tests:

- "Separate effect tests" which involve analytical configurations and a specific physical phenomenon, or which represent one reactor component. More than 1000 separate effect tests from 45 test facilities are used.
- "Integral effect test" performed on system facilities modeling whole reactor type circuits, intended to validate the capacity of the code to predict complex and inter-dependent thermal-hydraulic effects. About 20 effect tests from 8 system facilities are used.

Thus, the assessment strategy of the CATHARE code is divided into a qualification program and a verification program.

The qualification program aims at covering the whole range of flow patterns, physical processes and reactor components specific features. A list of experiments used for the qualification of the constitutive laws exists. Each experiment is related to a principal phenomenon and some of them are also related to a reactor component. The constitutive laws that are validated by these experiments are classified into three groups:

- Mechanical transfers,
- Interfacial heat and mass transfers,
- Wall heat transfers.

Some experiments are devoted to critical flows in nozzles of different sizes and shapes. They provide information on interfacial heat transfers in flashing flows, two phase wall friction and interfacial

friction in dispersed flows. All these processes control the break discharge flow rate.

Many experiments studied flow regimes and mechanical laws, particularly the interfacial friction. The duct geometries are:

- Horizontal or vertical tubes,
- Rod bundles (core geometry) or tube bundles (steam generators),
- Annuli (downcomer geometry),
- Geometry of the hot legs,
- Geometry of the U shaped intermediate leg.

Some experiments have been necessary to cover the whole spectrum of phenomena occurring during the reflooding of a core. The reflooding consists in rewetting a high temperature dry core by ECCS water:

- Wall heat fluxes were studied in tubes, rod bundle and tube bundle geometries,
- Direct contact condensation at ECCS injections were qualified with two test facilities at different scales,
- CCFL was studied for various geometries including scale 1 tests for the downcomer.

Experiments are also used to qualify:

- Phase separation phenomena at a T-junction,
- Lower plenum voiding,
- Entrainment and deentrainment in a upper plenum,
- Fuel behavior (clad ballooning, clad rupture, clad oxidation),
- Two-phase pump characteristics,
- Multi-dimensional effects in a core and in a downcomer.

All these separate effects tests are first used for the development or the improvement of the closure relationships. As the boundary conditions are well known this is the only way to determine the accuracy of each closure relationship. These qualification calculations are also used for:

- Giving the range of validity of closure relationship,
- Estimating the uncertainty on each closure relationship,
- Defining the best schematization of each component in relation to the physical situation,
- Defining the node size and time step required for the converged calculation.

The verification program aims at covering the whole range of accidental transients in pressurized water reactors. These are for example:

- Large Break Loss of Coolant Accidents (LBLOCA),
- Small Break Loss of Coolant Accidents (SBLOCA),
- Steam Generator Tube Ruptures (SGTR),
- Loss of Feed Water (LOFW),
- Steam Lines Breaks,
- Loss of Residual Heat Removal System.

All the existing system test facilities were used for the assessment of the successive CATHARE versions and revisions. These loops are the following: LOFT, LSTF, BETHSY, PKL, LOBI, SPES, PACTEL and PMK.

The CATHARE verification matrix is based on these facilities.

#### C.4.2 Description of the IRSN CATHARE Input Deck

The CATHARE input Deck is based on the RELPAP5 input deck given by the organizer of the BEMUSE phase 4. The CATHARE input deck is built with only 1D and OD components (AXIAL and VOLUME). The primary and secondary circuit as well as the choices of the modeling will be described precisely.

##### Primary Circuit

The primary circuit consists mainly of the reactor pressure vessel, four coolant loops each having a hot leg, a steam generator (a U-SG), a cold leg with primary coolant pump. The pressurizer is connected to the hot leg1. The nodalisation of the primary circuit is described in table C.6 and is illustrated thanks to GUTHARE (Graphical User Interface of caTHARE)

##### Reactor Pressure Vessel (RPV)

The reactor vessel is a cylindrical high-pressure vessel and is designed to contain the vessel internals and fuel assemblies of the core.

The modeling of the reactor vessel is realized with the help of CATHARE specific axial and volume elements as shown on figure.

##### Downcomer

The annular collector in the upper reactor vessel collecting water from the different cold legs of the four loops is represented by 2 volume elements: VOLDOWN1 and VOLDOWN2. The water collected into annular collector passes into the downcomer which is represented by 2 axial elements: DOWNCO1 and DOWNCO2. We use two downcomers in order to be not too conservative in the bypass phase of the ECCS. There is no crossflow between the two axial downcomers.

Elements	Quantities
Number of pipes	21
Number of volumes	15
Number of Boundary Conditions	1
Number of Double Ended Breaks	1
Number of 3D Modules	0
Number of Tee Sub-Modules	1
Number of 3D ports	0
Number of Volume ports	46
Number of Pipe Meshes	968
Number of 3D Meshes	0
Total Number of Hydraulic Modules	38
Total Accounted Scalar Meshes	1047

Table C.6: Nodalisation Code Resources of the primary circuit

### Lower Plenum

The lower portion of Lower Plenum (LP) is represented by a volume element, LPINF, and the upper part of LP is represented by an axial, TUYINF, associated to volume element, VOLINF. With this modeling, we can represent in a better mean the thermal stratification during the reflood phase of the LB-LOCA than with only one VOLUME element.

### Core

The core region is modeled by as illustrated on figure C.12 and C.13:

- an average channel modeled by an axial element, C MOY,
- a hot channel modeled by an axial, C CHAUD,
- a bypass modeled by an axial element, BYPASSCO.

There is no crossflow between the average and hot channel. The water coming from LP then passes into the core region where it takes the heat from the different fuel assemblies and then further gets collected in the Upper Plenum (UP).

### Upper Plenum and Upper head

The Upper plenum is modeled using a volume element UP associated to an axial element UPA. The upper head of the reactor pressure vessel is modeled using a volume element: UH. The hot water in the UP then flows to each hot leg of the four different loops. This modeling is chosen because we do not have enough information to represent the guide tubes of ZION. To represent a slightly warm dome and so the recirculation between the upper plenum and the upper head, we use 2 CANDLE (CANDUP and CANDUH) elements to bring some energy from the UP element to the UH element.

### Fuel Assemblies

In the average channel MOY (see figure 3), 2 kinds of fuel are modeled as in the recommendation:

- the fuel of the average core: 64 Fuel assemblies / 13056 rods,
- the fuel of the peripheral core: 64 Fuel assemblies / 13056 rods.

In the hot channel CHAUD (see figure 3), 3 kinds of fuel are modeled as in the recommendation:

- the fuel of the hot core: 64 Fuel assemblies / 13056 rods,
- the fuel of the hot assembly: 1 Fuel assembly / 203 rods,
- the fuel of the hot rod: 1 rod.

As in the recommendation, we put the hot core in the hot channel and not in the average channel in order to avoid having an overheated water channel in the core.

CCFL OPTION: We do not activate the CCFL option at the upper tie plate in the CATHARE input deck because we do not have enough information to evaluate the CCFL correlation.

#### REFLOOD OPTION:

We define for each channel a top-down and a bottom-up reflood module. In the average we associate them to the average core which has the biggest inertia and in the hot channel the hot core which in our point of view lead the hydraulic of the channel. In each channel during the transient, the fuels which are not associated to a REFLOOD MODULE (in CATHARE) have the same quench front as the fuels which are associated to the REFLOOD MODULE.

### Axial Power Profile

In our input deck, the fuels are modeled by heating WALL elements and not by a FUEL elements in order to impose precisely the conductivity and the capacity of the fuel and gap as in the recommendations [ref XXX] and because we do not have enough information to model precisely the fuel. We do not use advanced models for the fuel elements.

Because of this choice of modeling, we cannot model the power released directly to the moderator and we decide to integrate the moderator power to the fuel power. Finally we have a core power of 3250MW which is the value expected for the primary circuit. With this modeling, we will slightly overestimate the cladding temperature of the fuels. The linear heat generation rate profiles and core heat structure description are presented in figure C.14 and table C.7.

### The Loops

The loop 1, 3 and 4 are intact and the loop 2 is the broken loop. The following descriptions are related to the intact loop 1 (with the pressurizer) and the broken loop 2. The modeling of the loop 1 is exactly the same as the other intact loop the only exception being the pressurizer.

The intact loops are modeled (see on figure C.15) by:

Core Zone	Rod average) linear power (W/m)	Power per rod	Maximum linear power (W/m)	Number of rods	Fuel Power (kW)	Total power (MW)
1	18006	65901	22113	13056	860409	860.41
2	22506	82373	27630	13056	1075457	1075.46
3	27009	98852	33159	13056	1290613	1 290.61
4	31511	115330	38687	203	23412	23.41
5	3761	123565	41456	1	124	0.12
Total	-	-	-	39372	3250015	3250

Table C.7: Core heat structures features

- AXIAL element (HL1): hot leg
- 2 VOLUME elements (SG1IN and SG1OUT): steam generator channel head, modeling proposed in the CATHARE user guidelines [Ref. 3, 4, 5] because high velocities are expected in two phase flow.
- AXIAL element multiplied by 3388:U tubes
- AXIAL element (CL1): cold leg
- PUMP element (PUMP1): pump
- ACCU element (ACCU1): hydro accumulator
- SOURCE element (LPIS1): lower pressure injection system
- AXIAL element (SLINE): surge line of the pressurizer
- VOLUME element (PRZ): pressurizer
- SAFVALV element: safety valve at the top of the pressurizer

### The broken loop 2

The hydro accumulator and the LPIS (Lower pressure injection system) are not modeled on this loop as specified in the recommendations. The Double-ended break called RUPGUI is modeled with the RUPTURE element which simulates a guillotine rupture. Before the opening of the break, the two pipes CL2 and CL2DOWN are connected. After the opening the break, the element is replaced by two boundary conditions in pressure (BC4 element) at the extremity of the 2 pipes.

### Secondary Circuit

We model only the steam generator vessel of the secondary side. As we do not have enough information to model very precisely this secondary side, we try to use the information of the RELAP input deck. The nodalisation of the secondary circuit is described in table C.8.

The 4 steam generators modeling on the secondary side are the same. The Steam generator 1 as the others is modeled (see on figure C.17) by:

Elements	Quantities
Number of pipes	8
Number of volumes	8
Number of Boundary Conditions	8
Number of Double Ended Breaks	0
Number of 3D Modules	0
Number of Tee Sub-Modules	4
Number of 3D ports	0
Number of Volume ports	20
Number of Pipe Meshes	432
Number of 3D Meshes	0
Total Number of Hydraulic Modules	24
Total Accounted Scalar Meshes	476

Table C.8: Nodalisation Code Resources of the primary circuit

- Boundary condition BC3E element (FW1, steam generator 1): feed water
- AXIAL element (SG1SSD1, steam generator 1): downcomer of the steam generator
- VOLUME element (SG1VOL, steam generator 1): steam generator fictitious bottom
- AXIAL element (RISER1, steam generator 1): riser
- VOLUME element (SGDOM1, steam generator 1): dome
- Boundary condition BC5A element (SL1, steam generator 1): steam line



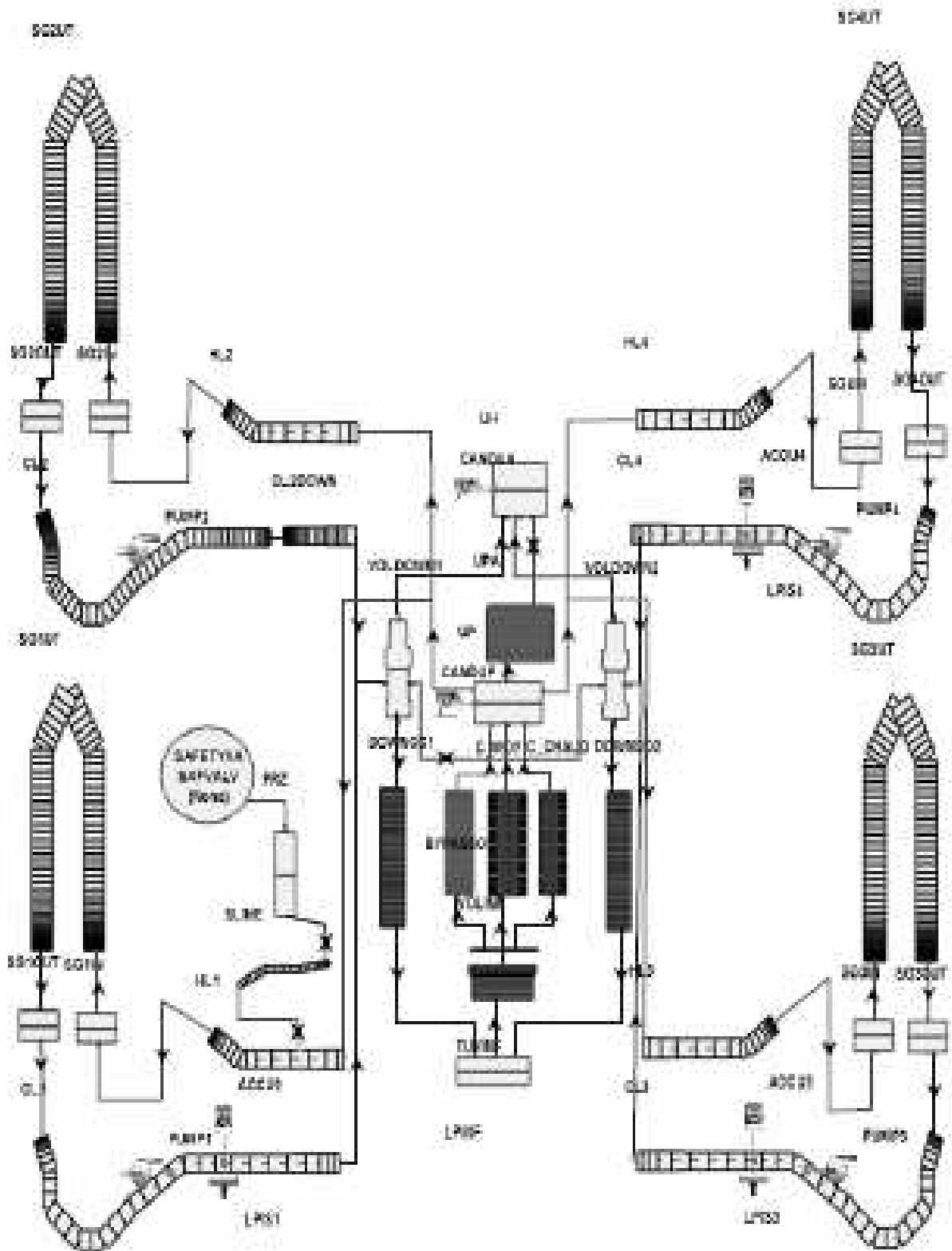


Figure C.11: Sketch of CATHARE input deck: Primary Side.

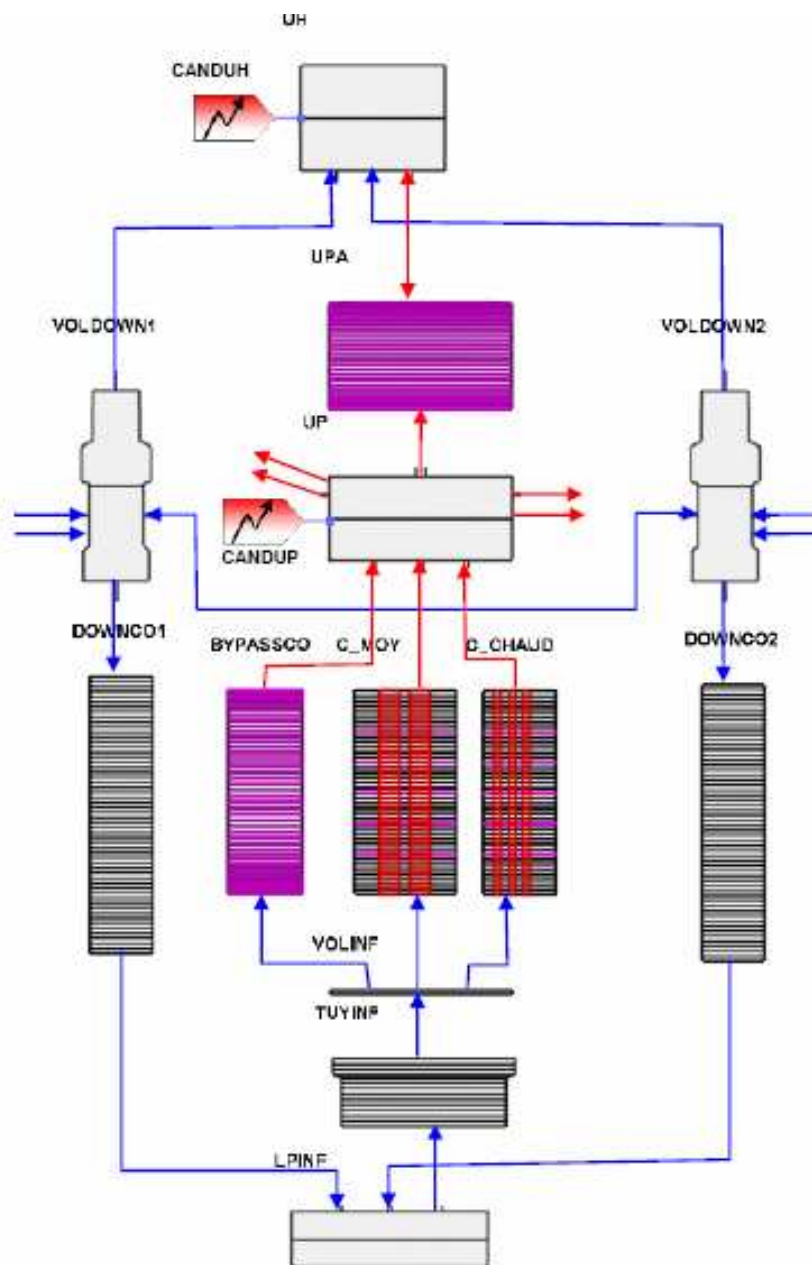


Figure C.12: Sketch of CATHARE input deck: Reactor Pressure Vessel.

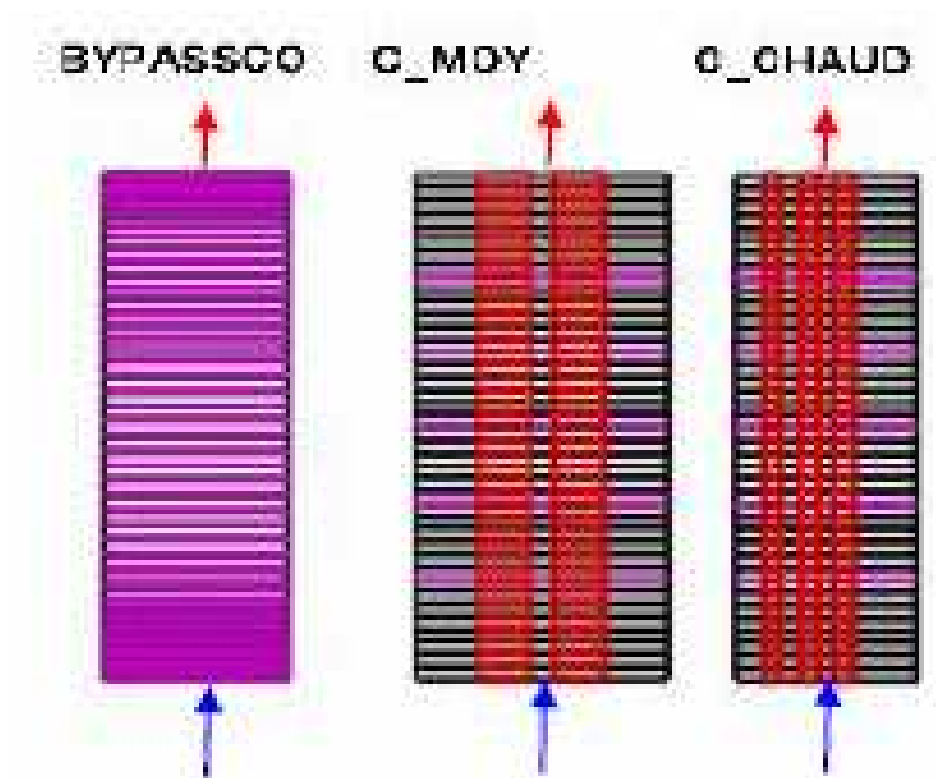


Figure C.13: 3.Sketch of CATHARE input deck: Core.

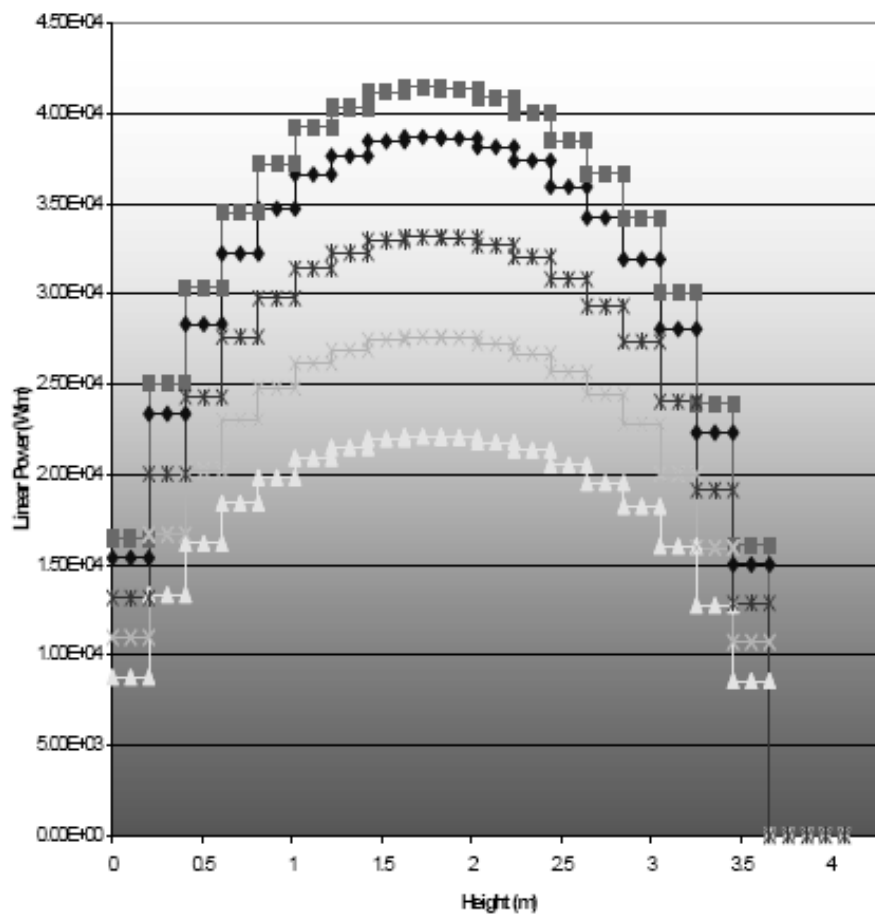


Figure C.14: Linear heat generation rate profiles.

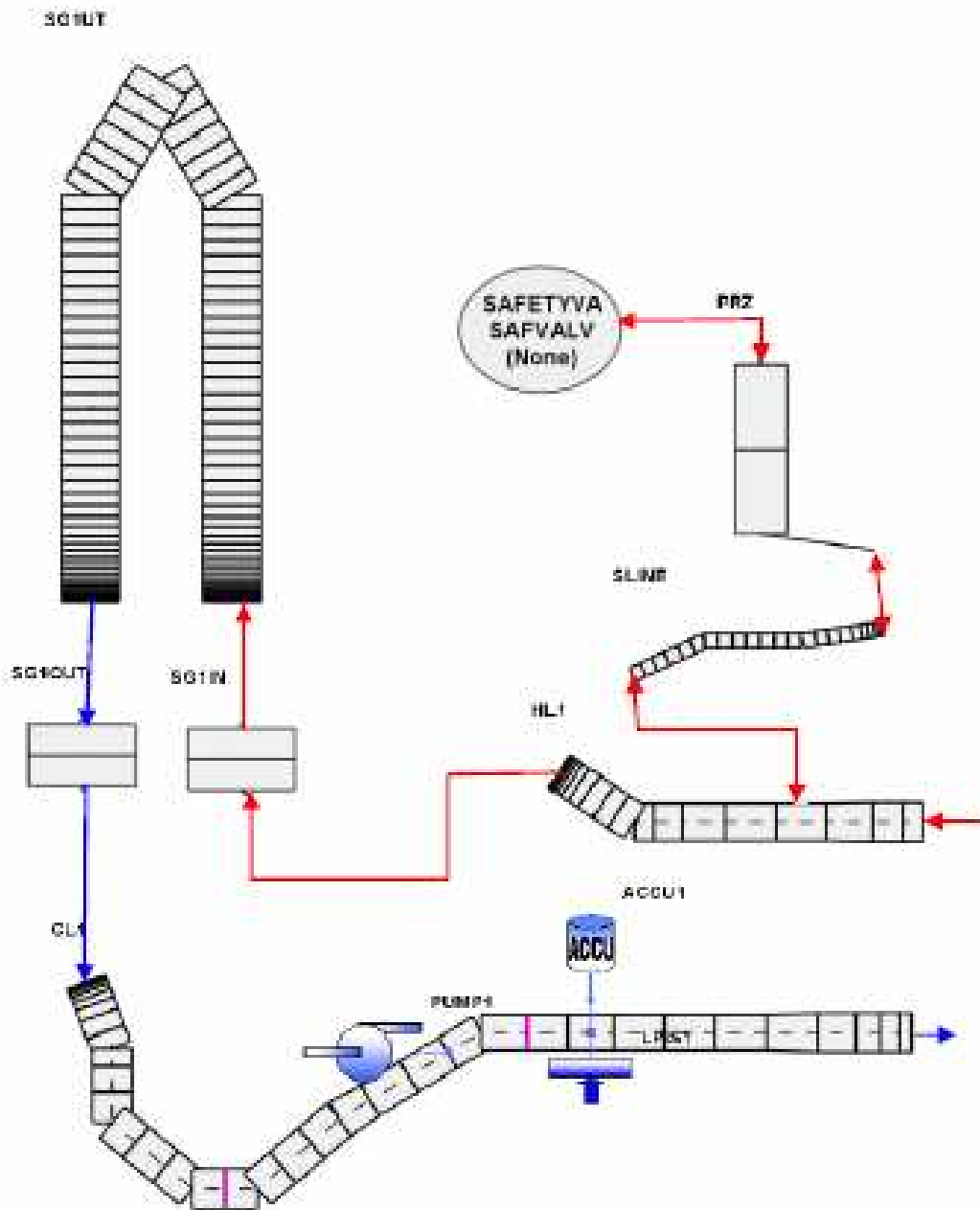


Figure C.15: Sketch of CATHARE input deck: intact loop 1.

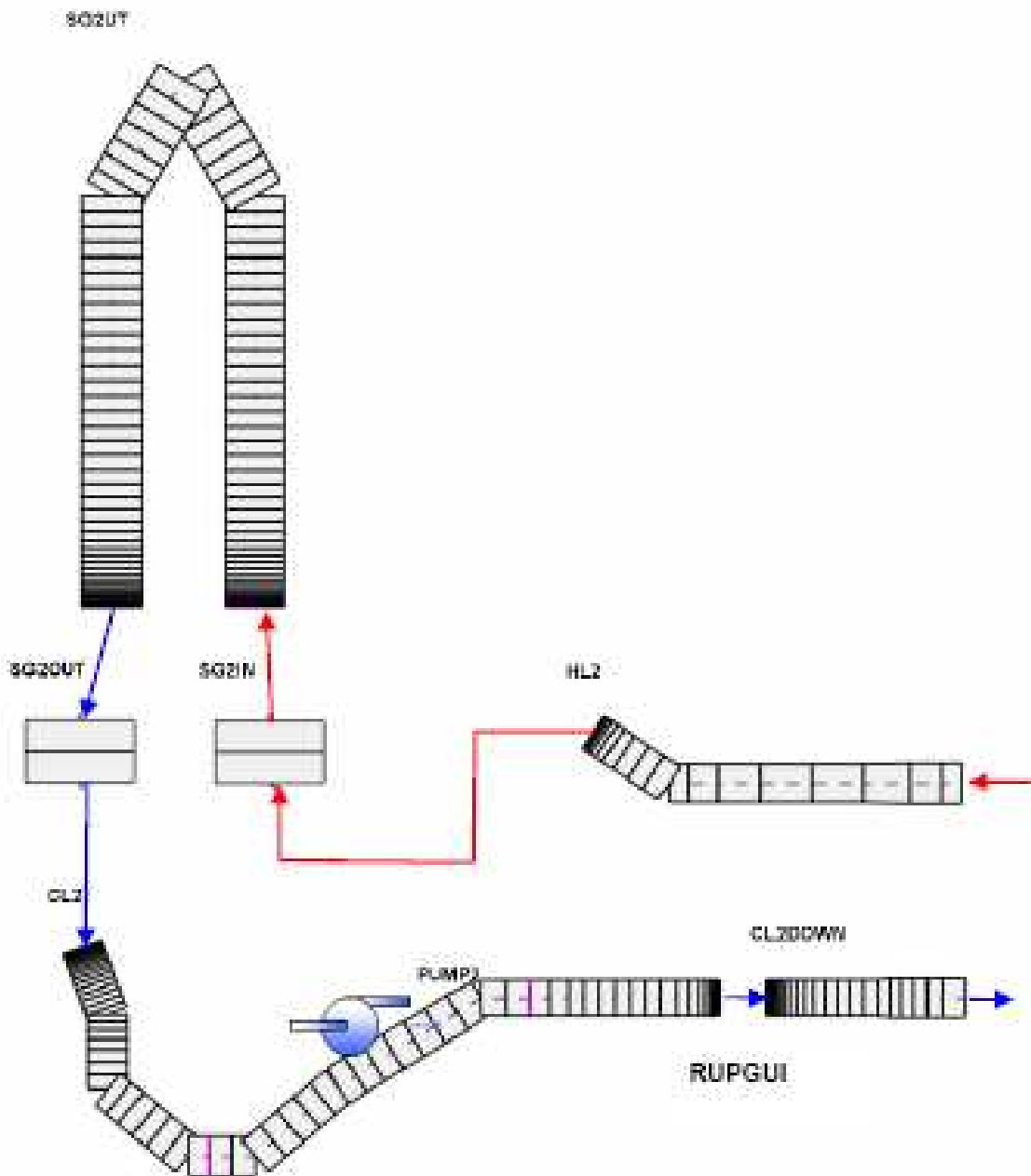


Figure C.16: Sketch of CATHARE input deck: broken loop 2.

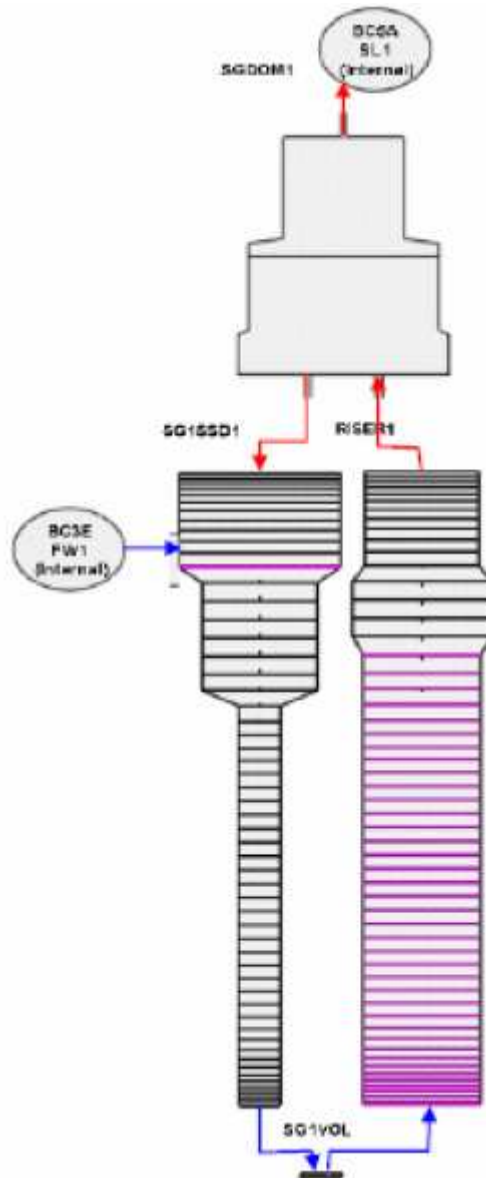


Figure C.17: 7.Sketch of CATHARE input deck: secondary side of the steam generator.

## C.5 JNES, Japan

### C.5.1 Description of the code: TRACE v4.05

**TRACE ver.4.05 is used in phase IV calculation.**

The TRAC/RELAP Advanced Computational Engine (TRACE – formerly called TRAC–M) is a best–estimate reactor systems code developed by the USNRC for analyzing transient neutronic–thermal–hydraulic behaviour in light water reactors. TRACE includes a full nonhomogeneous, nonequilibrium, two–fluid thermal–hydraulic model of two–phase flow.

### C.5.2 Description of the input deck

- **Geometric features:** number of hydraulic nodes, number of mesh points for heat structures, number of core channels, number of downcomers...

Reactor vessel (RV) including core is treated as three–dimensional nodalization and the other components are one–dimensional. RV is modelled by VESSEL component of TRACE code. RV is divided into 17–node for vertical direction, 6–ring for radial direction and 4–node for rotational direction (Figure C.18).

Thermal hydraulic regions of core channel are shown in Figure C.21. Reactor core consists of 8–node for vertical and 4–ring for radial. Core configuration and fuel assembly (FA) layout is shown in Figure C.22 based on the specification of Phase IV.

Four loops are modelled in this input deck, individually. One is broke loop and the others are intact (Figures C.19, C.20). Geometrical data, such as piping length, flow area, hydraulic diameter, is prepared with referring to the RELAP5 input deck and the excel sheet. There are 134 heat structures using HTSTR component based on the specification. These heat structures are applied to RV material, core barrel, fuel rods and steam generators (Figure C.23).

- **Models used:** activation of models such as CCFL, use of advanced options for fuel and/or gap...

The fine–mesh model is applied to fuel rods to calculate heat transfer of rod surface and cladding temperature. After reflood trip is set to on, reactor core is divided in detail for vertical direction and length of calculation node become smaller.

- **Nodalization sketch:**



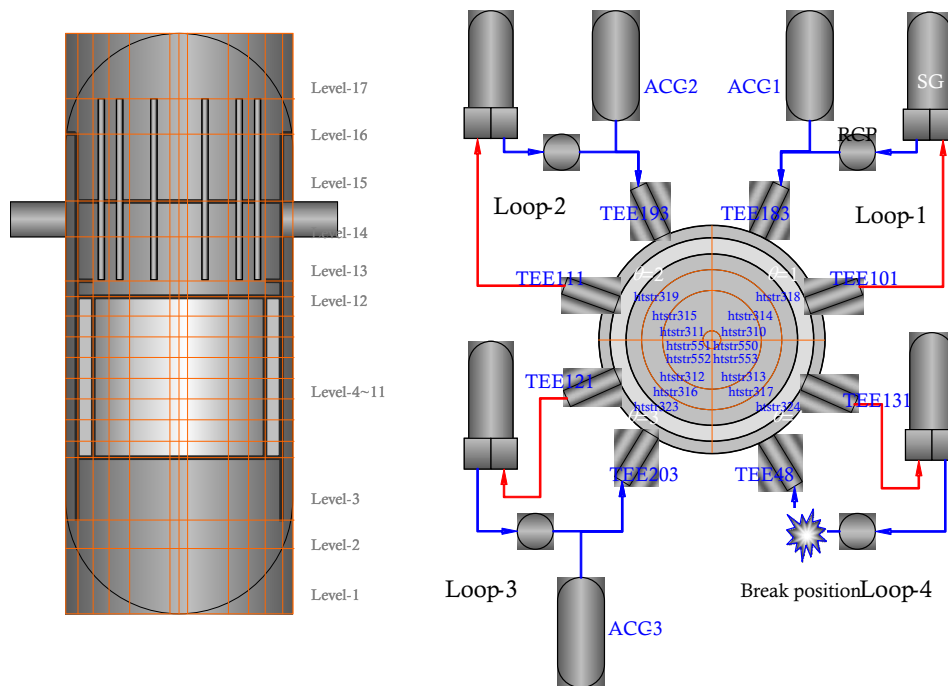


Figure C.18: Nodalization sketch for RV

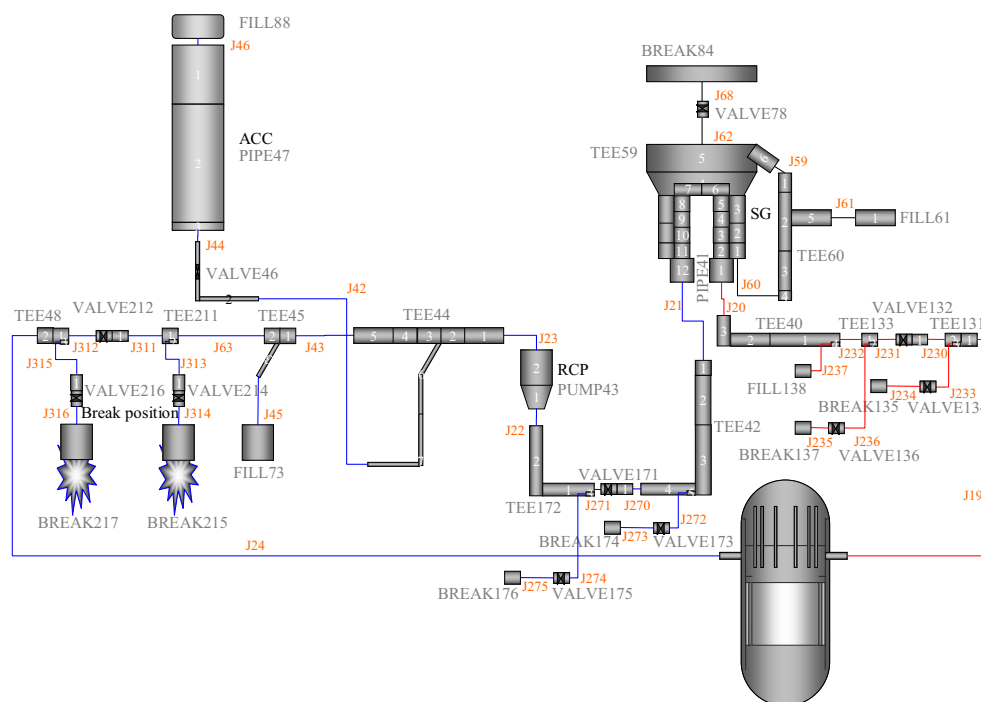


Figure C.19: Nodalization of broken loop



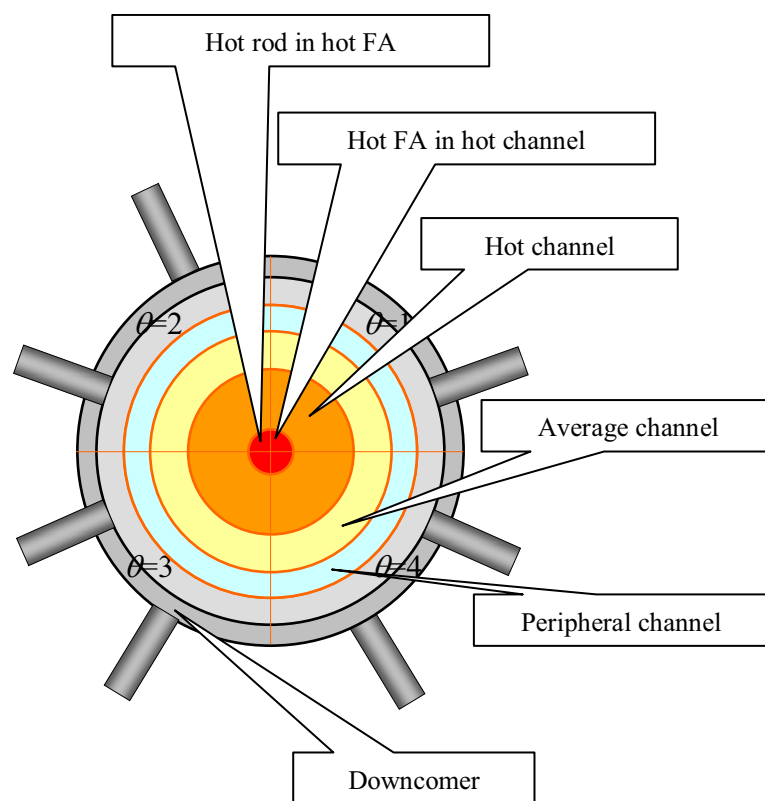


Figure C.21: Nodalization for core radial direction and FA layout  
(Hottest rod position is at  $\theta=1$ )

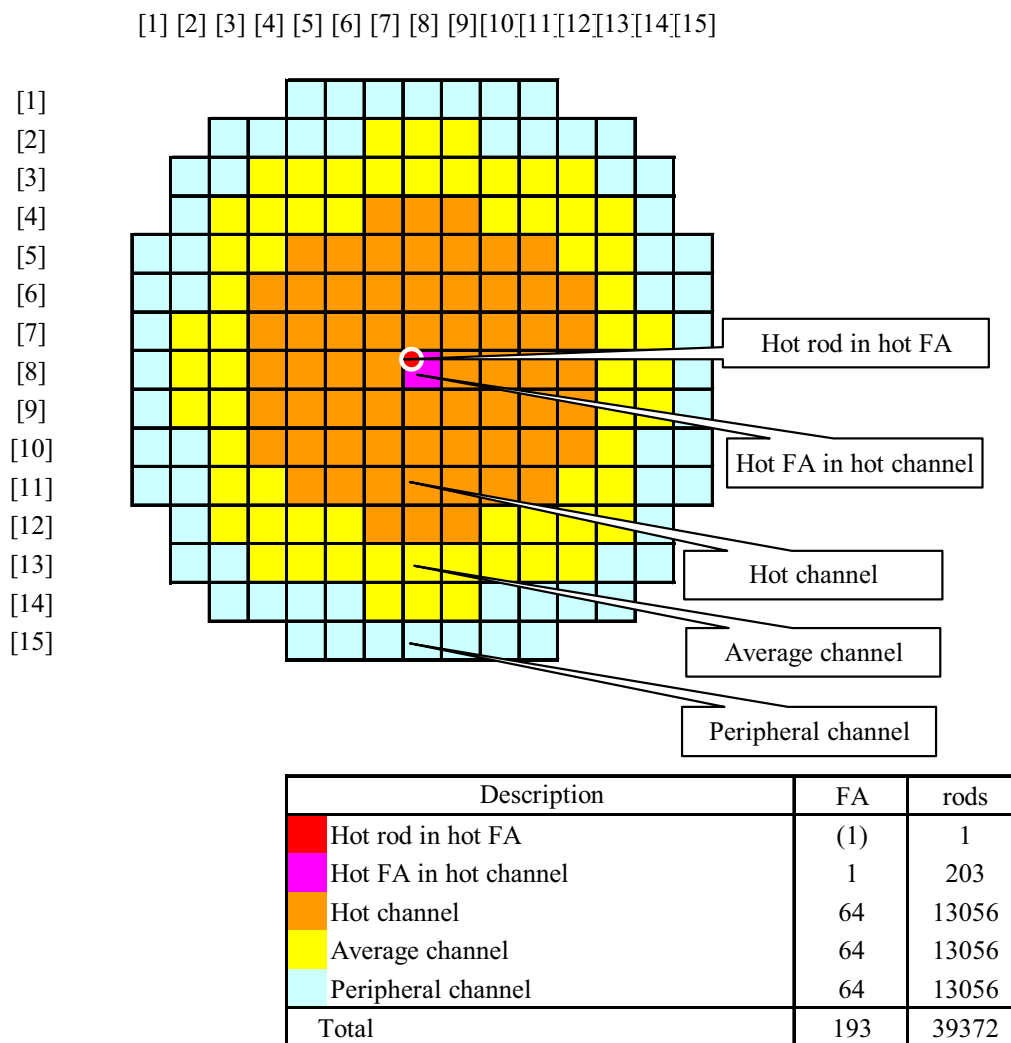


Figure C.22: Core configuration

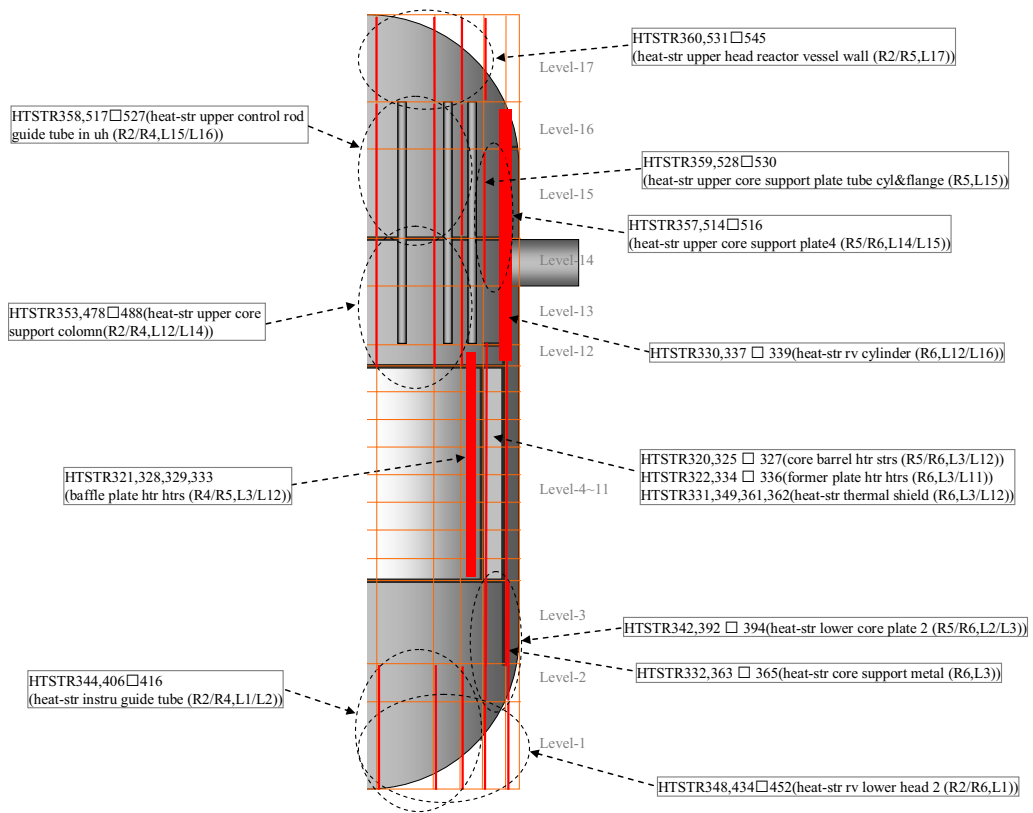


Figure C.23: Heat structures on RPV  
(Added heat structure number written in the specification 3.5)

Maximum linear heat generation rates (kW/m) for zones 2 and 5, for the following three locations: bottom of the core, 2/3 of the core, top of the core.

Please see the following figure. The linear heat generation rates are set based on the specification of phase IV.

Direct heating to moderator is not considered in TRACE code. Therefore, LHGR for moderator is added to LHGR for fuel. (e.g. maximum linear power of zone 5 is not 40.42 but 41.46 kW/m. Total power is 3250 MW<sub>t</sub>)

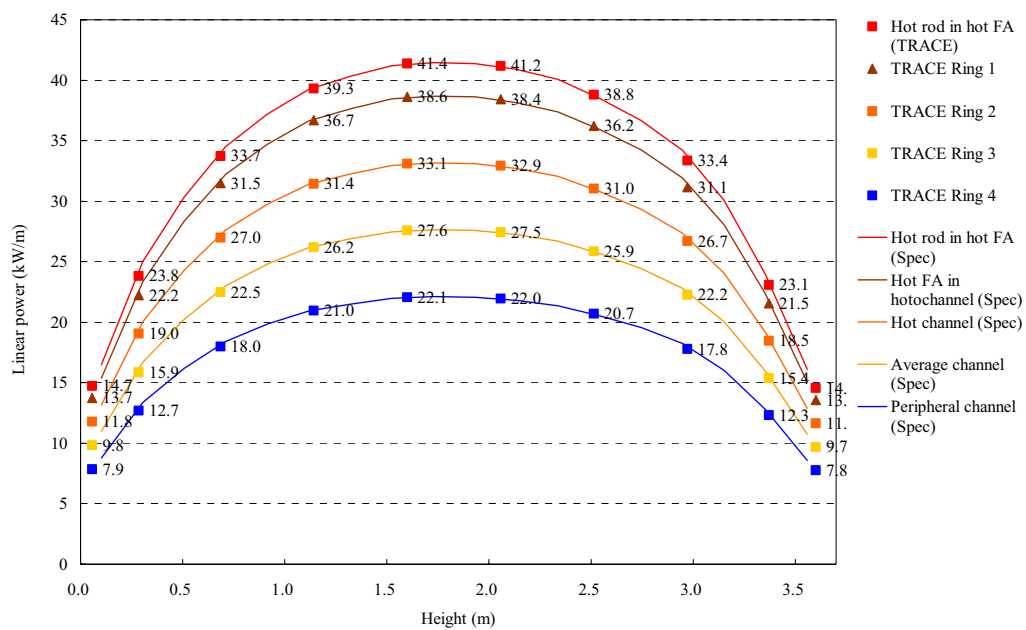


Figure C.24: Linear heat generation rate profile

## C.6 KAERI, South Korea

### C.6.1 Description of the Code: MARS 3.1

MARS(Multi-dimensional Analysis of Reactor Safety) code[1] is a realistic multi-dimensional thermal-hydraulic system analysis of light water reactor transients. The backbones of MARS code are the RELAP5/MOD3.2.1.2[2] and the COBRA-TF[3] codes of USNRC. The RELAP5 code is a versatile and robust system analysis code based on one-dimensional two-fluid model for two-phase flows whereas COBRA-TF code is based on a three-dimensional, two-fluid, three-field model. The two codes were consolidated into a single code by integrating the hydrodynamic solution schemes, and unifying various thermal-hydraulic models, EOS and I/O features.

The sources of the code were fully restructured using the modular data structure and a new dynamic memory allocation scheme of FORTRAN 90. MARS runs on Windows platform, and it is currently a popular multi-dimensional thermal-hydraulic tool in use for the analyses of reactor transients, experiment facility simulations and various safety research purposes. MARS can also be connected, by means of dynamic linkage using DLLs, to other codes such as 3D kinetics code MASTER and containment analysis codes, CONTAIN[4] and CONTEMPT[5]. TH modeling capability of the MARS is being improved and extended for application not only to light and heavy water reactors but also to research reactors and many advanced reactor types. The MARS can be running with the graphic system analyzer, ViSA, for a user-friendly computing environment.

A new multidimensional fluid model has been developed and implemented to the system analysis module of Version 2.3 in order to overcome some limitations of COBRA-TF 3D vessel module. The multidimensional model has been developed for porous media with a similarity of RELAP5-3D MULTID component model. However this model include not only 3D convection term but also diffusion terms in momentum equation, and 3D conduction and thermal mixing terms were also implemented to the energy equation. The simple Prantl's mixing length model was implemented as a turbulence model for two phase flow.

Property tables for gas and liquid metal have been generated for advanced reactor application, and brief models for new generation reactor with this property tables have been implanted in the MARS version 3.1.

### C.6.2 Description of the Input Deck

Zion RELAP5 input deck which supplied with BEMUSE 4 specification has been used as a base input for model. The original one-dimensional model has been built by modifying a general input deck for PWR simulating a SB-LOCA received from NRC. Many parts of NRC input deck has been changed in BEMUSE 4 specification. One-dimensional model consists of the intact and broken loops, the steam generator secondary of the intact loop, the pressurizer, the ECC system, and the reactor vessel, as shown in Figure C.25.

Three dimensional model of Zion vessel has been developed in this work. Vessel was divided into eight 45° azimuthal sectors and five radial rings, shown in Figure C.26. The eight azimuthal sectors corresponded to the eight nozzles connecting the loop and the vessel. Sector 7, 8 corresponded to the broken loop cold and hot leg position, sector 2,3,6 to the intact loop cold leg, and sector 1,4,5 to the intact loop hot leg. One outer radial ring represented the downcomer and the other four rings corresponded to hot-, average-, and peripheral channel regions of the core and core bypass region.



The axial nodalization of each component was based on the one-dimensional model, resulting in 2 levels in lower head, 2 lower plenum, 18 levels in core, 6 levels in upper plenum, and 4 levels in upper head regions.

The whole core contains 24 (3 radial x 8 azimuthal) fuel heat structures. Each fuel heat structure represents 8 fuel assemblies. Additional one hot assemble and hot rod were simulated in the eight hot channels respectively. All fuel structures were modeled as 18 axial nodes. Fuel power and volume fraction of each channel are assigned as BEMUSE4 input specifications.

Table C.9 shows the comparison of the number of the total volume, the number of the total junction, the mass of the total system and the volume of the total system. When the 3D model is compared to the 1D original model, the 3D model has 5 times larger number of the volume, 12 times that of the number of the junction and 6 times that of the number of the heat structure greater than those of the 1D model. Some differences in the system mass and volume were resulted but negligible to overall calculation.

	No. of volume	No. of junction	No. of heat structure	Total mass (kg)	Total volume (m <sup>3</sup> )
1D	252	257	216	488190	1134.4
3D	1372	3192	1441	488152	1135.4
3D/1D	5.4	12.4	6.67	0.99	1.0008

Table C.9: Comparisons of the 1D and 3D modeling.

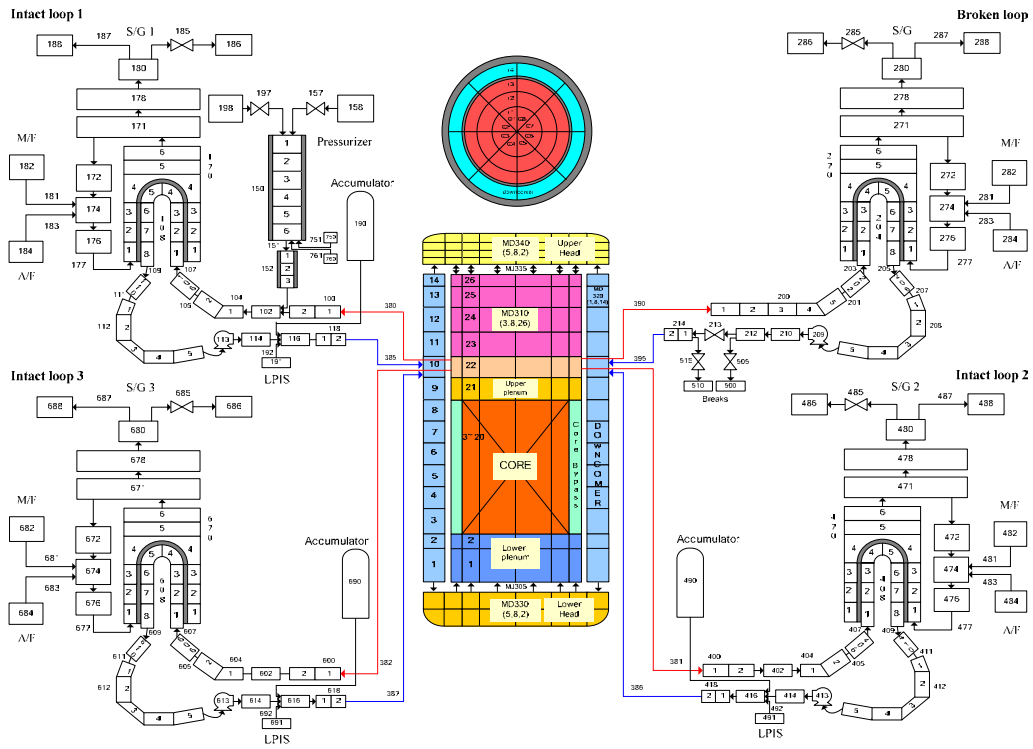


Figure C.25: Nodalization diagram of Zion NPP for MULTID component

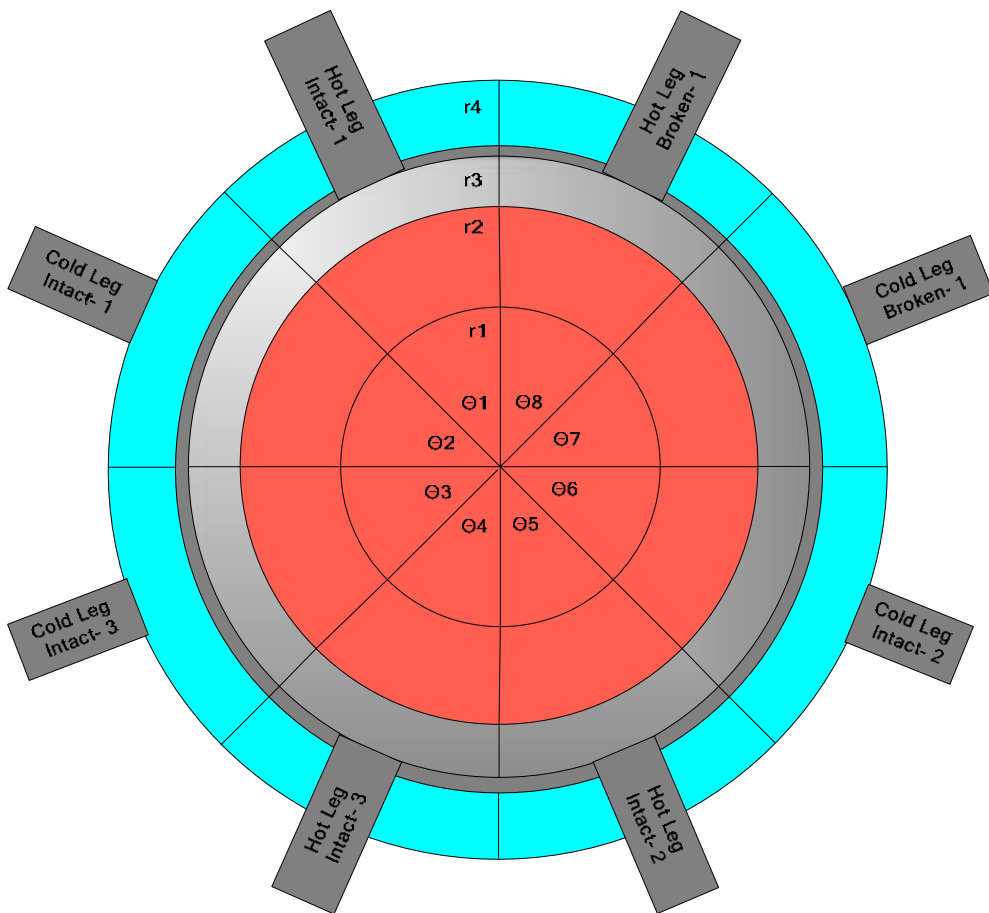


Figure C.26: Cross-sectional view of reactor vessel

### C.6.3 References

1. B.D.Chung, et.al., MARS 3.0 Code Manual, Volumes 1, Code Structure, System Modules, and Solution Methods, KAERI/TR-2812/2004, December 2004.
2. RELAP5/MOD3 Cod Manual Volume I: Code Structure, System Models, and Solution Methods, NUREG/CR-5535, U. S. Nuclear Regulatory Commission (1998).
3. M.J.Thurgood et al., COBRA/TRAC – A Thermal-Hydraulics Code for Transient Analysis of Nuclear Reactor Vessels and Primary Coolant Systems Volume 1, NUREG/CR-3046 PNL-4385, March 1983.
4. K.K. Murata, et. al, "Code Manual for CONTAIN2.0: A Computer Code for Nuclear Reactor Containment Analysis", Sandia National Laboratories, SAND97-1735, NUREG/CR-6533, June (1997).
5. C.C.Lin, et.al, "CONTEMPT4/MOD6 : A Multicompartment Containment System Analysis Program", Brookhaven National Laboratory, BNL-NUREG-51966, NUREG/CR-4547, March (1986).

## C.7 KINS, South Korea

### C.7.1 Description of the code: RELAP5/MOD3.3

The RELAP5 computer code is a light water reactor transient analysis code developed for the U.S. Nuclear Regulatory Commission (NRC) for use in rulemaking, licensing audit calculations, evaluation of operator guidelines, and as a basis for a nuclear plant analyzer. RELAP5 is a highly generic code that, in addition to calculating the behavior of a reactor coolant system during a transient, can be used for simulation of a wide variety of hydraulic and thermal transients in both nuclear and nonnuclear systems involving mixtures of steam, water, noncondensable, and solute. RELAP5/MOD3.3 has proven jointly by the NRC and a consortium consisting of several countries.

### C.7.2 Description of the input deck

#### Geometric features

Number of hydraulic nodes, number of mesh points for heat structures, number of core channels, number of downcomers

- Number of volumes = 252
- Number of junctions = 257
- Number of mesh points for heat structures = 2145
- Number of core channels = 1
- Number of downcomers = 1

#### Models used

Activation of models such as CCFL, use of advanced options for fuel and/or gap.

- CCFL model: not applied
- Reflood model: applied in heat structures of fuel
- Choking model: applied in broken area

### C.7.3 Nodalization sketch

See C.27.

### C.7.4 Maximum linear heat generation rates

Maximum linear heat generation rates (kW/m) for zones 2 and 5, for the following three locations: bottom of the core, 2/3 of the core, top of the core.

Zone 2: 10.987 kW/m (bottom), 26.712 kW/m (2/3), 10.734 kW/m (top)  
Zone 5: 16.481 kW/m (bottom), 38.832 kW/m (2/3), 16.102 kW/m (top)

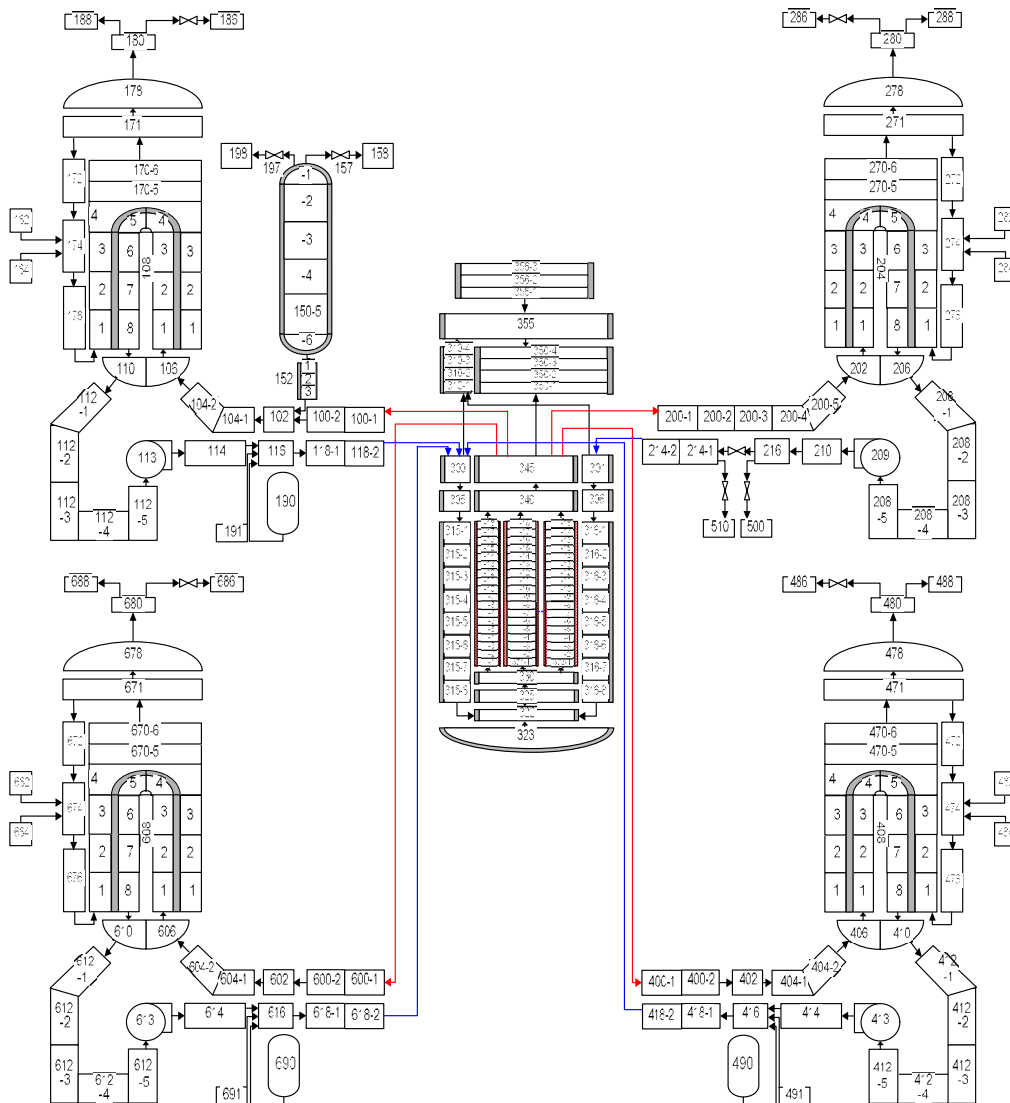


Figure C.27: Nodalization sketch

## C.8 NRI-1, Czech Republic

### C.8.1 Description of the code: RELAP5/MOD3.3

The code used for performing the ZION LBLOCA is RELAP5/MOD3.3 described in Refs NRI-1.1 and NRI-1.2.

### C.8.2 Description of the input deck

The "as-received" RELAP5/MOD3 input deck as described in Ref NRI-1.3 was modified in several steps. Firstly, the input deck was updated to meet input requirements as described in ref NRI-1.2, namely to add junction hydraulic diameter and CCFL data cards to primary system model components. Secondly, the axial nodalization of downcomer and radial nodalization of core region was changed. Right hand side boundary control volumes of heat structures representing fuel rods were re-specified that each heat structure (except the hot rod in hot fuel assembly) had its own hydraulic channel. Cross flows at each axial elevation were modeled. Radial nodalization of heat structures modeling fuel rods was changed. Resulting input deck consists of 306 control volumes, 368 junctions, and 216 heat structures having totally 2055 mesh points.

In the next step, the code models were activated as follows:

- Original RELAP5/MOD3 break flow model (Ransom-Trapp model) with default discharge coefficients was applied for break junctions (c505, c515).
- CCFL models were activated for junctions located at upper downcomer, upper core plate, upper plenum, and steam generator tube bundle inlet.
- The boundary conditions representing the containment pressure were re-specified in order to model "null transient" in steady state part of the code run.
- Decay heat power table was updated to include the data for transient time after 60 s.
- The base case as well as the sensitivity cases was analyzed up to 500 seconds in the transient. The steady state was calculated for 400 s.

#### **Nodalization sketch.**

Since the "as-received" input deck technique was generally used, Figure 2 in Ref NRI-1.3 applies. Components c331 through c339 were used to replace the core region model.

#### **Maximum linear heat generation rates.**

Since the "as-received" input deck technique was generally used, the data from Table 13 in Ref NRI-1.3 apply.

## C.9 PSI, Switzerland

### C.9.1 Description of the code: TRACEv5.0rc3

The code used for the BEMUSE Programme Phase IV at PSI is TRACE (Transient Analysis Computation Engine) version 5.0rc3, released in January 2007. TRACEv5.0rc3 is the latest in a series of advanced, best-estimate reactor system codes developed by the U.S. Nuclear Regulatory Commission (with the involvement of Los Alamos National Laboratory, Integrated Systems Laboratory (ISL), The Pennsylvania State University (PSU) and Purdue University) for analyzing transient and stationary neutronic/thermal-hydraulic behaviour of Light Water Reactors (LWRs). The code is a result of a consolidation of the capabilities of previous USNRC supported codes, such as TRAC-PF1, TRAC-BF1, RELAP-5 and RAMONA. The most important models of TRACE include multidimensional two-phase flow, non-equilibrium thermodynamics, generalized heat transfer, reflood, level tracking and reactor kinetics. The set of coupled partial differential equations, together with the necessary closure relationships, are solved in a staggered (momentum solved at cell edges) finite difference mesh. Heat transfer is treated semi-implicitly, while the hydrodynamic equations (1, 2 and 3 Dimensional) make use of a multi-step time differencing scheme (SETS) that allows the material Courant limit to be violated, thus resulting in large time step sizes for slow transients, and fast running capabilities. The system of coupled non-linear PDEs is solved by means of a Newton-Raphson iterative method, which results in a set of linearized algebraic equations in pressure, whose results is obtained by direct matrix inversion. A full two-fluid (6-equations) model is used to evaluate the gas-liquid flow, with an additional mass balance equation to describe a non-condensable gas field, and an additional transport equation to track dissolved solute in the liquid field.

The model for a specific nuclear power plant is built by connecting modular components with each other. TRACE components currently include pipes and tees (PIPE, TEE), pressure boundary condition (BREAK), flow boundary condition (FILL), three-dimensional component to simulate the reactor pressure vessel and its associated internals (VESSEL), heat conductors (HTSTR), heaters (HEATR), power in/out (POWER), channels (CHAN), jet pumps (JETP), separator (SEPD), plena (PLENUM), pressurizers (PRIZR), pumps (PUMP), valves (VALVE), radiation heat transfer (RADENC), turbines (TURB) and external components (EXTERNAL). In addition, it is possible to include control actions during the transients, through a built-in control system capability.

#### Description of the input deck

The RELAP5 input deck supplied with the BEMUSE 4 specifications has been used as basis to build the TRACE deck of the Zion NPP. The nodalization consists of three intact loops and one broken loop, the pressurizer, four steam generators, three emergency water injections systems (one for each intact loop) and three accumulators. A scheme of the nodalization is reported in Fig. 1. As in the original RELAP5 deck, the break has been modeled by means of three valves (217, 219, 221), where valve 221 closes at the time of the break initiation, while valves 217 and 219 open to the containment pressure boundary conditions specified by means of the BREAK components 218 and 220. The nodalization includes 71 hydraulic components (6 breaks, 11 fills, 21 pipes, 4 pumps, 1 pressurizer, 17 tees, 10 valves, 1 three-dimensional vessel), 74 hydraulic connections and 86 heat structures.

The reactor pressure vessel is modeled by means of a three-dimensional component, nodalized with 27 axial locations, 4 azimuthal sectors and 6 radial rings. The radial rings are subdivided as follows: ring 1 for the core hot assembly and hot rod; ring 2 for the core hot channel; ring 3 for the core average channel; ring 4 for the core peripheral channel; ring 5 for the bypass; ring 6 for the downcomer.



A scheme of the reactor vessel and the core is reported in Fig. 2. For the core nodalization 18 axial locations are used. Each of the 5 core regions (peripheral channel, average channel, hot channel, hot assembly and hot rod) is represented by means of 4 separated heat structures, each of them associated to one of the four azimuthal sectors respectively (in total 20 powered heat structures). The fuel rods are nodalized with 18 axial locations and 9 radial nodes (6 for the fuel pellet, 1 for the gap, 2 for the cladding). According to the latest BEMUSE 4 specifications, hot dimensions are assumed for the fuel in the whole core. The steady-state is performed by using the special TRACE option of constrained steady-state (CSS) combined with the definition of hydraulic path steady-state initialization (HPSI). To achieve a correct heat balance between the primary and secondary side, the heat structure flow area had to be reduced of about 22%. No adjustment of the pumps speed was required to achieve the specified nominal flow-rate in the primary loops.

The maximum linear heat generation rates for zones 2 and 5 are reported in Table 1 for three axial locations, respectively:

- bottom of the core (0.4 - 0.6 m).
- 2/3 of the core (1.6 - 1.8 m).
- Top of the core (2.8 - 3.0 m)

Axial location [m]	ZONE 2 Linear power (kW/m)	ZONE 5 Linear power (kW/m)
0.51	20.244	30.367
1.73	27.636	41.454
2.95	22.804	34.207

Table C.10: Maximum linear heat generation rates for Zones 2 and 5

### Special models used

The critical flow model is activated for all components connected to a pressure boundary condition, so that critical flow at the break is taken into account. The default critical flow model in TRACE is based on Ransom and Trapp's formulation. Reflood models are used (since TRACE version 4.260, reflood set of physical models does not need to be manually switched on by the user). According to BEMUSE 4 specifications: the CCFL model is activated for the core upper tie plate. As by specification, the Wallis model is selected with slope  $m = 1$  and intercept  $c = 0.8625$ ; the fuel gap is simulated as a heat slab with prescribed heat conduction and heat capacity.

### Comments on sensitivity study

For the sensitivity study cold fuel dimensions have been used for the reference calculation. The strongest influence on the PCT is given by changing fuel dimensions from cold to hot conditions (cold conditions gives a PCT 85 K higher than the one obtained with hot dimensions). A strong influence on the PCT is found also when the fuel or the gap conductivity is varied or if the maximum linear power of the hot rod is changed. The strongest influence on the reflooding time is given by the change of containment pressure evolution and by the change in decay power.

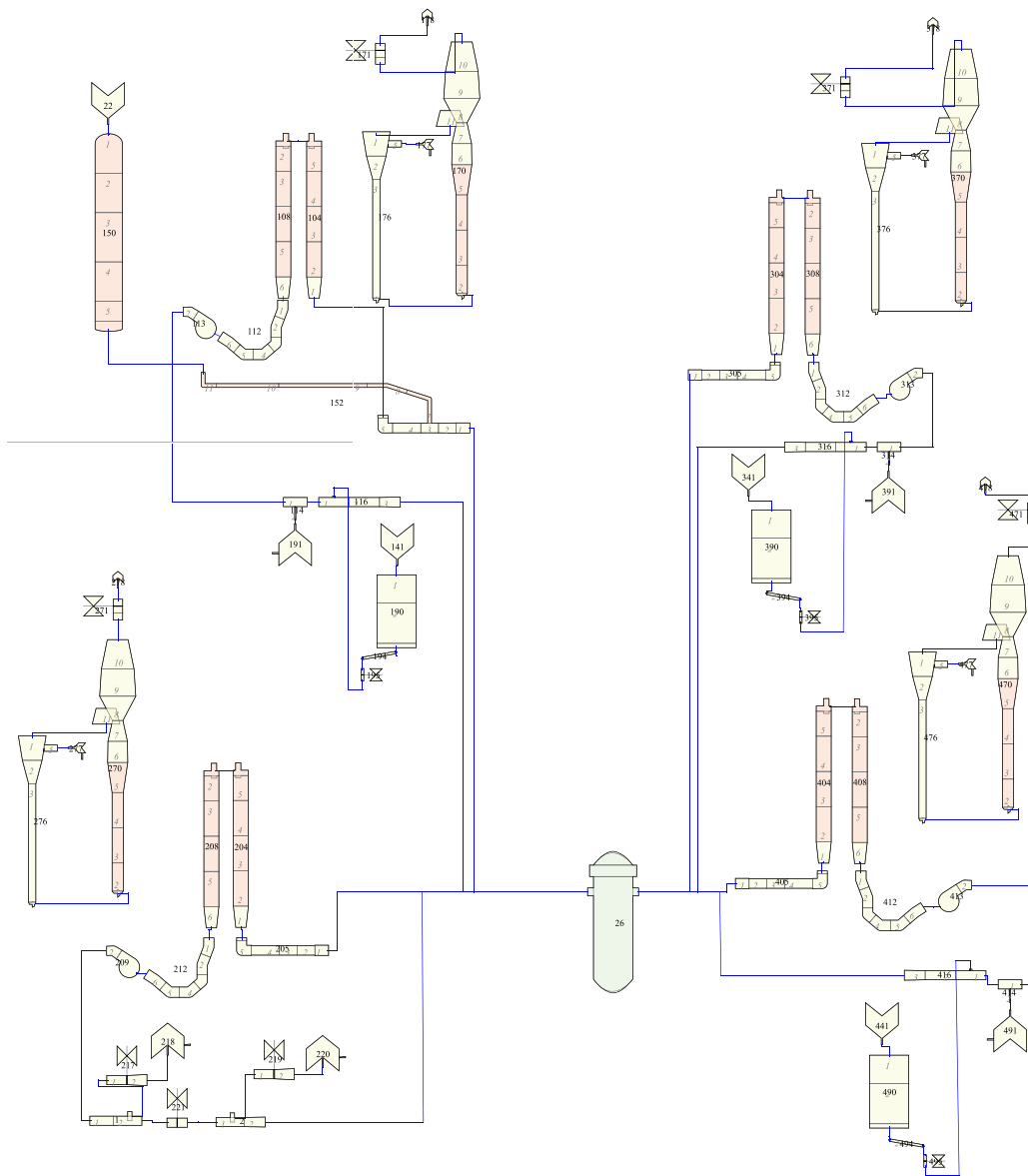


Figure C.28: TRACE nodalization for Zion NPP

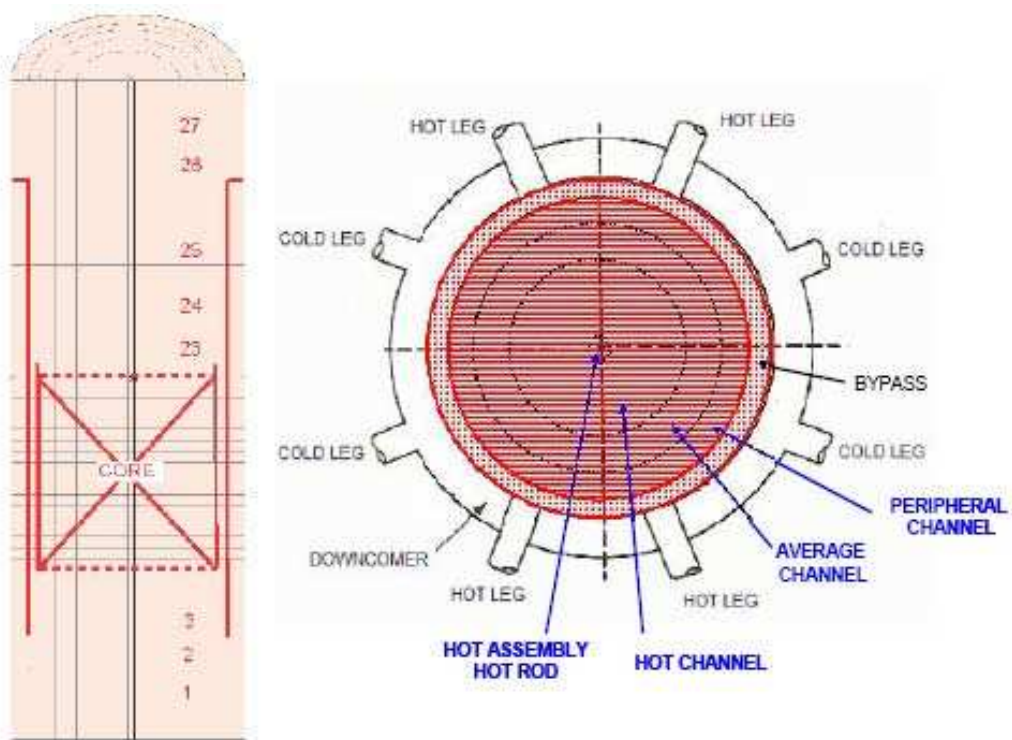


Figure C.29: Vessel nodalization

## C.10 UNIPI1 Italy

### C.10.1 CODES AND INPUTS

#### Description of the Code RELAP5 Mod3.2

The light water reactor (LWR) transient analysis code, RELAP5, was developed at the Idaho National Engineering Laboratory (INEL) for the U.S. Nuclear Regulatory Commission (NRC). Code uses include analyses required to support rulemaking, licensing audit calculations, evaluation of accident mitigation strategies, evaluation of operator guidelines, and experiment planning analysis. RELAP5 has also been used as the basis for a nuclear plant analyzer. Specific applications have included simulations of transients in LWR systems such as loss of coolant, anticipated transients without scram (ATWS), and operational transients such as loss of feedwater, loss of offsite power, station blackout, and turbine trip. RELAP5 is a highly generic code that, in addition to calculating the behavior of a reactor coolant system during a transient, can be used for simulation of a wide variety of hydraulic and thermal transients in both nuclear and nonnuclear systems involving mixtures of steam, water, noncondensable, and solute.

The MOD3 version of RELAP5 has been developed jointly by the NRC and a consortium consisting of several countries and domestic organizations that were members of the International Code Assessment and Applications Program (ICAP) and its successor organization, Code Applications and Maintenance Program (CAMP). Credit also needs to be given to various Department of Energy sponsors, including the INEL laboratory-directed discretionary funding program. The mission of the RELAP5/MOD3 development program was to develop a code version suitable for the analysis of all transients and postulated accidents in LWR systems, including both large- and small-break loss-of-coolant accidents (LOCAs) as well as the full range of operational transients.

The RELAP5/Mod3.2 code [1, 2] code is based on a non-homogeneous and non-equilibrium model for the twophase system that is solved by a fast, partially implicit numerical scheme to permit economical calculation of system transients. The objective of the RELAP5 development effort from the outset was to produce a code that included important first-order effects necessary for accurate prediction of system transients but that was sufficiently simple and cost effective so that parametric or sensitivity studies were possible.

The code includes many generic component models from which general systems can be simulated. The component models include pumps, valves, pipes, heat releasing or absorbing structures, reactor point kinetics, electric heaters, jet pumps, turbines, separators, accumulators, and control system components. In addition, special process models are included for effects such as form loss, flow at an abrupt area change, branching, choked flow, boron tracking, and non-condensable gas transport.

In particular, the control volume has a direction associated with it that is positive from the inlet to the outlet. The fluid scalar properties, such as pressure, energy, density and void fraction, are represented by the average fluid condition and are viewed as being located at the control volume center. The fluid vector properties, i.e. velocities, are located at the junctions and are associated with mass and energy flow between control volumes. Control volumes are connected in series using junctions to represents flow paths.

Heat flow paths are also modeled in a one-dimensional sense, using a staggered mesh to calculate temperatures and heat flux vectors. The heat structure is thermally connected to the hydrodynamic control volumes through heat flux that is calculated using a boiling heat transfer formulation. The heat structures are used to simulate pipe walls, heater elements, nuclear fuel pills and heat exchanger surfaces.

The system mathematical models are coupled into an efficient code structure. The code includes extensive input checking capability to help the user discover input errors and inconsistencies. Also

included are free-format input, restart, renodalization, and variable output edit features. These user conveniences were developed in recognition that generally the major cost associated with the use of a system transient code is in the engineering labor and time involved in accumulating system data and developing system models, while the computer cost associated with generation of the final result is usually small.

The development of the models and code versions that constitute RELAP5 has spanned approximately 17 years from the early stages of RELAP5 numerical scheme development to the present. RELAP5 represents the aggregate accumulation of experience in modeling reactor core behavior during accidents, two-phase flow processes, and LWR systems. The code development has benefited from extensive application and comparison to experimental data in the LOFT, PBF, Semiscale, ACRR, NRU, and other experimental programs.

### Description of the Input

The RELAP5/Mod3.2 ZION NPP model nodalization is shown in Figure C.30. The vessel model (Figure C.31) consists of 23 hydraulic components which are connected by 50 junctions. The down-comer (DC) is nodalized by two channels made with two BRANCHES and one PIPE (with 8 control volumes) each. One DC channel (360) has a volume and flow area equivalent to 3/4 of the total DC volume and flow area and it is connected with the three intact loop via the respective cold legs. The second DC channel (370) is connected to the broken loop. Cross flow junctions between the two DC channels have been implemented as suggested in the specification [3].

The reactor core is represented by two hydraulic channels, modelled by two PIPE (830 and 840) subdivided in 18 hydraulic volumes. The PIPE 830 simulates 2/3 of the total volume and flow area of the core and it is associated with the peripheral and average fuel bundles (see Figure C.32). The PIPE 840 simulates the remaining 1/3 of the core and has been coupled with the hot fuel bundle, hot fuel channel and hot fuel rod. Core cross flow junctions (899) has been considered as suggested in the specification [3]. Loss coefficients (forward and reverse) have been introduced for simulating the 5 grid spacers. A core bypass (800) is simulated with a 18 nodes PIPE.

The 193 fuel assembly (FA) have been arranged in the following five groups of HEAT STRUCTURES as depicted by Fig. 3:

- The first represents the RELAP5 average fuel rod in the peripheral channel and includes 64 NPP FA,
- The second represents the RELAP5 average rod in the average channel and includes 64 NPP FA
- The third represents the RELAP5 average rod in the hot channel and includes 64 NPP FA
- The fourth represents the RELAP5 average rod in the hot fuel assembly
- The fifth represents the RELAP5 hot rod in the hot fuel assembly.

The subdivision of the ZION NPP power among the five groups has been done in agreement with the values in Table C.11 and taking into account the direct moderator heating (about 2.5%). The linear power associated to each axial piece of the five heat structures is represented in Figure C.33. Geometrical features of the fuel pins and fuel pellets have been considered (hot condition) using data in Table C.12. Finally, the following choices have been adopted:

- Bottom-up and top down reflood model for all five RELAP5 heat structures;
- CCFL model at core tie plate using Wallis correlation;

Core Zone per rod	Rod average linear power (kW/m)	Power (kW)	Maximum linear power (kW/m)	Number of rods	Fuel Power (kW)	Moderator Power (kW)	Total Power (MW)
1	17.56	64.25	21.56	13056	838881.02	21509.77	860.39
2	21.94	80.32	26.94	13056	10487601.27	26887.21	1075.49
3	26.33	96.38	32.33	13056	1258321.53	32264.65	1290.59
4	30.72	112.44	37.72	203	22825.71	585.27	23.41
5	32.92	120.47	40.42	1	120.47	3.09	0.12
<b>Total</b>				39372	3168750	81250	3250

Table C.11: ZION NPP power subdivision among the five RELAP5 group of heat structures.

PARAMETER	UNIT	VALUE
<b>Fuel Pin</b>		
Outside diameter	mm	10.71
Cladding thickness	mm	0.61
Gap thickness	mm	0.054
Active fuel length	m	3.66
<b>Fuel pellet</b>		
Diameter	mm	9.38

Table C.12: Fuel rod characteristics (hot condition for the average rod).

- Gap thermal conductivity introduced by mean of a table from the specification [3].

Each of the four loops (three intact - Figure C.34 - and one broken - Figure C.35) is explicitly modelled with their own steam generators also considering the objective to develop a multi purpose nodalization (i.e. valid for other kind of transients). The pressurizer (PIPE 150) is connected to the hot leg (PIPE 100 and PIPE 102) of loop 1 via the surgeline (PIPE 152). Five zones may be recognized in the secondary side of each steam generator: 1) the downcomer; 2) the riser zone, essentially including the U-tubes; 3) the top of the vessel, including the separator, and the steam dome regions; 4) the steam line downstream the dome; 5) the feed water line (simulated with the time dependent junction (181) and the time dependent volume (182) connected to the top of the downcomer. The degree of detail of the nodalization is commensurate to what considered in the primary loop. In particular, the heights of the riser volumes are the same as the heights of the corresponding rising and descending nodes of the primary side U-tubes (slicing nodalization technique). The component 172 simulates the separator that is necessary in the code model in order to achieve quality equal to one in the steam dome.

The double end guillotine break (full open area equal to 0.3832 m<sup>2</sup>) is located in the cold leg (PIPE 212 and 214) of the loop 2 (Figure C.35) and it is simulated by three VALVEs (213, 515 and 505). Volumes 500 and 510 (TMDPVOL) simulate the containment with pressure imposed as a function of time after the break [3]. The RELAP5 Mod3.2 default Henry-Fauske critical flow model is adopted.

Moreover the following can be noted:

- The hydro accumulators (190, 490, 690) have been simulated with proper ACCUM components with 4.14 MPa as pressure set-point. Accumulators are isolated when their level falls below 0.14 m in order to avoid the injection of non condensables in the primary system;
- The LPIS system is nodalized by time dependent volumes (191, 491 and 691) and time dependent junctions (192, 492 and 692) by which the LPIS mass flow rate is imposed as function of pressure. The LPIS pressure set point is 1.42 MPa;
- The reactor coolant pumps trip at the same time of the break;

TOTAL NUMBER OF HYDRAULIC NODES	286
TOTAL NUMBER OF JUNCTIONS	294
TOTAL NUMBER OF HEAT STRUCTURES	247
TOTAL NUMBER OF MESH POINTS	2238
NUMBER OF CORE CHANNELS (without bypass)	2
NUMBER OF AXIAL CORE NODES PER CHANNEL	18

Table C.13: RELAP5 nodalization code resources.

PARAMETERS	HOT ROD IN HOT FA (ZONE 5)			AVERAGE ROD IN AVERAGE CHANNEL (ZONE 2)		
	Bottom Level 0 to 1.22 m	2/3 Core Height 1.22 to 2.44 m	Top Level 2.44 to 3.66 m	Bottom Level 0 to 1.22 m	2/3 Core Height 1.22 to 2.44 m	Top Level 2.44 to 3.66 m
Maximum Linear Power (KW/m)	36.28	40.42	37.56	24.19	26.94	25.04
Elevation from BAF (m)	1.11	1.73	2.54	1.11	1.73	2.54
Azimuthal Position	NA	NA	NA	NA	NA	NA

Table C.14: Maximum linear power and location.

- The reactor coolant pump velocities are imposed as a function of time after the break;
- A decay power curve is imposed by reactor power multiplier specified as a function of time after the break;
- The steam line and the feed water line were isolated at 10 s and 20 s respectively after the break;
- A null transient of 200 s was run for achieving a steady state. The transient was run for 500 s.

Table C.13 summarizes the main nodalization code resources used, whereas Table C.14 contains the maximum linear powers considered in the axial discretization of the linear power profiles and the corresponding elevations for the six temperature time trends reported in Section 2.

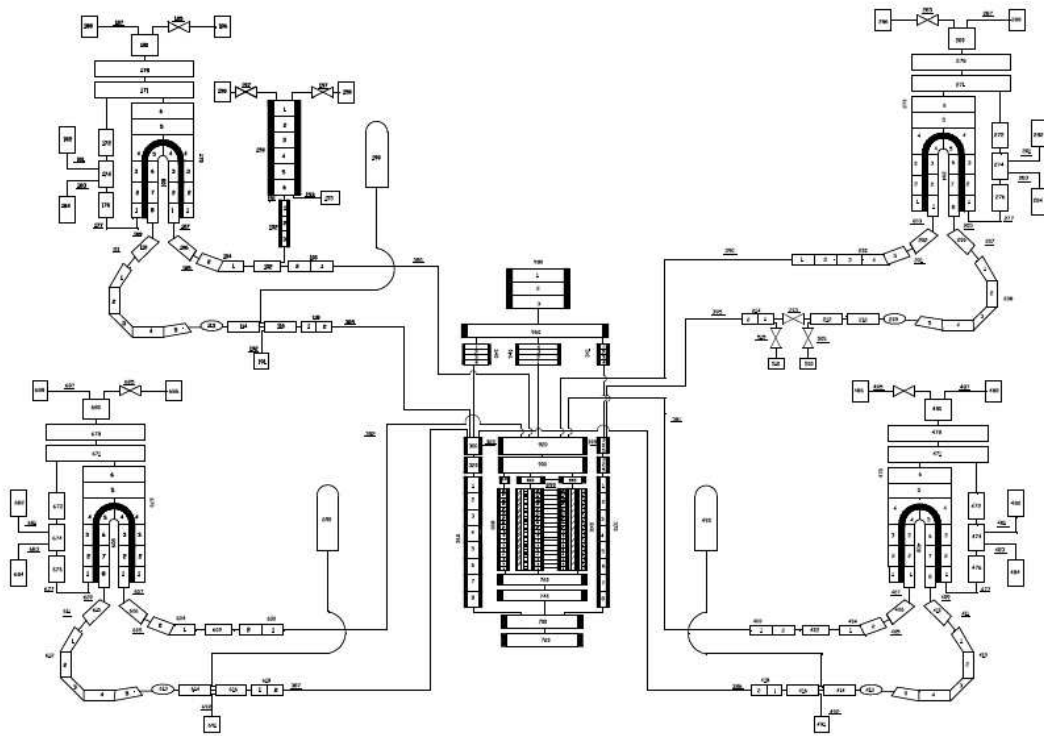


Figure C.30: General nodalization



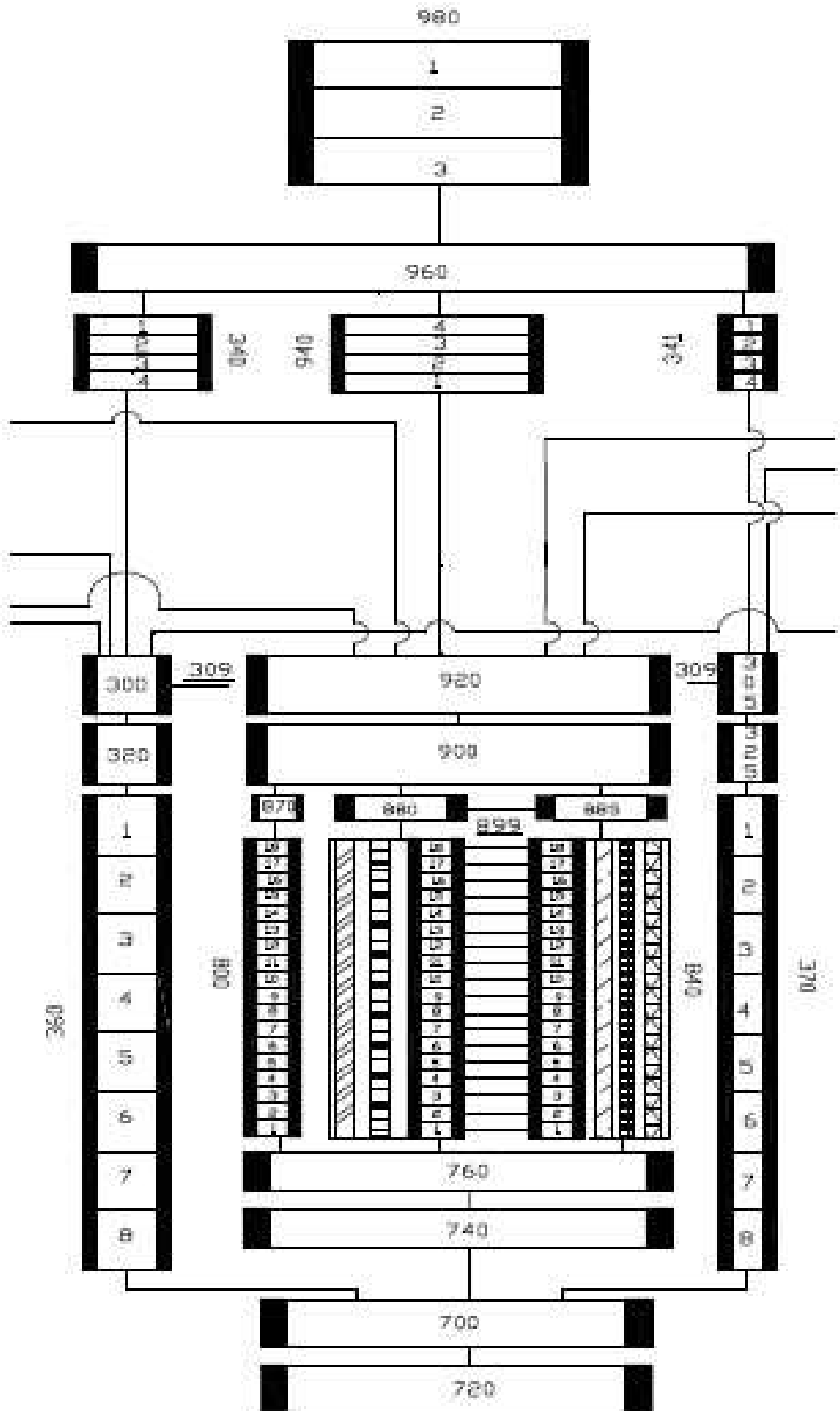


Figure C.31: Vessel nodalization

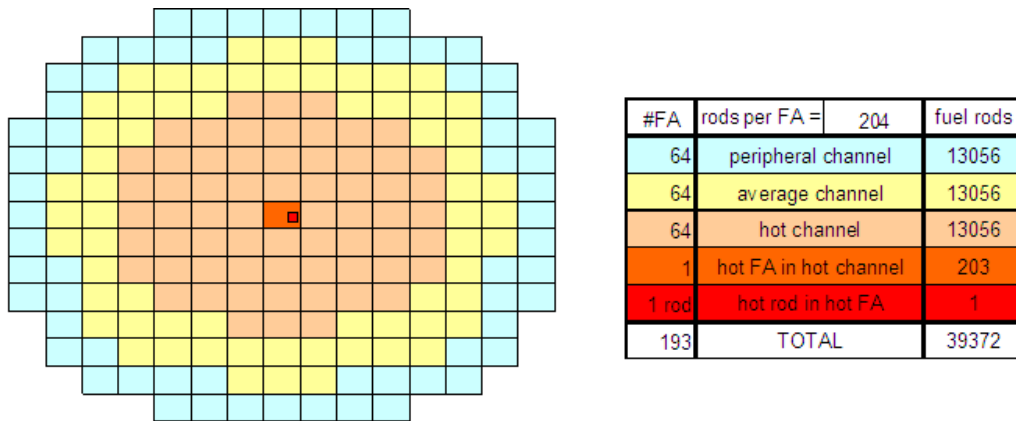


Figure C.32: Vessel nodalization

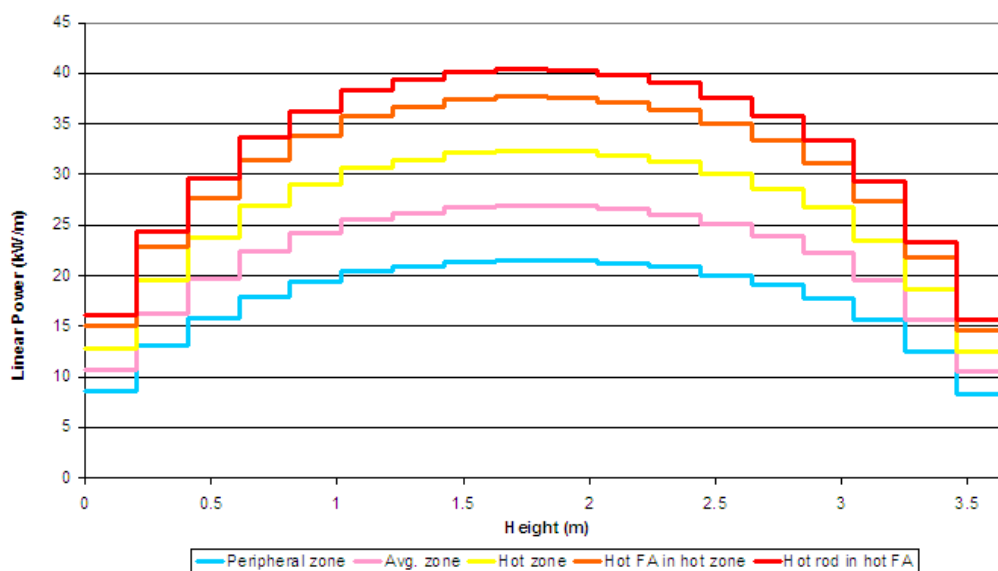


Figure C.33: Vessel nodalization

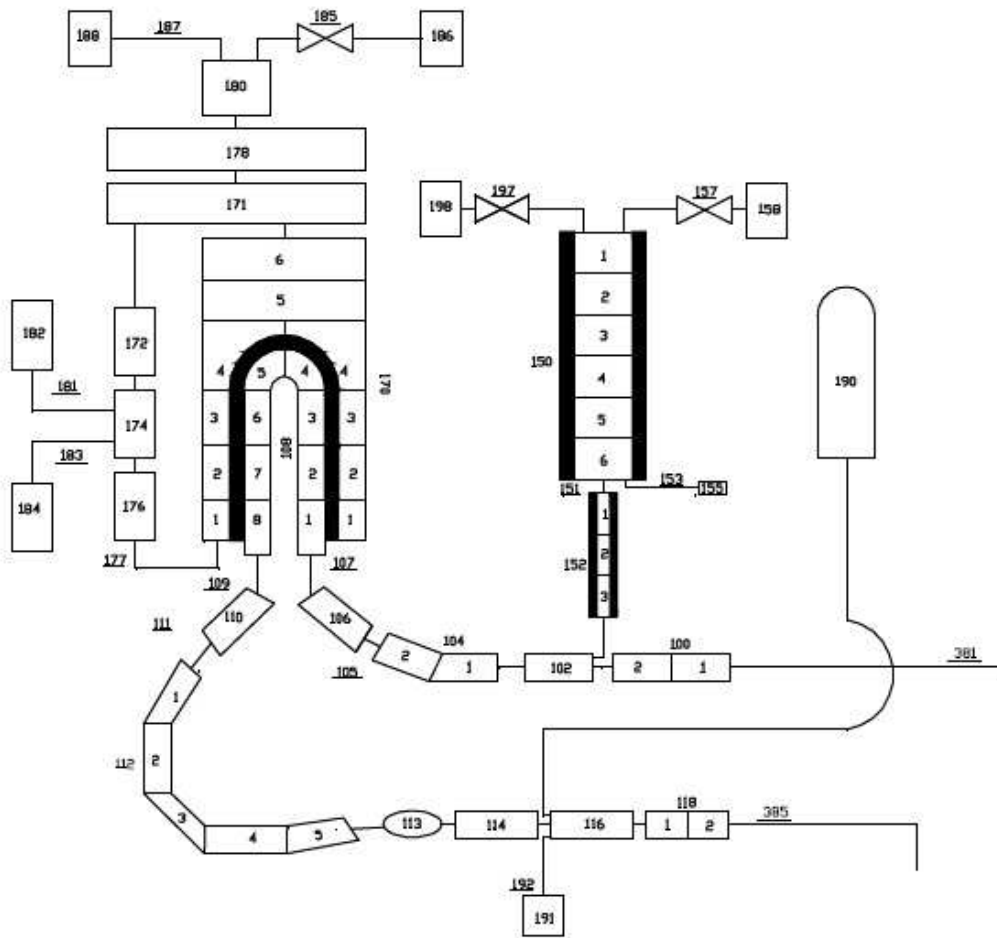


Figure C.34: Vessel nodalization

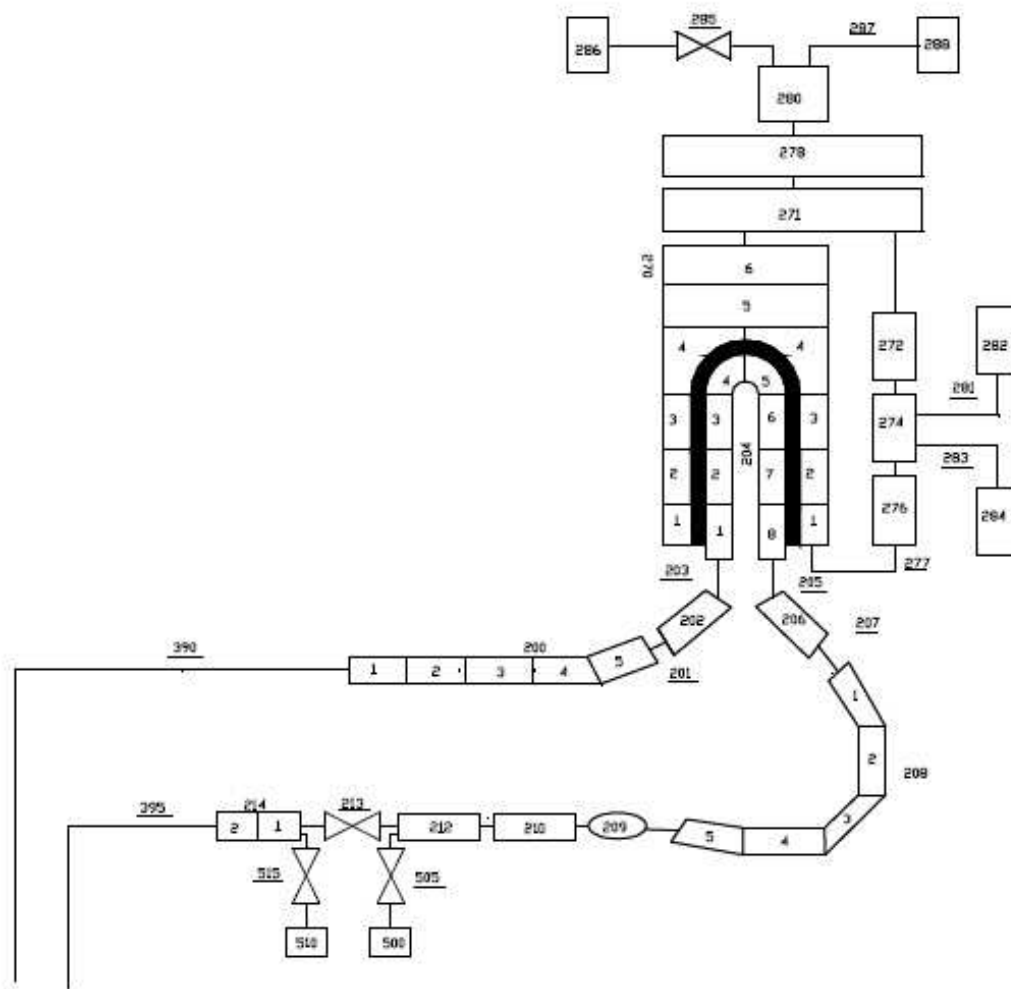


Figure C.35: Vessel nodalization

**REFERENCES**

1. W. H. Ramson, "Relap5/Mod2 code manual: user guide and input requirements", NUREG/CR-4312 EGG-2396, Idaho (USA), March 1997.
2. The Relap5 Code Development Team, "Relap5/Mod3 code manual", NUREG/CR-5535-V4, Idaho (USA), June 1995.
3. M. Perez, F. Reventos, Ll. Batet, "Phase 4 of BEMUSE Programme: Simulation of a LB-LOCA in ZION Nuclear Power Plant. Input and Output Specifications" rev. 3, Universitat Politecnica de Catalunya, Spain, 2007.
4. F. D'Auria, N. Debrechin, and G. M. Galassi, "Outline of the Uncertainty Methodology based on Accuracy Extrapolation", J. Nuclear Technology, 109,1,21 (1995).
5. A. Petruzzi, et. Al, BEMUSE Phase II Report, "Re-analysis of the ISP-13 Exercise, Post Test Analysis of the LOFT, L2-5 Test Calculation", Appendix B, "Description of the Procedure to Qualify the Nodalization and to Analyze the Code Results", NEA/CSNI/R(2006)2, November 2005.
6. A. Petruzzi, "RELAP5 Mod3.2 Post Test Analysis and CIAU Uncertainty Evaluation of LOFT Experiment L2-5", NT 558, rev.1, Internal Document, October 2005.

## C.11 UNIPI-2, Italy

### C.11.1 Description of the code: Cathare2 v2.5\_1

The development of the CATHARE (Code for Analysis of Thermalhydraulics during an Accident of Reactor and safety Evaluation) code was initiated in 1979. It is a joint effort of CEA, IPSN, EDF and FRAMATOME.

The objectives of the code are:

- perform safety analyses with best estimate calculations of thermalhydraulic transients in Pressurized Water Reactors for postulated accidents or other incidents, such as LBLOCA, SBLOCA, SGTR, Loss of RHR, Secondary breaks, Loss of Feed-Water,
- quantify the conservative analyses margin,
- investigate Plant Operating and Accident Management Procedures,
- be used as a plant analyzer, in a full scope training simulator providing real time calculation.

Its applications are limited to transients during which no severe damage occurs to fuel rods. The code is based on a 2-fluid 6-equation model. The presence of non condensable gases (such as nitrogen, hydrogen, air) can be modeled by one to four additive transport equations. A non-volatile component (as boron) and activity can be treated by the code. The code is able to model any kind of experimental facility or PWR (western type and VVER), and is usable for other reactors (fusion reactor, RBMK reactors, BWR, research reactors). At the present time, CATHARE extension for gas reactors (High Temperature Reactor "HTR", Gas Turbine Modular Helium Reactor "GT MHR", etc.) is under way, in particular gas turbine and gas compressor modules will be developed very soon. The code is used for research, safety and design purposes. The applications mainly concern plant system and component designs, the definition and verification of emergency operating procedures, investigations for new types of core management, new reactors and system designs, the preparation and interpretation of experimental programs. For safety analysis, a methodology has been developed in order to evaluate uncertainties on the code predictions.

CATHARE has a modular structure. Several modules can be assembled to represent the primary and secondary circuits of any reactor and of any separate-effect or integral test facility.

The modules are below summarized.

- The 1-D module to describe pipe flow.
- The 1-D module with tee used to represent a main pipe (1-D module) with a lateral branch (tee-branch). The T module predicts phase separation phenomena, and a specific modeling effort has been paid for cases where the flow is stratified in the main pipe.
- The volume module, a two-node module used to describe large size plena with several connections, such as the pressurizer, the accumulator, the steam generator dome or the lower plenum and upper plenum of a PWR. The volume predicts level swell, total or partial fluid stratification and phase separation phenomena at the junctions.
- The 3-D module to describe multidimensional effects in the vessel.

To complete the modeling of the circuits, sub-modules can be connected to the main modules:

- the CCFL module which may be connected at any junctions, or at any vector node of the 1-D module, in order to predict the counter current flow limitation in complex geometries such as the upper core plate and the inlet of SG tubes,
- the multi-layer wall module in which radial conduction is calculated,
- the reflooding model with 2-D heat conduction in the wall or fuel rod for predicting quench front progression: both bottom up quenching and top-down quenching can be predicted,
- the fuel pin thermo-mechanics sub-module, which can predict fuel cladding deformation, creep, rupture, clad oxidation and thermal exchanges,
- heat exchangers between two circuits or between two elements of a circuit,
- the point neutronics module (a 3-D neutronics code can also be coupled to CATHARE),
- the accumulator sub-module,
- sources and sinks, breaks, SGTR,
- 1-node pump,
- pressurizer sub-module based on Volume module with specific features
- valves, safety valves, check valves, flow limiters,
- boundary conditions.

### C.11.2 Description of the input deck

ZION NPP nodalization by Cathare2 v2.5.1 code

General information

A detailed nodalization reproducing each geometrical zone (data permitting) of the NPP geometry and system has been developed. In principle, it should be suitable for different types of transients without changes in the schematization. For this reason the typical scheme for the LB-LOCA analysis (i.e. two channels for the core simulation, etc.) has not fully taken into account.

The Zion NPP nodalization is shown in Fig. C.36, Fig. C.37. The entire input deck consists of more than 2400 nodes. More details regarding the adopted code resources can be found in Table C.15. The nodalization has been developed using from the data available in the RELAP5 nodalization released in the frame of the BEMUSE Project and labeled “zion\_rev2.inp”.

The main peculiarities of the ZION NPP model are hereafter summarized.

- Five independent hydraulic channels (plus the bypass channel) and active thermal structures are used for the core schematization (peripheral, average and hot zones, and hot assembly and hot rod).
- The thermal structures of the core are simulated with WALL component. The axial power profile implemented is derived by RELAP5 input data. The axial profiles of the power density generated by each single pin belonging to the different thermal structures are showed in Fig. C.38. For sake of completeness in Fig. C.39 and Table C.16, it is reported the linear power versus height and also the linear power in the zone 2 and 5 corresponding to the position TOP, 2/3 and BOTTOM of the core.

- The material proprieties embedded in the code are used, with the exception of UO<sub>2</sub> and gap. In these cases the thermal conductivity and capacity, provided with the RELAP5 input deck, have been implemented in the specific subroutines.
- The annular down-comer of the NPP, where the four cold legs joined to the RPV, is modeled by 8 components. Four of them are directly connected to the end of the cold legs, the others model the portion (1/8 of the circular sector without the CL connection).
- Each of the 4 RCP/SG modules is explicitly modeled. The explicit model has been adopted for coherence with the Relap5 input deck and considering the objective to develop a multi purpose nodalization. Four loops are identical and they are modeled with the same schematization.
- The hydro-accumulators are simulated with proper ACCU components. The line connecting the hydro-accumulators and the CL has been included in the specification of the component.
- The LPIS system is modeled with a source component in which the mass flow, as function of the pressure and the temperature of the liquid, is defined with proper REALIST command.
- The break is connected to the loop #2. The break tubes have been linked to CL 2 through a TEE-BRANCH component. It is modeled by two axial component and a valve component linked between them.
- The PRZ is connected to the hot leg of loop 1 through a TEE BRANCH component. The surge line is modeled with an axial component. The option PRSRIZER has been enabled: this increases the heat transfer between upper and lower sub-volumes in the PRZ element during steady-state calculation, in order to reduce the time constants associated with PRZ dynamics.
- Each of four steam generators has been modeled separately, but the SL have not been modeled and they are simulated with a BCONDIT component directly connected to the dome of the SG.
- The pumps have been modeled with a PUMPCHAR operator linked to the CL. The data of the pump were taken directly by the RELAP5 nodalization.
- The steady state is performed running the a null transient of 500s without any control system: the results obtained demonstrate that the nodalization reaches a stable steady state.
- The special gadget bottom-top REFLOOD has been developed and activated during the LB-LOCA transient.



#	PARAMETER	VALUE
<b>HYDRAULIC ELEMENTS (Cathare2 V2.5)</b>		
1	Total Number of Hydraulic Modules (primary side)	55
	Total Number of Scalar Meshes (primary side)	1954
	Total Number of Hydraulic Modules (secondary side)	24
	Total Number of Scalar Meshes (secondary side)	476
	TOTAL NUMBER OF HYDRAULIC MODULES	79
	TOTAL NUMBER OF SCALAR MESHES	2430
2	Number of Junction (primary side)	95
	Number of Junction (secondary side)	24
	NUMBER OF JUNCTIONS	119
<b>HEAT STRUCTURES (Cathare2 V2.5)</b>		
3	NUMBER OF HEAT STRUCTURES (not including the zone — Utubes and risers – of the heat exchange primary to secondary side)	41
4	TOTAL NUMBER OF MESH POINTS	12017
5	NUMBER OF CORE ACTIVE STRUCTURES – AXIAL	40
6	NUMBER OF CORE ACTIVE STRUCTURES – RADIAL	12
7	NUMBER OF EXCHANGE COMPONENTS (the zone — Utubes and risers – of the heat exchange primary to secondary side)	8
8	NUMBER OF MESHES IN THE EXCHANGE COMPONENTS (the zone — Utubes and risers – of the heat exchange primary to secondary side)	1824

Table C.15: Overview of Cathare2 code resources

L (m)	AVERAGE ZONE Linear Power(kW/m)	HOT ROD Linear Power (kW/m)	Position
0.3	16.69698	25.04541	Bottom of the core
2.44	26.70725	40.06082	2/3 of the core
3.36	15.94776	23.92164	Top of the core

Table C.16: Maximum linear heat generation rates (kW/m) for zones 2 and 5 in the locations required for the submission results

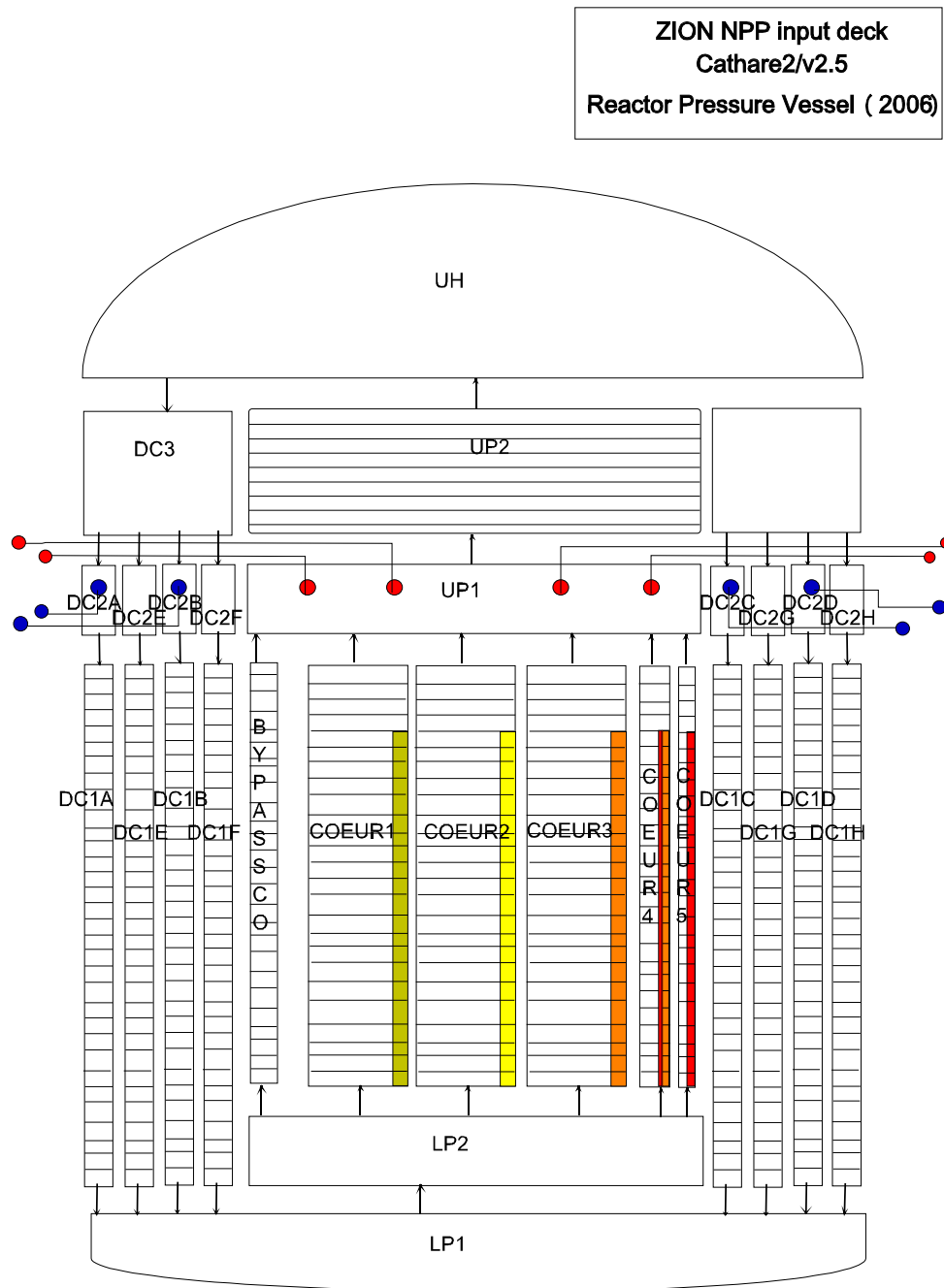
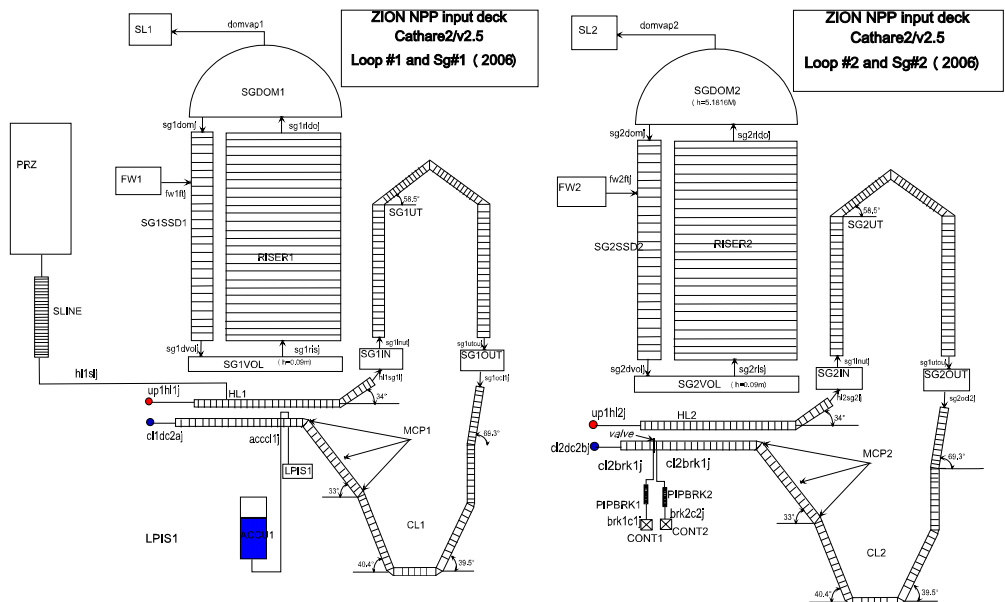
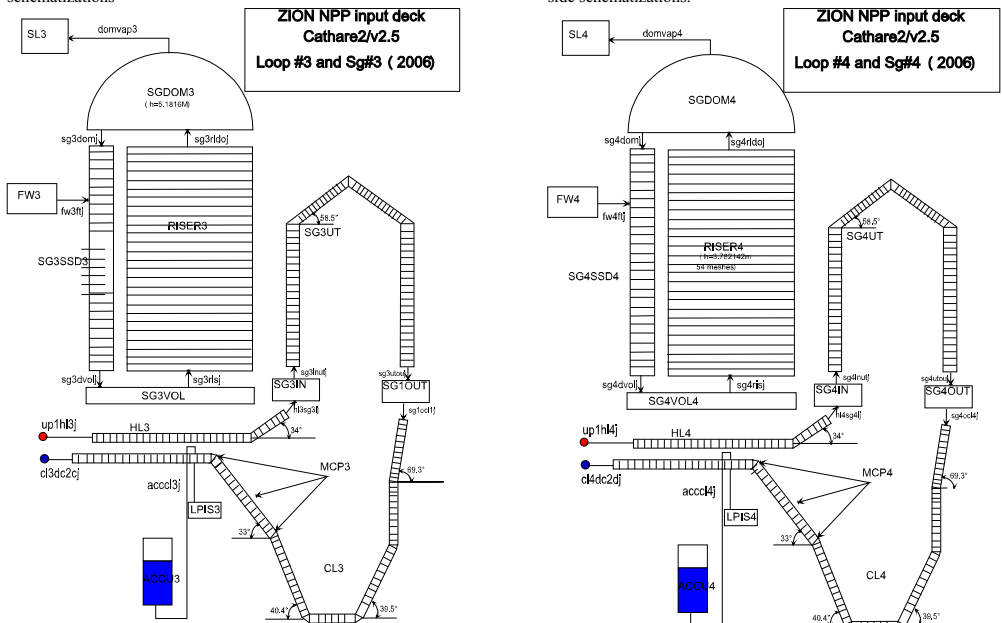


Figure C.36: Vessel nodalization



(a) SG #1 and loop #1 primary side and SG #1 housing secondary side schematizations. (b) SG #2 and loop #2 primary side and SG #2 housing secondary side schematizations.



(c) SG #3 and loop #3 primary side and SG #3 housing secondary side schematizations. (d) SG #4 and loop #4 primary side and SG #4 housing secondary side schematizations.

Figure C.37: Loops nodalization

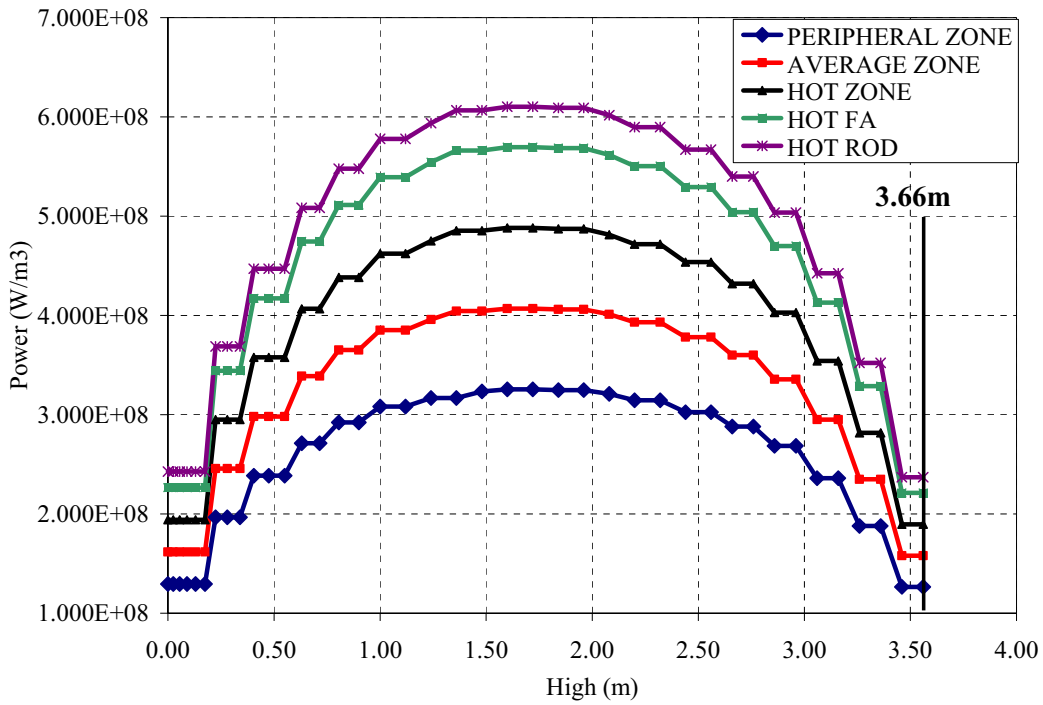


Figure C.38: Power generation.

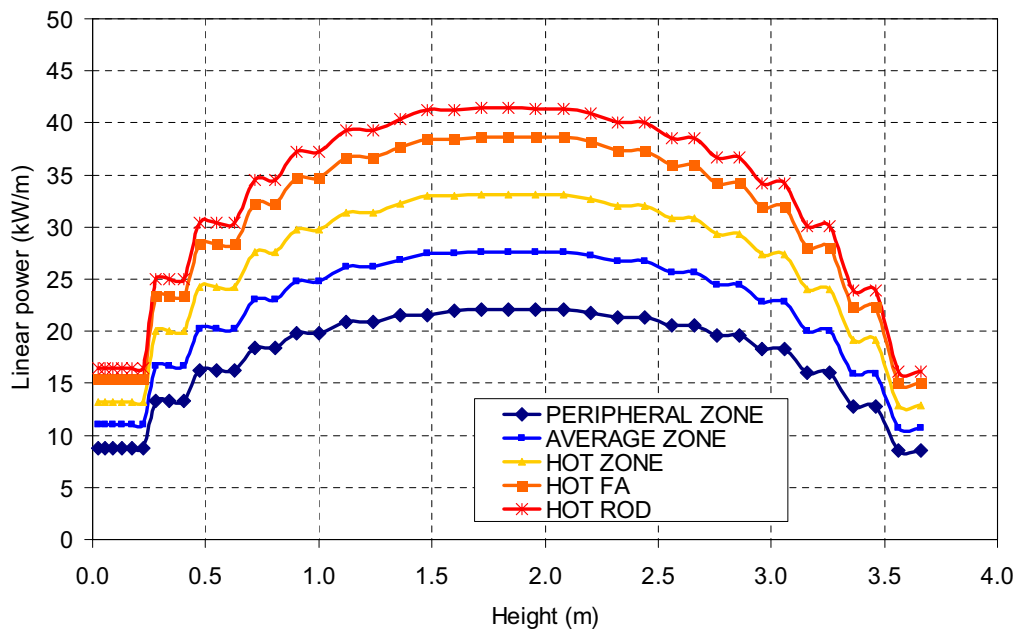


Figure C.39: Linear power generation.

## C.12 UPC, Spain

### C.12.1 Description of the code: RELAP5/MOD3.3

The code used is RELAP5, developed at IDAHO NATIONAL ENGINEERING LABORATORY (INEL) for the US Nuclear Regulatory Commission (NRC). Different versions of RELAP5 have been internationally validated through different international programs (ICAP, CAMP, etc.). The version used for this analysis is RELAP5/MOD3.3, the last version released from CAMP (Code Applications and Maintenance Program). The objective of the RELAP5/MOD3.3 development program was to develop a code version suitable for the analysis of all transients and postulated accidents, including both large and small break LOCA. The results of the code calculations have been compared with an experimental data base of IET and SET to obtain a qualitative and quantitative evaluation of how the code simulates the phenomena of interest and its applicability to the specific scenario.

### C.12.2 Description of the input deck

Modifications performed on the R5 - input deck supplied for BEMUSE phase IV:

- Core Nodalization
  - Two core channels:
    - \* Pipe 435 with peripheral and average fuel heat structures associated (HSs zones 1 and 2)
    - \* Pipe 436 with hot fuel heat structures associated (HSs 3, 4 and 5)
  - Area of the hydrodynamic channels was calculated according to the number of rods associated.
  - Cross flow junctions at the 18 nodes of the core pipes with no loss coefficients input.
  - Bundle option activated in both hydrodynamic components and heat structures.
  - Reflood activated using option 1 of R5 code.
- Downcomer Nodalization
  - 4 downcomers, one per loop.
  - Cross flow junctions at all nodes except for the inner - cold leg connection. itemVolume in order to avoid unrealistic fluid bypass, no loss coefficients input.
- Reflood options
  - Reflood activated using option 1 of R5 code.
- Break Nodalization
  - Trip valves type with no loss coefficients.
  - Ransom-Trapp choked flow model with default code coefficients.
- Gap / fuel
  - Hot dimensions for all fuel rods.
  - No use of gap conductance model: thermal conductivity is introduced by means of a table.

- CCFL

- CCFL option activated in core to upper tie plate junctions. Wallis correlation and values given in the specifications document were used.

Bundle option was activated in both hydrodynamic component and heat structures for SG U-tubes secondary side and for the core channels.

Accumulators are isolated when their level falls below 0.14 m in order to avoid non condensable in the primary system.

The input deck runs 1400 seconds of steady state and 600 seconds of transient.

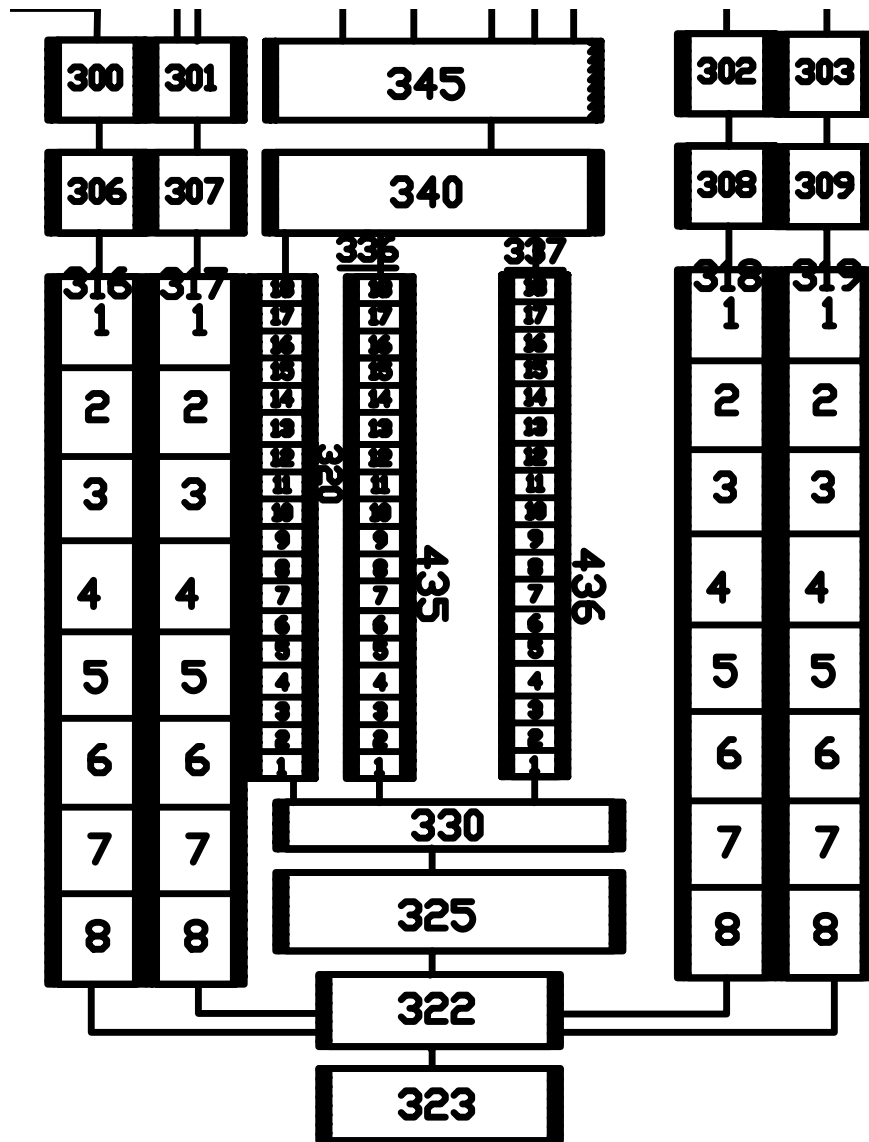


Figure C.40: UPC — Core nodalization

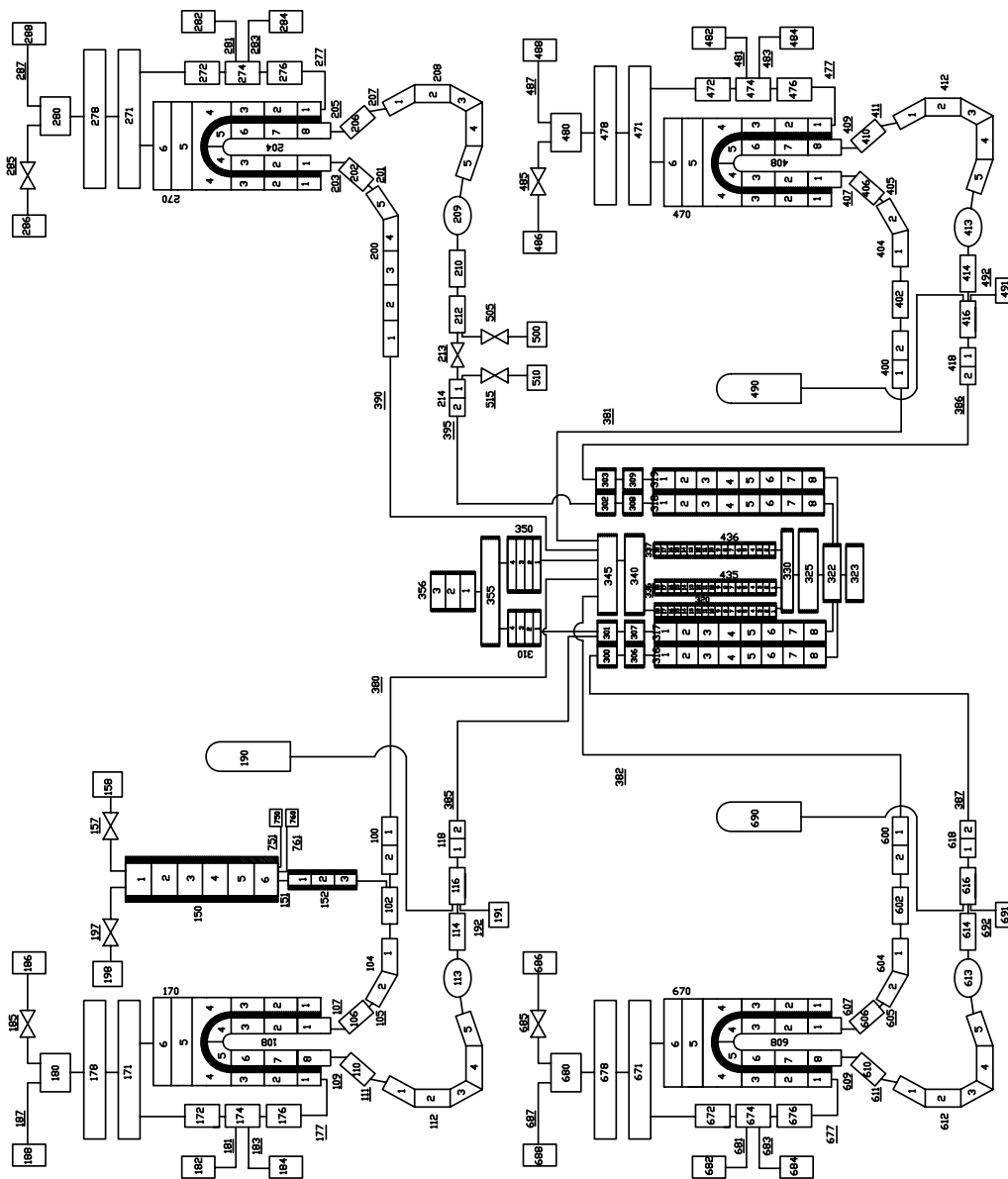


Figure C.41: UPC — Nodalization sketch



APPENDIX D

# Steady state achievement

**Coordinators:** F.Reventós (UPC), M.Pérez (UPC), L. Batet (UPC), R. Pericas (UPC)

**Participating Organizations and Authors**

AEKI, Hungary	I. Trosztel, I. Tóth
CEA, France	P. Bazin, A. de Crécy, P. Germain
FSUE EDO GUIDROPRESS, Russia	S. Borisov
GRS, Germany	H. Glaeser, T. Skorek
IRSN, France	J. Joucla, P. Probst
JNES, Japan	A. Ui
KAERI, South Korea	B. D. Chung
KINS, South Korea	D.Y. Oh
NRI-1, Czech Republic	M. Kyncl, R. Pernica
PSI, Switzerland	A. Manera
UNIPI-1, Italy	F. D'Auria, A. Petruzzi
UNIPI-2, Italy	F. D'Auria, A. Del Nevo
UPC, Spain	M. Pérez, F. Reventós, L. Batet



## D.1 AEKI, Hungary

Pressure distribution values for AEKI group are in Table D.1 and depicted in Figure D.1 Reference curve built by coordinators as participants agreed on the 5th meeting.

N°	Position along the loop	Calculated value (MPa)
1	Hot leg inlet HL IN	15,49
2	Hot leg outlet HL OUT	15,48
3	Steam generator inlet plenum SG IN	15,49
4	U-tube top UT Top	15,37
5	Steam generator outlet plenum SG OUT	15,37
6	Downstream SG outlet nozzle OUT SG NOZZLE	15,32
7	Bottom of loop seal LOOP SEAL	15,34
8	Pump inlet PUMP IN	15,30
9	Pump outlet PUMP OUT	15,86
10	Cold leg inlet CL IN	15,86
11	Cold leg outlet CL OUT	15,81
12	Lower plenum (0.2 m from bottom of vessel) LP	15,74
13	Bottom of active core BAF	15,73
14	Top of active core TAF	15,59

Table D.1: AEKI — Pressure distribution along the loop

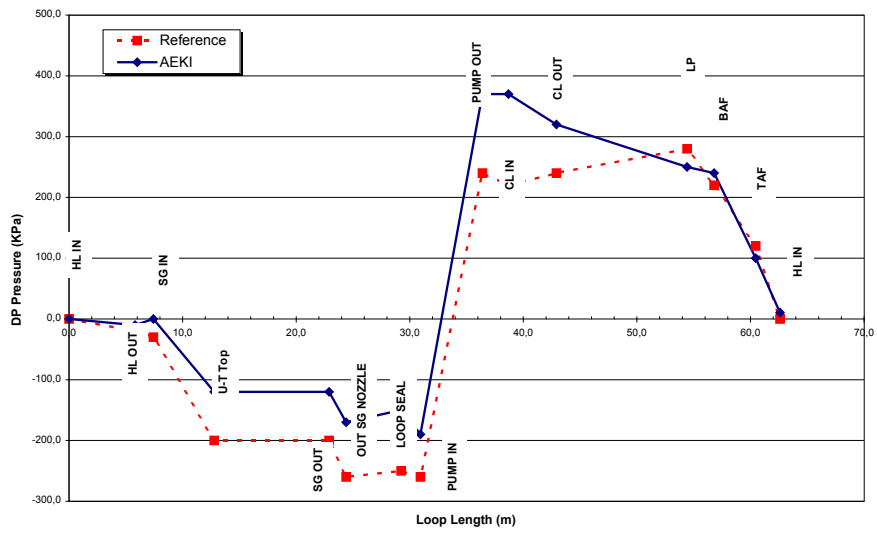


Figure D.1: AEKI — Normalized pressure distribution versus loop length

N°		Unit	DATA
<b>Nodalization development</b>			
1	Primary circuit volume (with pressurizer, WITHOUT accumulators) - volume of the pipes	$m^3$	346,14
2	Secondary circuit volume - volume of the pipes (4 SG)	$m^3$	825,66
4	Core heat transfer surface area	$m^2$	4848,5
5	SG U-tubes heat transfer external surface area (without tube sheet) (4 SG)	$m^3$	20800
6	Core heat transfer volume (volume surrounding active core) (coolant volume)	$m^3$	17,4
7	SG U-tubes heat transfer volume (without tube sheet) (U-tubes structure volume)	$m^3$	48,4
8	Maximum of the axial power distribution for the average rod in average channel (zone 2)	kW/m	27
9	Maximum of the axial power distribution for the hot rod in hot fuel assembly (zone 5)	kW/m	40,5
<b>Steady State</b>			
1	Core power	MW	3250,2
2	Heat transfer in the steam generators (4 loops)	MW	3260,5
3	Primary system hot leg pressure	MPa	15,49
4	Pressurizer pressure (top volume)	MPa	15,4
5	Steam generator 1 exit pressure	MPa	6,705
6	Accumulator 1 pressure	MPa	4,14
7	Intact HL 1 temperature (near vessel)	K	603,2
8	Intact CL 1 temperature (near vessel)	K	571,6
9	Reactor vessel downcomer temperature	K	571,6
10	Broken loop HL temperature (near vessel)	K	603,2
11	Broken loop CL temperature (near vessel)	K	571,5
12	Pressurizer temperature (lower volume)	K	617,4
13	Rod surface temperature (hot rod in hot channel , 1.6 - 1.8 m)	K	621,3
14	Upper header temperature	K	570,5
15	Reactor coolant pump of loop 1 velocity	rpm	1176
16	Reactor pressure vessel pressure loss	kPa	319,4
17	Core pressure loss	kPa	153,4
18	Primary system total loop pressure loss	kPa	603,6
19	Steam generator 1 pressure loss	kPa	118,5
20	Primary system total mass inventory (with pressurizer, without accumulators)	kg	228990
21	Steam generator 1 total mass inventory	kg	72590
22	Primary system total loop coolant mass flow	kg/s	17353
23	Steam generator 1 feedwater mass flow	kg/s	438
24	Core coolant mass flow	kg/s	17115
25	Core bypass mass flow (LP-UP)	kg/s	220,7
26	Pressurizer level (collapsed)	m	8,81
27	Secondary side downcomer level	m	11,94

Table D.2: AEKI — Nodalization and steady state data table

## D.2 CEA, France

Pressure distribution values for CEA group are in Table D.3 and depicted in Figure D.2 Reference curve built by coordinators as participants agreed on the 5th meeting.

N°	Position along the loop		Calculated value (MPa)
1	Hot leg inlet	HL IN	15,633
2	Hot leg outlet	HL OUT	15,615
3	Steam generator inlet plenum	SG IN	15,64
4	U-tube top	UT Top	15,425
5	Steam generator outlet plenum	SG OUT	15,409
6	Downstream SG outlet nozzle	OUT SG NOZZLE	15,364
7	Bottom of loop seal	LOOP SEAL	15,383
8	Pump inlet	PUMP IN	15,362
9	Pump outlet	PUMP OUT	15,932
10	Cold leg inlet	CL IN	15,932
11	Cold leg outlet	CL OUT	15,898
12	Lower plenum (0.2 m from bottom of vessel)	LP	15,851
13	Bottom of active core	BAF	15,777
14	Top of active core	TAF </td <td>15,69</td>	15,69

Table D.3: CEA — Pressure distribution along the loop

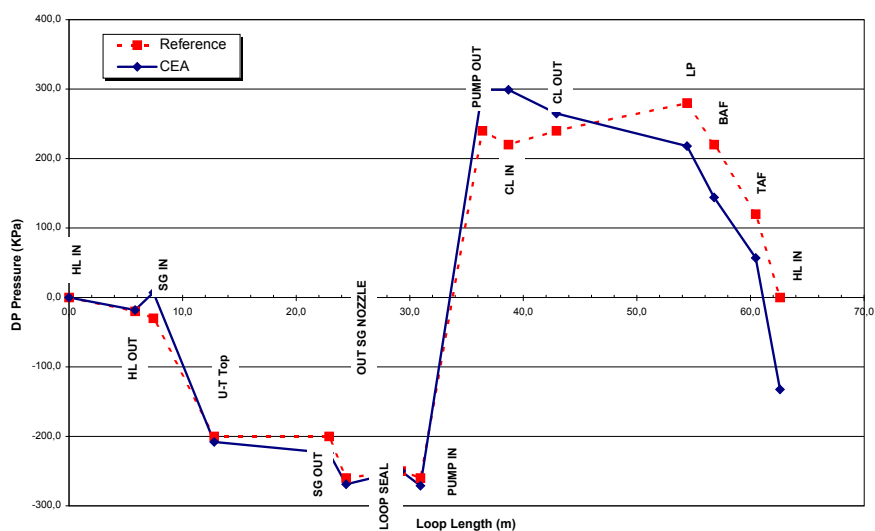


Figure D.2: CEA — Normalized pressure distribution versus loop length

N°		Unit	DATA
<b>Nodalization development</b>			
1	Primary circuit volume (with pressurizer, WITHOUT accumulators) - volume of the pipes	$m^3$	352,7
2	Secondary circuit volume - volume of the pipes	$m^3$	662,5
4	Core heat transfer surface area	$m^2$	4844
5	SG U-tubes heat transfer external surface area (without tube sheet)	$m^2$	19295
6	Core heat transfer volume (volume surrounding active core)	$m^3$	18,16
7	SG U-tubes heat transfer volume (without tube sheet)	$m^3$	84,1
8	Maximum of the axial power distribution for the average rod in average channel (zone 2)	kW/m	27,56
9	Maximum of the axial power distribution for the hot rod in hot fuel assembly (zone 5)	kW/m	41,34
<b>Steady State</b>			
1	Core power	MW	3250
2	Heat transfer in the steam generators (4 loops)	MW	3263,6
3	Primary system hot leg pressure	MPa	15,633
4	Pressurizer pressure (top volume)	MPa	15,533
5	Steam generator 1 exit pressure	MPa	6,72
6	Accumulator 1 pressure	MPa	4,137
7	Intact HL 1 temperature (near vessel)	K	602,63
8	Intact CL 1 temperature (near vessel)	K	571,65
9	Reactor vessel downcomer temperature	K	571,62
10	Broken loop HL temperature (near vessel)	K	602,64
11	Broken loop CL temperature (near vessel)	K	571,66
12	Pressurizer temperature (lower volume)	K	618,09
13	Rod surface temperature (hot rod in hot channel , 1.6 - 1.8 m)	K	620,94
14	Upper header temperature	K	575,75
15	Reactor coolant pump of loop 1 velocity	rpm	1134
16	Reactor pressure vessel pressure loss	kPa	264,6
17	Core pressure loss	kPa	166,6
18	Primary system total loop pressure loss	kPa	569,7
19	Steam generator 1 pressure loss	kPa	230,2
20	Primary system total mass inventory (with pressurizer, without accumulators)	kg	231296
21	Steam generator 1 total mass inventory	kg	48540
22	Primary system total loop coolant mass flow	kg/s	17298
23	Steam generator 1 feedwater mass flow	kg/s	440
24	Core coolant mass flow	kg/s	17058
25	Core bypass mass flow (LP-UP)	kg/s	217,5
26	Pressurizer level (collapsed)	m	8,82
27	Secondary side downcomer level	m	12,2

Table D.4: CEA — Nodalization and steady state data table

### D.3 EDO, Russia

Reference curve built by coordinators as participants agreed on the 5th meeting.

Power plant geometry is assumed according to [1]. Initial and boundary conditions are assumed according to the data presented in [1]: reactor plant initial power, primary and secondary pressure, reactor inlet temperature, pressurizer coolant level are from Tables. Working equipment parameter variation (frequency of RCP revolutions, boron solution supply from low pressure pumps) was simulated according to Tables.

The TECH-M-97 code simulates the equipment characteristic only of the WWER plant therefore during a fulfillment LB LOCA calculations the horizontal steam generator was simulated. Geometrical characteristic of steam generators (volume, heat transfer surface area, steam and water volume relation), secondary coolant parameters (pressure, feedwater flowrate and temperature) are assumed according to [1]. Maximum value of linear heat flux for a hot fuel rod in hot FA and average channel amounts to 41,6 and 27,6 kW/m, respectively. Table 5 contains data about the nodalization development and the steady state achievement. Variation of reactor plant main parameters under steady-state conditions (primary and secondary side pressure, primary system total loop coolant mass flow, pressurizer collapsed level) is presented in coming Figures D.3. Parameter variation is not above 0,6/100 within 100 s of the process.

Pressure distribution values for EDO group are in Table D.5 and depicted in Figure D.4

N°	Position along the loop	Calculated value (MPa)
1	Hot leg inlet HL IN	15.5
2	Hot leg outlet HL OUT	15.491
3	Steam generator inlet plenum SG IN	15.469
4	U-tube top UT Top	15.286
5	Steam generator outlet plenum SG OUT	15.245
6	Downstream SG outlet nozzle OUT SG NOZZLE	15.26
7	Bottom of loop seal LOOP SEAL	15.265
8	Pump inlet PUMP IN	15.255
9	Pump outlet PUMP OUT	15.812
10	Cold leg inlet CL IN	15.812
11	Cold leg outlet CL OUT	15.8
12	Lower plenum (0.2 m from bottom of vessel) LP	15.71
13	Bottom of active core BAF	15.708
14	Top of active core TAF	15.545

Table D.5: EDO — Pressure distribution along the loop



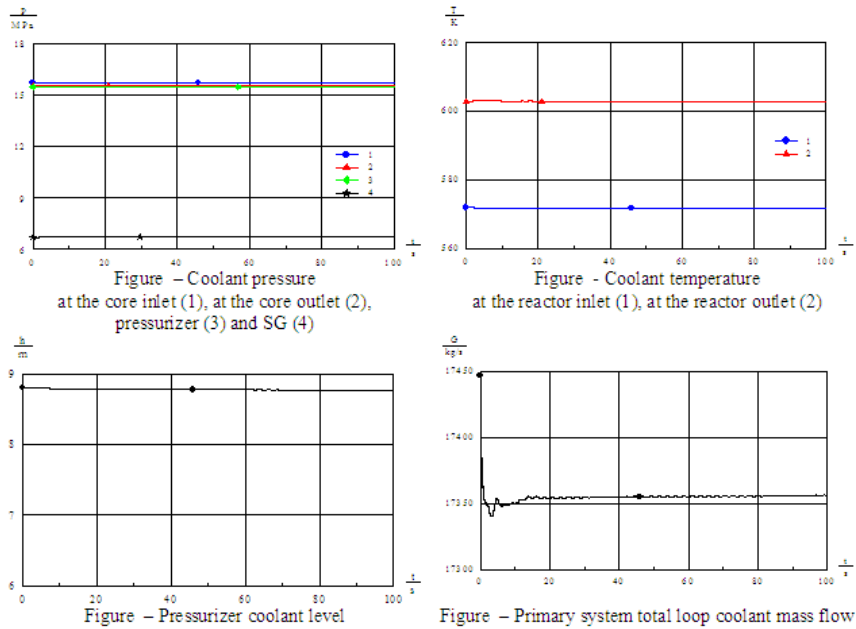


Figure D.3: Relevant time trends.

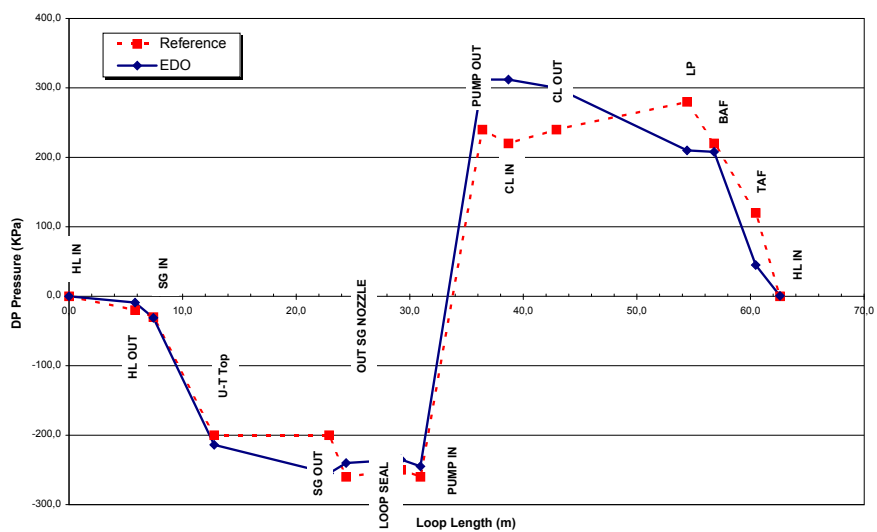


Figure D.4: EDO — Normalized pressure distribution versus loop length

N°		Unit	DATA
<b>Nodalization development</b>			
1	Primary circuit volume (with pressurizer, WITHOUT accumulators) - volume of the pipes	$m^3$	353,3
2	Secondary circuit volume - volume of the pipes	$m^3$	664,664
4	Core heat transfer surface area	$m^2$	4843,98
5	SG U-tubes heat transfer external surface area (without tube sheet)	$m^2$	20309,18
6	Core heat transfer volume (volume surrounding active core)	$m^3$	18,154
7	SG U-tubes heat transfer volume (without tube sheet)	$m^3$	21,695
8	Maximum of the axial power distribution for the average rod in average channel (zone 2)	kW/m	27,6
9	Maximum of the axial power distribution for the hot rod in hot fuel assembly (zone 5)	kW/m	41,6
<b>Steady State</b>			
1	Core power	MW	3250,00
2	Heat transfer in the steam generators (4 loops)	MW	3250,00
3	Primary system hot leg pressure	MPa	15,50
4	Pressurizer pressure (top volume)	MPa	15,45
5	Steam generator 1 exit pressure	MPa	6,71
6	Accumulator 1 pressure	MPa	4,10
7	Intact HL 1 temperature (near vessel)	K	603,08
8	Intact CL 1 temperature (near vessel)	K	571,91
9	Reactor vessel downcomer temperature	K	571,91
10	Broken loop HL temperature (near vessel)	K	603,08
11	Broken loop CL temperature (near vessel)	K	571,91
12	Pressurizer temperature (lower volume)	K	617,5
13	Rod surface temperature (hot rod in hot channel , 1.6 - 1.8 m)	K	620,75
14	Upper header temperature	K	603,05
15	Reactor coolant pump of loop 1 velocity	rpm	1146,5
16	Reactor pressure vessel pressure loss	kPa	266,50
17	Core pressure loss	kPa	163
18	Primary system total loop pressure loss	kPa	569,4
19	Steam generator 1 pressure loss	kPa	220
20	Primary system total mass inventory (with pressurizer, without accumulators)	kg	211600
21	Steam generator 1 total mass inventory	kg	42800
22	Primary system total loop coolant mass flow	kg/s	17357
23	Steam generator 1 feedwater mass flow	kg/s	440
24	Core coolant mass flow	kg/s	17092
25	Core bypass mass flow (LP-UP)	kg/s	265
26	Pressurizer level (collapsed)	m	8,8
27	Secondary side downcomer level	m	2,4

Table D.6: EDO — Nodalization and steady state data table

### D.3.1 References

8. M. Pérez, F. Reventós, Ll. Batet, "Phase 4 of BEMUSE Programme: Simulation of a LB-LOCA in ZION Nuclear Power Plant. Input and Output Specifications" rev. 3, Universitat Politècnica de Catalunya, Spain, 2007

## D.4 GRS, Germany

Pressure distribution values for GRS group are in Table D.7 and depicted in Figure D.5 Reference curve built by coordinators as participants agreed on the 5th meeting.

N°	Position along the loop		Calculated value (MPa)
1	Hot leg inlet	HL IN	15,51
2	Hot leg outlet	HL OUT	15,5
3	Stem generator inlet plenum	SG IN	15,51
4	U-tube top	UT Top	15,32
5	Steam generator outlet plenum	SG OUT	15,3
6	Downstream SG outlet nozzle	OUT SG NOZZLE	15,25
7	Bottom of loop seal	LOOP SEAL	15,26
8	Pump inlet	PUMP IN	15,23
9	Pump outlet	PUMP OUT	15,79
10	Cold leg inlet	CL IN	15,79
11	Cold leg outlet	CL OUT	15,78
12	Lower plenum (0.2 m from bottom of vessel)	LP	15,75
13	Bottom of active core	BAF	15,73
14	Top of active core	TAF	15,62

Table D.7: GRS — Pressure distribution along the loop

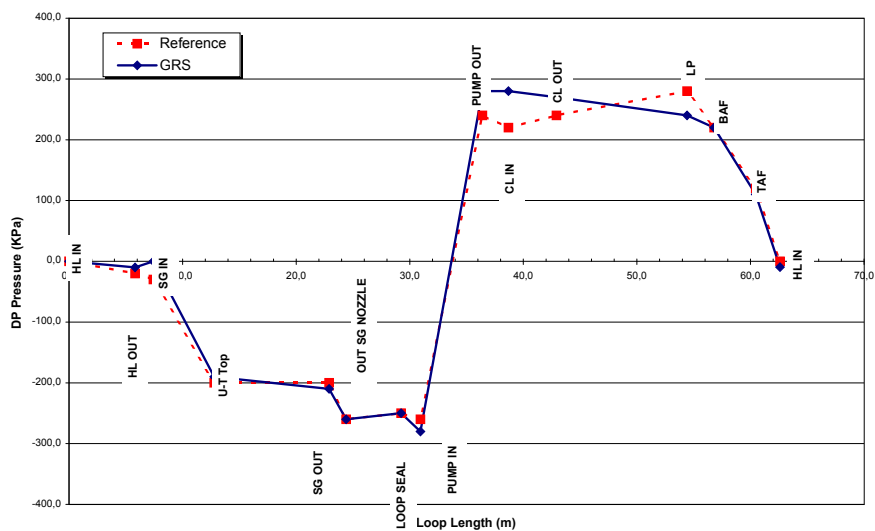


Figure D.5: GRS — Normalized pressure distribution versus loop length

N°		Unit	DATA
<b>Nodalization development</b>			
1	Primary circuit volume (with pressurizer, WITHOUT accumulators) - volume of the pipes	$m^3$	346,1
2	Secondary circuit volume - volume of the pipes	$m^3$	818,2
4	Core heat transfer surface area	$m^2$	4844
5	SG U-tubes heat transfer external surface area (without tube sheet)	$m^2$	16704
6	Core heat transfer volume (volume surrounding active core)	$m^3$	17,42
7	SG U-tubes heat transfer volume (without tube sheet)	$m^3$	20,14
8	Maximum of the axial power distribution for the average rod in average channel (zone 2)	kW/m	26,92
9	Maximum of the axial power distribution for the hot rod in hot fuel assembly (zone 5)	kW/m	40,4
<b>Steady State</b>			
1	Core power	MW	3250
2	Heat transfer in the steam generators (4 loops)	MW	3260,8
3	Primary system hot leg pressure	MPa	15,51
4	Pressurizer pressure (top volume)	MPa	15,42
5	Steam generator 1 exit pressure	MPa	6,71
6	Accumulator 1 pressure	MPa	4,146
7	Intact HL 1 temperature (near vessel)	K	603,1
8	Intact CL 1 temperature (near vessel)	K	571,5
9	Reactor vessel downcomer temperature	K	571,5
10	Broken loop HL temperature (near vessel)	K	603,1
11	Broken loop CL temperature (near vessel)	K	571,5
12	Pressurizer temperature (lower volume)	K	617,8
13	Rod surface temperature (hot rod in hot channel , 1.6 - 1.8 m)	K	622,1
14	Upper header temperature	K	598,9
15	Reactor coolant pump of loop 1 velocity	rpm	1176
16	Reactor pressure vessel pressure loss	kPa	266
17	Core pressure loss	kPa	134
18	Primary system total loop pressure loss	kPa	604,2
19	Steam generator 1 pressure loss	kPa	243
20	Primary system total mass inventory (with pressurizer, without accumulators)	kg	228950
21	Steam generator 1 total mass inventory	kg	72890
22	Primary system total loop coolant mass flow	kg/s	17352
23	Steam generator 1 feedwater mass flow	kg/s	439
24	Core coolant mass flow	kg/s	17113
25	Core bypass mass flow (LP-UP)	kg/s	221
26	Pressurizer level (collapsed)	m	8,8
27	Secondary side downcomer level	m	11,94

Table D.8: GRS — Nodalization and steady state data table

## D.5 IRSN, France

Pressure distribution values for IRSN group are in Table D.9 and depicted in Figure D.6 Reference curve built by coordinators as participants agreed on the 5th meeting.

N°	Position along the loop		Calculated value (MPa)
1	Hot leg inlet	HL IN	15,55
2	Hot leg outlet	HL OUT	15,53
3	Stem generator inlet plenum	SG IN	15,53
4	U-tube top	UT Top	15,34
5	Steam generator outlet plenum	SG OUT	15,33
6	Downstream SG outlet nozzle	OUT SG NOZZLE	15,28
7	Bottom of loop seal	LOOP SEAL	15,30
8	Pump inlet	PUMP IN	15,24
9	Pump outlet	PUMP OUT	15,79
10	Cold leg inlet	CL IN	15,77
11	Cold leg outlet	CL OUT	15,79
12	Lower plenum (0,2 m from bottom of vessel)	LP	15,84
13	Bottom of active core	BAF	15,79
14	Top of active core	TAF	15,69

Table D.9: IRSN — Pressure distribution along the loop

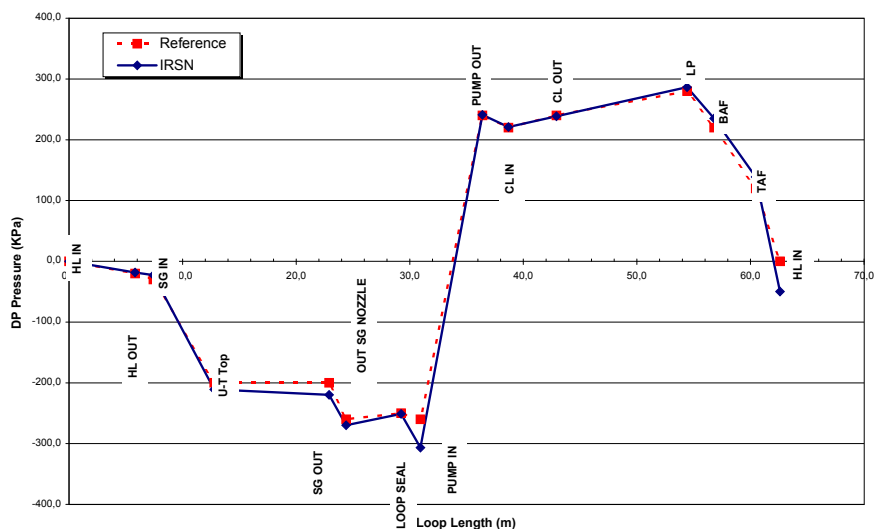


Figure D.6: IRSN — Normalized pressure distribution versus loop length

N°		Unit	DATA
<b>Nodalization development</b>			
1	Primary circuit volume (with pressurizer, WITHOUT accumulators) - volume of the pipes	$m^3$	353
2	Secondary circuit volume - volume of the pipes	$m^3$	668
4	Core heat transfer surface area	$m^2$	4.481
5	SG U-tubes heat transfer external surface area (without tube sheet)	$m^2$	17.897
6	Core heat transfer volume (volume surrounding active core)	$m^3$	20,30
7	SG U-tubes heat transfer volume (without tube sheet)	$m^3$	87,84
8	Maximum of the axial power distribution for the average rod in average channel (zone 2)	kW/m	26,94
9	Maximum of the axial power distribution for the hot rod in hot fuel assembly (zone 5)	kW/m	40,42
<b>Steady State</b>			
1	Core power	MW	3250
2	Heat transfer in the steam generators (4 loops)	MW	3248
3	Primary system hot leg pressure	MPa	15,55
4	Pressurizer pressure (top volume)	MPa	15,44
5	Steam generator 1 exit pressure	MPa	7,30
6	Accumulator 1 pressure	MPa	4,14
7	Intact HL 1 temperature (near vessel)	K	602,7
8	Intact CL 1 temperature (near vessel)	K	571,8
9	Reactor vessel downcomer temperature	K	571,8
10	Broken loop HL temperature (near vessel)	K	602,7
11	Broken loop CL temperature (near vessel)	K	571,8
12	Pressurizer temperature (lower volume)	K	617,4
13	Rod surface temperature (hot rod in hot channel , 1.6 - 1.8 m)	K	621,1
14	Upper header temperature	K	575,9
15	Reactor coolant pump of loop 1 velocity	rpm	1146,0
16	Reactor pressure vessel pressure loss	kPa	108
17	Core pressure loss	kPa	102
18	Primary system total loop pressure loss	kPa	239
19	Steam generator 1 pressure loss	kPa	197
20	Primary system total mass inventory (with pressurizer, without accumulators)	kg	305522
21	Steam generator 1 total mass inventory	kg	49530
22	Primary system total loop coolant mass flow	kg/s	17345
23	Steam generator 1 feedwater mass flow	kg/s	453
24	Core coolant mass flow	kg/s	17109
25	Core bypass mass flow (LP-UP)	kg/s	216
26	Pressurizer level (collapsed)	m	8,87
27	Secondary side downcomer level	m	12,50

Table D.10: IRSN — Nodalization and steady state data table

## D.6 JNES, Japan

Pressure distribution values for JNES group are in Table D.11 and depicted in Figure D.7 Reference curve built by coordinators as participants agreed on the 5th meeting.

N°	Position along the loop		Calculated value (MPa)
1	Hot leg inlet	HL IN	15,528
2	Hot leg outlet	HL OUT	15,518
3	Steam generator inlet plenum	SG IN	15,529
4	U-tube top	UT Top	15,349
5	Steam generator outlet plenum	SG OUT	15,347
6	Downstream SG outlet nozzle	OUT SG NOZZLE	15,283
7	Bottom of loop seal	LOOP SEAL	15,294
8	Pump inlet	PUMP IN	15,266
9	Pump outlet	PUMP OUT	15,832
10	Cold leg inlet	CL IN	15,806
11	Cold leg outlet	CL OUT	15,793
12	Lower plenum (0.2 m from bottom of vessel)	LP	15,821
13	Bottom of active core	BAF	15,737
14	Top of active core	TAF	15,641

Table D.11: JNES — Pressure distribution along the loop

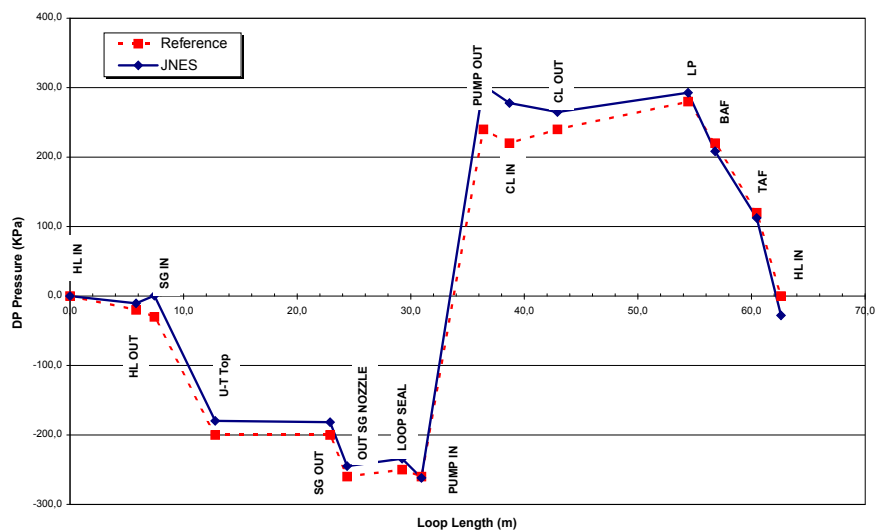


Figure D.7: JNES — Normalized pressure distribution versus loop length

N°		Unit	CALC DATA
<b>Nodalization development</b>			
1	Primary circuit volume (with pressurizer, WITHOUT accumulators) - volume of the pipes	$m^3$	335,517
2	Secondary circuit volume - volume of the pipes	$m^3$	535,060
4	Core heat transfer surface area	$m^2$	4,841E+03
5	SG U-tubes heat transfer external surface area (without tube sheet)	$m^2$	1,913E+04
6	Core heat transfer volume (volume surrounding active core)	$m^3$	19,379
7	SG U-tubes heat transfer volume (without tube sheet)	$m^3$	22,914
8	Maximum of the axial power distribution for the average rod in average channel (zone 2)	kW/m	27,631
9	Maximum of the axial power distribution for the hot rod in hot fuel assembly (zone 5)	kW/m	41,456
<b>Steady State</b>			
1	Core power	MW	3250,000
2	Heat transfer in the steam generators (4 loops)	MW	3247,801
3	Primary system hot leg pressure	MPa	15,528
4	Pressurizer pressure (top volume)	MPa	15,342
5	Steam generator 1 exit pressure	MPa	4,880
6	Accumulator 1 pressure	MPa	4,140
7	Intact HL 1 temperature (near vessel)	K	602,6
8	Intact CL 1 temperature (near vessel)	K	570,2
9	Reactor vessel downcomer temperature	K	570,3
10	Broken loop HL temperature (near vessel)	K	602,6
11	Broken loop CL temperature (near vessel)	K	570,2
12	Pressurizer temperature (lower volume)	K	617,4
13	Rod surface temperature (hot rod in hot channel , 1.6 - 1.8 m)	K	626,7
14	Upper header temperature	K	606,5
15	Reactor coolant pump of loop 1 velocity	rpm	1096,3
16	Reactor pressure vessel pressure loss	kPa	264,880
17	Core pressure loss	kPa	95,850
18	Primary system total loop pressure loss	kPa	264,880
19	Steam generator 1 pressure loss	kPa	182,180
20	Primary system total mass inventory (with pressurizer, without accumulators)	kg	2,176E+05
21	Steam generator 1 total mass inventory	kg	5,527E+04
22	Primary system total loop coolant mass flow	kg/s	1,700E+04
23	Steam generator 1 feedwater mass flow	kg/s	4,053E+02
24	Core coolant mass flow	kg/s	1,675E+04
25	Core bypass mass flow (LP-UP)	kg/s	2,231E+02
26	Pressurizer level (collapsed)	m	8,736
27	Secondary side downcomer level	m	13,782

Table D.12: JNES — Nodalization and steady state data table



## D.7 KAERI, South Korea

Pressure distribution values for KAERI group are in Table D.13 and depicted in Figure D.8 Reference curve built by coordinators as participants agreed on the 5th meeting.

N°	Position along the loop		Calculated value (MPa)
1	Hot leg inlet	HL IN	15,5377
2	Hot leg outlet	HL OUT	15,5133
3	Stem generator inlet plenum	SG IN	15,477
4	U-tube top	UT Top	15,3659
5	Steam generator outlet plenum	SG OUT	15,3453
6	Downstream SG outlet nozzle	OUT SG NOZZLE	15,2935
7	Bottom of loop seal	LOOP SEAL	15,3043
8	Pump inlet	PUMP IN	15,2954
9	Pump outlet	PUMP OUT	15,8189
10	Cold leg inlet	CL IN	15,8066
11	Cold leg outlet	CL OUT	15,8241
12	Lower plenum (0.2 m from bottom of vessel)	LP	15,7268
13	Bottom of active core	BAF	15,7086
14	Top of active core	TAF	15,618

Table D.13: KAERI — Pressure distribution along the loop

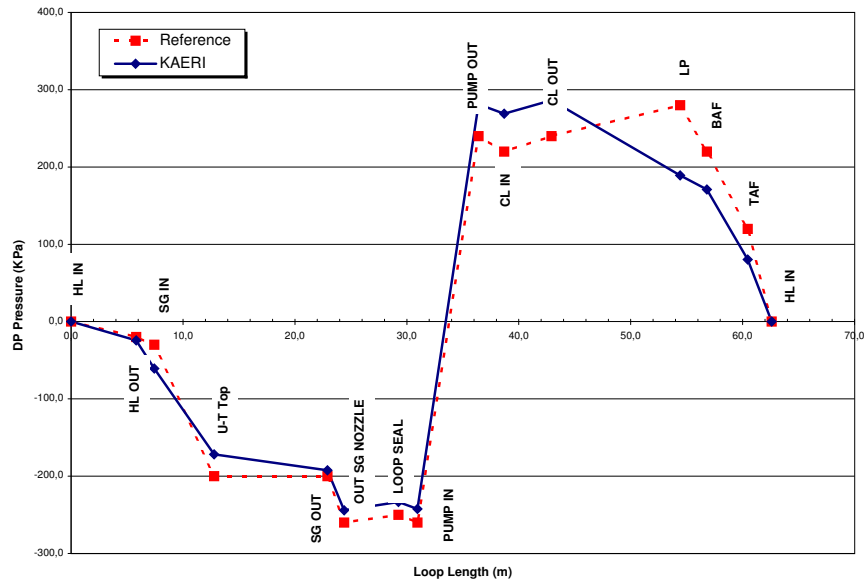


Figure D.8: KAERI — Normalized pressure distribution versus loop length

N°	Quantity	Unit	Calc. data
<b>Nodalization development</b>			
1	Primary circuit volume (with pressurizer)	m <sup>3</sup>	398,625
2	Secondary circuit volume		664,68
4	Core heat transfer surface area	m <sup>2</sup>	4844
5	SG U-tubes heat transfer external surface area (without tube sheet)		19134.9
6	Core heat transfer volume (volume surrounding active core)	m <sup>3</sup>	20.22
7	SG U-tubes heat transfer volume (without tube sheet)		87.85
8	Maximum of the axial power distribution for the average rod in average channel (zone 2)	kW/m	26.94
9	Maximum of the axial power distribution for the hot rod in hot fuel assembly (zone 5)		40.42
<b>Steady State</b>			
1	Core power	MW	3250
2	Heat transfer in the steam generators (4 loops)		3264.9
3	Primary system hot leg pressure	MPa	15.5377
4	Pressurizer pressure		15.5155
5	Steam generator 1 exit pressure		6.7404
6	Accumulator 1 pressure		4.1368
7	Intact HL 1 temperature (near vessel)	K	603.732
8	Intact CL 1 temperature (near vessel)		571.83
9	Reactor vessel downcomer temperature		571.791
10	Broken loop HL temperature (near vessel)		603.708
11	Broken loop CL temperature (near vessel)		571.813
12	Pressurizer temperature (lower volume)		607.505
13	Rod surface temperature (hot rod in hot channel, 1.6-1.8 m)		625.45
14	Upper header temperature		602.402
15	Reactor coolant pump of loop 1 velocity	rpm	1146.49
16	Reactor pressure vessel pressure loss	kPa	286.4
17	Core pressure loss		116.5
18	Primary system total loop pressure loss		1148.7
19	Steam generator 1 pressure loss		159.995
20	Primary system total mass inventory (with pressurizer, without accumulators)	kg	231847
21	Steam generator 1 total mass inventory		48065
22	Primary system total loop coolant mass flow	kg/s	17060.3
23	Steam generator 1 feedwater mass flow		439.23
24	Core coolant mass flow		16746.47
25	Core bypass mass flow (LP-UP)		293.316
26	Pressurizer level (collapsed)	m	8.861542
27	Secondary side or downcomer level		12.88902

Table D.14: KAERI — Nodalization and steady state data table

## D.8 KINS, South Korea

Pressure distribution values for KINS group are in Table D.15 and depicted in Figure D.9 Reference curve built by coordinators as participants agreed on the 5th meeting.

N°	Position along the loop	Calculated value (MPa)
1	Hot leg inlet HL IN	15.5351
2	Hot leg outlet HL OUT	15.5155
3	Steam generator inlet plenum SG IN	15.5122
4	U-tube top UT Top	15.3393
5	Steam generator outlet plenum SG OUT	15.3452
6	Downstream SG outlet nozzle OUT SG NOZZLE	15.2806
7	Bottom of loop seal LOOP SEAL	15.2912
8	Pump inlet PUMP IN	15.2818
9	Pump outlet PUMP OUT	15.7861
10	Cold leg inlet CL IN	15.795
11	Cold leg outlet CL OUT	15.7915
12	Lower plenum (0.2 m from bottom of vessel) LP	15.8283
13	Bottom of active core BAF	15.7503
14	Top of active core TAF	15.6571

Table D.15: KINS — Pressure distribution along the loop

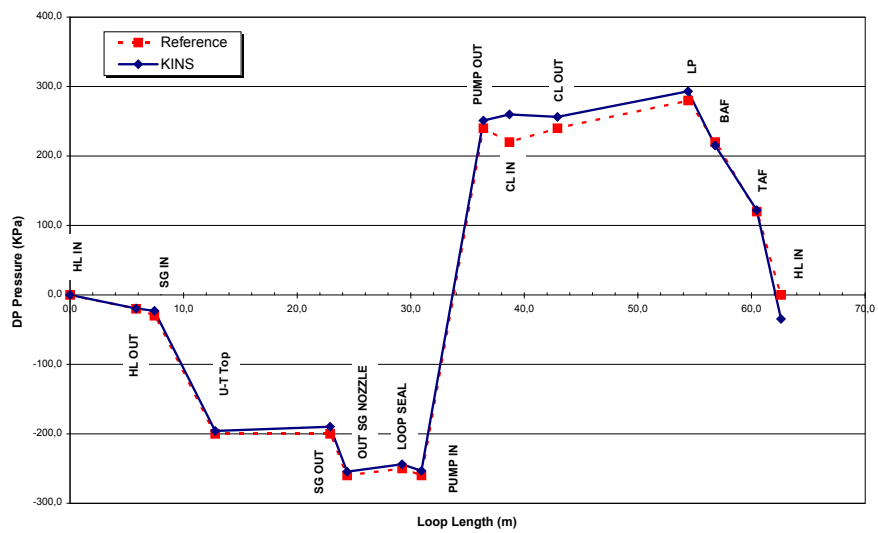


Figure D.9: KINS — Normalized pressure distribution versus loop length

N°	Quantity	Unit	Calc. data
<b>Nodalization development</b>			
1	Primary circuit volume (with pressurizer)	m <sup>3</sup>	352,94
2	Secondary circuit volume		664,68
4	Core heat transfer surface area	m <sup>2</sup>	4847,60
5	SG U-tubes heat transfer external surface area (without tube sheet)		19134,82
6	Core heat transfer volume	m <sup>3</sup>	20,23
7	SG U-tubes heat transfer volume (without tube sheet)		87,87
8	Maximum of the axial power distribution for the average rod in average channel (zone 2)	kW/m	26,95
9	Maximum of the axial power distribution for the hot rod in hot fuel assembly (zone 5)		40,00
<b>Steady State</b>			
1	Primary circuit power balance	MW	3250
2	Secondary circuit power balance		3253,8
3	Primary system hot leg pressure	MPa	15,54
4	Pressurizer pressure		15,52
5	Steam generator 1 exit pressure		6,74
6	Accumulator 1 pressure		4,14
7	Intact HL 1 temperature (near vessel)	K	603,22
8	Intact CL 1 temperature (near vessel)		572,01
9	Reactor vessel downcomer temperature		571,98
10	Broken loop HL temperature (near vessel)		603,22
11	Broken loop CL temperature (near vessel)		571,97
12	Pressurizer temperature		608,08
13	Rod surface temperature (hot rod in hot channel - middle position)		624,71
14	Reactor coolant pump of loop 1 velocity	rpm	1153,08
15	Reactor pressure vessel pressure loss	kPa	133,60
16	Core pressure loss		93,20
17	Primary system total loop pressure loss		513,20
18	Steam generator 1 pressure loss		167,00
19	Primary system total mass inventory (with pressurizer)	kg	2360660,00
20	Steam generator 1 total mass inventory		47789,00
21	Primary system total loop coolant mass flow	kg/s	17366,00
22	Steam generator 1 feedwater mass flow		439,23
23	Core coolant mass flow		17146,20
24	Core bypass mass flow (LP-UP)		219,28
25	Pressurizer level (collapsed)	m	8,84
26	Secondary side or downcomer level		12,43

Table D.16: KINS — Nodalization and steady state data table

## D.9 NRI-1, Czech Republic

Pressure distribution values for NRI-1 group are in Table D.17 and depicted in Figure D.10 Reference curve built by coordinators as participants agreed on the 5th meeting.

N°	Position along the loop		Calculated value (MPa)
1	Hot leg inlet	HL IN	15,5418
2	Hot leg outlet	HL OUT	15,521
3	Stem generator inlet plenum	SG IN	15,5173
4	U-tube top	UT Top	15,3142
5	Steam generator outlet plenum	SG OUT	15,2971
6	Downstream SG outlet nozzle	OUT SG NOZZLE	15,2397
7	Bottom of loop seal	LOOP SEAL	15,251
8	Pump inlet	PUMP IN	15,2417
9	Pump outlet	PUMP OUT	15,7924
10	Cold leg inlet	CL IN	15,799
11	Cold leg outlet	CL OUT	15,7946
12	Lower plenum (0.2 m from bottom of vessel)	LP	15,83
13	Bottom of active core	BAF	15,7567
14	Top of active core	TAF	15,6548

Table D.17: NRI-1 — Pressure distribution along the loop

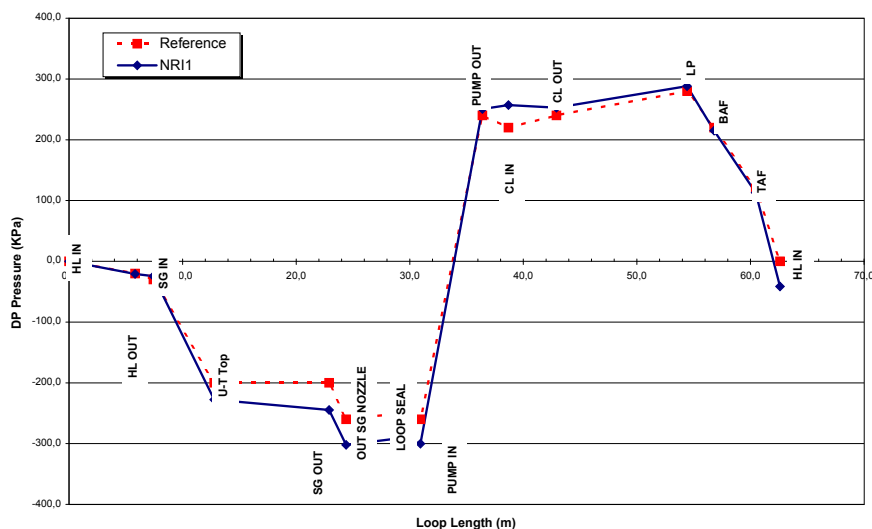


Figure D.10: NRI-1 — Normalized pressure distribution versus loop length

N°		Unit	CALC DATA
<b>Nodalization development</b>			
1	Primary circuit volume (with pressurizer, WITHOUT accumulators) - volume of the pipes	$m^3$	352,907
2	Secondary circuit volume - volume of the pipes	$m^3$	664,664
4	Core heat transfer surface area	$m^2$	4847,59
5	SG U-tubes heat transfer external surface area (without tube sheet)	$m^2$	19134,82
6	Core heat transfer volume (volume surrounding active core)	$m^3$	20,227
7	SG U-tubes heat transfer volume (without tube sheet)	$m^3$	83,405
8	Maximum of the axial power distribution for the average rod in average channel (zone 2)	kW/m	26,94
9	Maximum of the axial power distribution for the hot rod in hot fuel assembly (zone 5)	kW/m	40,42
<b>Steady State</b>			
1	Core power	MW	3250
2	Heat transfer in the steam generators (4 loops)	MW	3255
3	Primary system hot leg pressure	MPa	15,54
4	Pressurizer pressure (top volume)	MPa	15,52
5	Steam generator 1 exit pressure	MPa	6,74
6	Accumulator 1 pressure	MPa	4,14
7	Intact HL 1 temperature (near vessel)	K	604,48
8	Intact CL 1 temperature (near vessel)	K	571,74
9	Reactor vessel downcomer temperature	K	571,72
10	Broken loop HL temperature (near vessel)	K	604,48
11	Broken loop CL temperature (near vessel)	K	571,7
12	Pressurizer temperature (lower volume)	K	608,46
13	Rod surface temperature (hot rod in hot channel , 1.6 - 1.8 m)	K	614,34
14	Upper header temperature	K	590,02
15	Reactor coolant pump of loop 1 velocity	rpm	1146,5
16	Reactor pressure vessel pressure loss	kPa	252,8
17	Core pressure loss	kPa	165,8
18	Primary system total loop pressure loss	kPa	550,7
19	Steam generator 1 pressure loss	kPa	220,2
20	Primary system total mass inventory (with pressurizer, without accumulators)	kg	233811
21	Steam generator 1 total mass inventory	kg	47496
22	Primary system total loop coolant mass flow	kg/s	16491
23	Steam generator 1 feedwater mass flow	kg/s	439
24	Core coolant mass flow	kg/s	16250
25	Core bypass mass flow (LP-UP)	kg/s	241
26	Pressurizer level (collapsed)	m	8,84
27	Secondary side downcomer level	m	12,1

Table D.18: NRI-1 — Nodalization and steady state data table



## D.10 PSI, Switzerland

Pressure distribution values for PSI group are in Table D.19 and depicted in Figure D.11 Reference curve built by coordinators as participants agreed on the 5th meeting.

N°	Position along the loop	Calculated value (MPa)
1	Hot leg inlet HL IN	15,6079
2	Hot leg outlet HL OUT	15,579
3	Steam generator inlet plenum SG IN	15,5769
4	U-tube top UT Top	15,4006
5	Steam generator outlet plenum SG OUT	15,4008
6	Downstream SG outlet nozzle OUT SG NOZZLE	15,3579
7	Bottom of loop seal LOOP SEAL	15,3744
8	Pump inlet PUMP IN	15,3518
9	Pump outlet PUMP OUT	15,9047
10	Cold leg inlet CL IN	15,8825
11	Cold leg outlet CL OUT	15,8868
12	Lower plenum (0.2 m from bottom of vessel) LP	15,8123
13	Bottom of active core BAF	15,8086
14	Top of active core TAF	15,7135

Table D.19: PSI — Pressure distribution along the loop

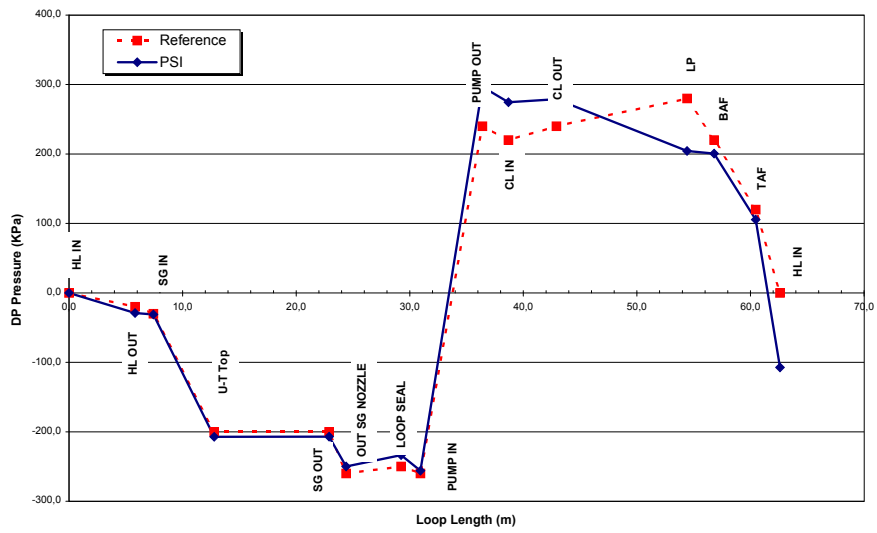


Figure D.11: PSI — Normalized pressure distribution versus loop length

N°	Quantity	Unit	Calc. data
<b>Nodalization development</b>			
1	Primary circuit volume (with pressurizer)	m <sup>3</sup>	340
2	Secondary circuit volume		668
4	Core heat transfer surface area	m <sup>2</sup>	4844
5	SG U-tubes heat transfer external surface area (without tube sheet)		14806
6	Core heat transfer volume	m <sup>3</sup>	17,2
7	SG U-tubes heat transfer volume (without tube sheet)		87,86
8	Maximum of the axial power distribution for the average rod in average channel (zone 2)	kW/m	27,63
9	Maximum of the axial power distribution for the hot rod in hot fuel assembly (zone 5)		41,45
<b>Steady State</b>			
1	Primary circuit power balance	MW	3250
2	Secondary circuit power balance		3249
3	Primary system hot leg pressure	MPa	15,6079
4	Pressurizer pressure		15,51
5	Steam generator 1 exit pressure		6,72
6	Accumulator 1 pressure		4,14
7	Intact HL 1 temperature (near vessel)	K	603,6
8	Intact CL 1 temperature (near vessel)		572,4
9	Reactor vessel downcomer temperature		572,3
10	Broken loop HL temperature (near vessel)		603,9
11	Broken loop CL temperature (near vessel)		572,4
12	Pressurizer temperature		617,95
13	Rod surface temperature (hot rod in hot channel - middle position)		617,8
14	Reactor coolant pump of loop 1 velocity	rpm	1146,83
15	Reactor pressure vessel pressure loss	kPa	278,9
16	Core pressure loss		94,8
17	Primary system total loop pressure loss		552,9
18	Steam generator 1 pressure loss		176,1
19	Primary system total mass inventory (with pressurizer)	kg	221672
20	Steam generator 1 total mass inventory		53838
21	Primary system total loop coolant mass flow	kg/s	17356,8
22	Steam generator 1 feedwater mass flow		440
23	Core coolant mass flow		17121,97
24	Core bypass mass flow (LP-UP)		234,82
25	Pressurizer level (collapsed)	m	8,8
26	Secondary side or downcomer level		12,6

Table D.20: PSI — Nodalization and steady state data table

## D.11 UNIP11, Italy

### D.11.1 NODALIZATION QUALIFICATION PROCESS AND RESULTS

#### Steps of the ZION NPP nodalization qualification process

The UMAE (Uncertainty Methodology based on Accuracy Extrapolation) procedure is adopted for qualifying the ZION NPP nodalization. More details about the methodology can be found in literature [4, 5].

The flow chart of the UMAE is depicted in Figure D.12 and the steps (i, j, k, m) of the loop GI are the ones to be satisfied when qualifying a NPP nodalization. In particular:

- The NPP nodalization (block i) must be set-up following the same guidelines (i.e. model options, nodalization strategy,...) as in the case of the ITF. In other words, this means that the ZION NPP nodalization has been developed taking into account the choices and the experience deriving from the nodalization of LOFT ITF carried out in the framework of BEMUSE Phase 2 [6]. This step is fully described in Section 1.1;
- The qualification at 'steady state' level (block j) of the plant nodalization is obtained using similar criteria adopted for the ITF in loop FG (i.e. demonstration of the achievement of a stationary behaviour of time trends, analysis of the pressure drops along the length of the NPP loops, achievement of the nominal NPP conditions,...). This step is described in Section 2.2;
- The qualification at 'on transient' level (blocks j and k) of the plant nodalization is obtained through the analysis of the Relevant Thermohydraulic Aspects (RTA) of the analysed NPP transient (in similar way to what performed in the loop FG for an ITF). Showing that the NPP nodalization produces results in agreement with one of the ITF experiments (block k) positively completes the qualification process. A qualified plant nodalization is made available (block m) from fulfilling the previous steps of the UMAE and it is called ASM (Analytical Simulation Model). These steps are described in Sections 2.3 and 2.4 where the Kv-scaling calculation (or similarity analysis) of the ZION NPP nodalization to the LOFT L2-5 experiment is also discussed.

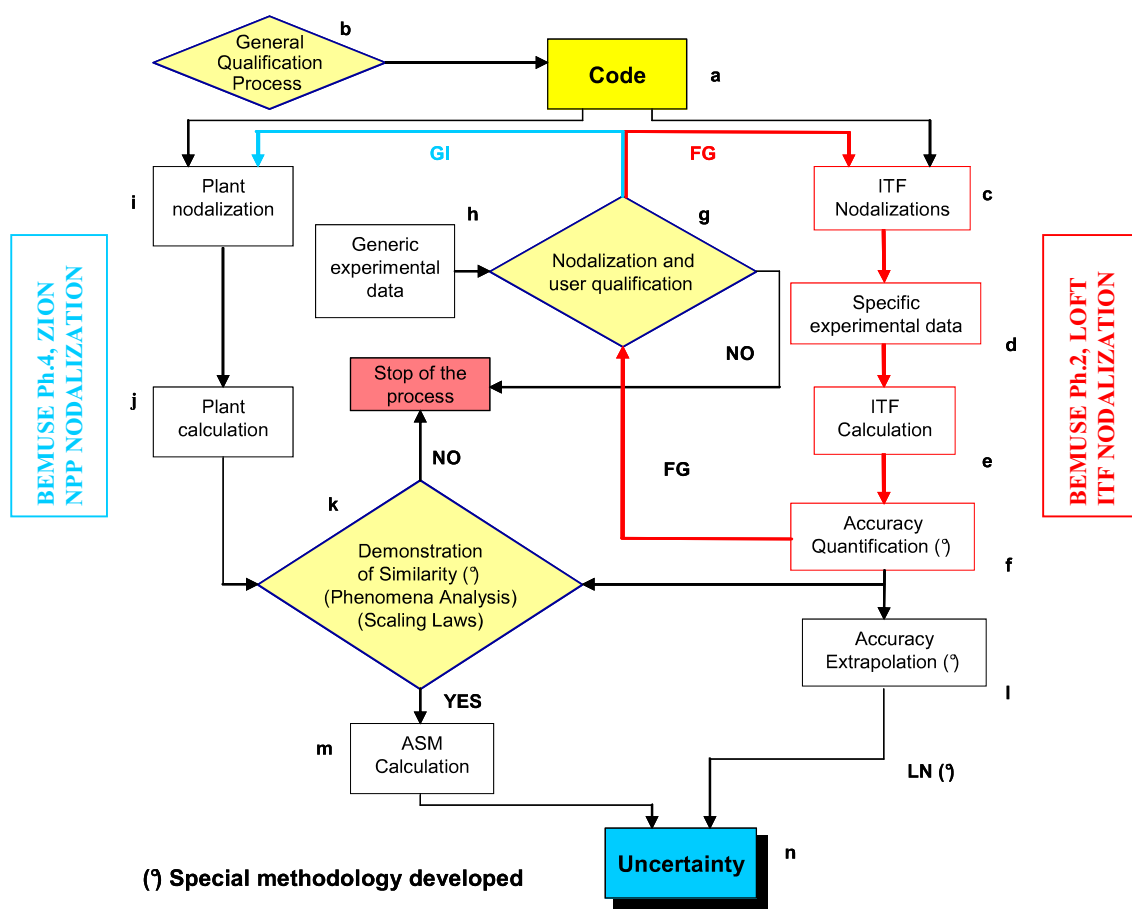


Figure D.12: Simplified flow diagram of the UMAE.

### RELAP5 ZION NPP: Steady state achievement

A steady state calculation has been achieved by running a 'null transient' of 200 s. The application of the procedures at block 'i' led to a qualified nodalization at steady-state level. The related results are shown in Table D.22 and in Figure D.13, where calculated values (taken at 200 s of calculation) are compared with reference data from the specification. The analysis of data brings to the following conclusions:

- The calculated values are stable, i.e. solutions are stable with an inherent drift  $\leq 1\%$  / 100 s.
- A good agreement (indispensable condition to be confident in the capabilities of the adopted nodalization to reproduce the phenomena expected for the selected transient) between calculated and reference values (from the specification) of the pressure distribution along the loop has been obtained, as shown in Table D.21 and in Figure D.13.
- The criteria for the nodalization qualification are fulfilled through the complete comparison between the calculated values of the quantities in Table D.22 and the corresponding reference data in the specification.

N°	Position along the loop	Calculated value (MPa)
1	Hot leg inlet HL IN	15,5005
2	Hot leg outlet HL OUT	15,4810
3	Steam generator inlet plenum SG IN	15,4704
4	U-tube top UT Top	15,2976
5	Steam generator outlet plenum SG OUT	15,2952
6	Downstream SG outlet nozzle OUT SG NOZZLE	15,2308
7	Bottom of loop seal LOOP SEAL	15,2415
8	Pump inlet PUMP IN	15,2321
9	Pump outlet PUMP OUT	15,7537
10	Cold leg inlet CL IN	15,7366
11	Cold leg outlet CL OUT	15,7547
12	Lower plenum (0.2 m from bottom of vessel) LP	15,7906
13	Bottom of active core BAF	15,7178
14	Top of active core TAF	15,6208

Table D.21: UNIP11 — Pressure distribution along the loop

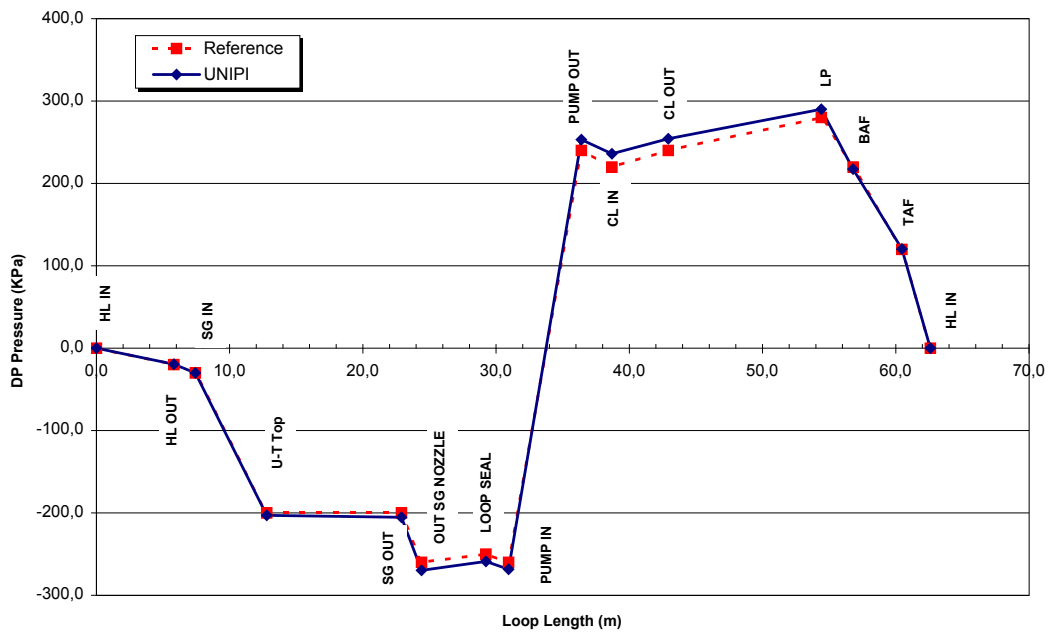


Figure D.13: UNIPI1 — Normalized pressure distribution versus loop length

N°	Quantity	Unit	Calc. data
<b>Nodalization development</b>			
1	Primary circuit volume (with pressurizer)	m <sup>3</sup>	352,91
2	Secondary circuit volume		661,91
4	Core heat transfer surface area	m <sup>2</sup>	4847,84
5	SG U-tubes heat transfer external surface area (without tube sheet)		19134,82
6	Core heat transfer volume	m <sup>3</sup>	18,16
7	SG U-tubes heat transfer volume (without tube sheet)		87,86
8	Maximum of the axial power distribution for the average rod in average channel (zone 2)	kW/m	26,94
9	Maximum of the axial power distribution for the hot rod in hot fuel assembly (zone 5)		40,42
<b>Steady State</b>			
1	Primary circuit power balance	MW	3250,00
2	Secondary circuit power balance		3255,10
3	Primary system hot leg pressure	MPa	15,50
4	Pressurizer pressure		15,48
5	Steam generator 1 exit pressure		6,71
6	Accumulator 1 pressure		4,14
7	Intact HL 1 temperature (near vessel)	K	602,50
8	Intact CL 1 temperature (near vessel)		571,20
9	Reactor vessel downcomer temperature		571,15
10	Broken loop HL temperature (near vessel)		602,50
11	Broken loop CL temperature (near vessel)		571,15
12	Pressurizer temperature		617,29
13	Rod surface temperature (hot rod in hot channel - middle position)		623,79
14	Reactor coolant pump of loop 1 velocity		rpm
15	Reactor pressure vessel pressure loss	kPa	254.14 / 109.62
16	Core pressure loss		159.2 / 96.95
17	Primary system total loop pressure loss		521,67
18	Steam generator 1 pressure loss		175,18
19	Primary system total mass inventory (with pressurizer)	kg	233656,00
20	Steam generator 1 total mass inventory		37777,00
21	Primary system total loop coolant mass flow	kg/s	17386,00
22	Steam generator 1 feedwater mass flow		439,23
23	Core coolant mass flow		17145,90
24	Core bypass mass flow (LP-UP)		217,26
25	Pressurizer level (collapsed)	m	8,78
26	Secondary side or downcomer level		11,90

Table D.22: UNIPI1 — Nodalization and steady state data table



**REFERENCES**

1. W. H. Ramson, "Relap5/Mod2 code manual: user guide and input requirements", NUREG/CR-4312 EGG-2396, Idaho (USA), March 1997.
2. The Relap5 Code Development Team, "Relap5/Mod3 code manual", NUREG/CR-5535-V4, Idaho (USA), June 1995.
3. M. Perez, F. Reventos, Ll. Batet, "Phase 4 of BEMUSE Programme: Simulation of a LB-LOCA in ZION Nuclear Power Plant. Input and Output Specifications" rev. 3, Universitat Politecnica de Catalunya, Spain, 2007.
4. F. D'Auria, N. Debrechin, and G. M. Galassi, "Outline of the Uncertainty Methodology based on Accuracy Extrapolation", J. Nuclear Technology, 109,1,21 (1995).
5. A. Petruzzi, et. Al, BEMUSE Phase II Report, "Re-analysis of the ISP-13 Exercise, Post Test Analysis of the LOFT, L2-5 Test Calculation", Appendix B, "Description of the Procedure to Qualify the Nodalization and to Analyze the Code Results", NEA/CSNI/R(2006)2, November 2005.
6. A. Petruzzi, "RELAP5 Mod3.2 Post Test Analysis and CIAU Uncertainty Evaluation of LOFT Experiment L2-5", NT 558, rev.1, Internal Document, October 2005.

## D.12 UNIPI-2, Italy

Pressure distribution values for UNIPI-2 group are in Table D.23 and depicted in Figure D.14 Reference curve built by coordinators as participants agreed on the 5th meeting.

N°	Position along the loop		Calculated value (MPa)
1	Hot leg inlet	HL IN	15,537703
2	Hot leg outlet	HL OUT	15,519224
3	Stem generator inlet plenum	SG IN	15,476744
4	U-tube top	UT Top	15,32925
5	Steam generator outlet plenum	SG OUT	15,315611
6	Downstream SG outlet nozzle	OUT SG NOZZLE	15,270176
7	Bottom of loop seal	LOOP SEAL	15,289702
8	Pump inlet	PUMP IN	15,270621
9	Pump outlet	PUMP OUT	15,788698
10	Cold leg inlet	CL IN	—
11	Cold leg outlet	CL OUT	15,791321
12	Lower plenum (0.2 m from bottom of vessel)	LP	15,810917
13	Bottom of active core	BAF	15,763505
14	Top of active core	TAF	15,674151

Table D.23: UNIPI-2 — Pressure distribution along the loop

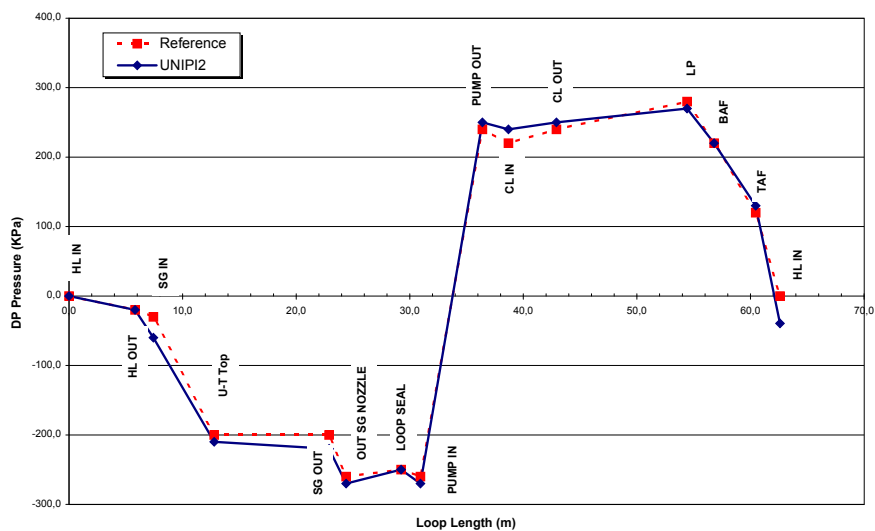


Figure D.14: UNIPI-2 — Normalized pressure distribution versus loop length

N°		Unit	DATA
<b>Nodalization development</b>			
1	Primary circuit volume (with pressurizer, WITHOUT accumulators) - volume of the pipes	$m^3$	352,8
2	Secondary circuit volume - volume of the pipes (only 1 SG)	$m^3$	166,9
4	Core heat transfer surface area	$m^2$	4843,97
5	SG U-tubes heat transfer external surface area (without tube sheet) (external surface 1 SG)	$m^2$	5039,10
6	Core heat transfer volume (volume surrounding active core)	$m^3$	2,79
7	SG U-tubes heat transfer volume (without tube sheet)	$m^3$	24,13
8	Maximum of the axial power distribution for the average rod in average channel (zone 2)	kW/m	27,64
9	Maximum of the axial power distribution for the hot rod in hot fuel assembly (zone 5)	kW/m	41,45
<b>Steady State</b>			
1	Core power	MW	3252
2	Heat transfer in the steam generators (4 loops)	MW	3270
3	Primary system hot leg pressure	MPa	15,54
4	Pressurizer pressure (top volume)	MPa	15,44
5	Steam generator 1 exit pressure	MPa	6,82
6	Accumulator 1 pressure	MPa	4,14
7	Intact HL 1 temperature (near vessel)	K	599,0
8	Intact CL 1 temperature (near vessel)	K	567,4
9	Reactor vessel downcomer temperature	K	567,4
10	Broken loop HL temperature (near vessel)	K	599,0
11	Broken loop CL temperature (near vessel)	K	567,4
12	Pressurizer temperature (lower volume)	K	618,1
13	Rod surface temperature (hot rod in hot channel , 1.6 - 1.8 m)	K	635,0
14	Upper header temperature	K	568,0
15	Reactor coolant pump of loop 1 velocity	rpm	1146,5
16	Reactor pressure vessel pressure loss (from CL-1 outlet to HL - 0.1m -from the vessel)	kPa	235,000
17	Core pressure loss (average channel h1=0.025m and h2=4.04m from active core bottom)	kPa	91,000
18	Primary system total loop pressure loss (MCP outlet - MCP inlet)	kPa	504,000
19	Steam generator 1 pressure loss (primary side from HL outlet to loop seal inlet, loop 1)	kPa	254,000
20	Primary system total mass inventory (with pressurizer, without accumulators)	kg	234283
21	Steam generator 1 total mass inventory	kg	49615
22	Primary system total loop coolant mass flow	kg/s	17344
23	Steam generator 1 feedwater mass flow	kg/s	440
24	Core coolant mass flow	kg/s	17252
25	Core bypass mass flow (LP-UP)	kg/s	221
26	Pressurizer level (collapsed)	m	8,77
27	Secondary side downcomer level	m	12,20

Table D.24: UNIPI-2 — Nodalization and steady state data table

## D.13 UPC, Spain

Pressure distribution values for UPC group are in Table D.25 and depicted in Figure D.15 Reference curve built by coordinators as participants agreed on the 5th meeting.

N°	Position along the loop	Calculated value (MPa)
1	Hot leg inlet HL IN	15.53
2	Hot leg outlet HL OUT	15.51
3	Steam generator inlet plenum SG IN	15.51
4	U-tube top UT Top	15.33
5	Steam generator outlet plenum SG OUT	15.34
6	Downstream SG outlet nozzle OUT SG NOZZLE	15.28
7	Bottom of loop seal LOOP SEAL	15.29
8	Pump inlet PUMP IN	15.28
9	Pump outlet PUMP OUT	15.79
10	Cold leg inlet CL IN	15.80
11	Cold leg outlet CL OUT	15.79
12	Lower plenum (0.2 m from bottom of vessel) LP	15.83
13	Bottom of active core BAF	15.75
14	Top of active core TAF	15.66

Table D.25: UPC — Pressure distribution along the loop

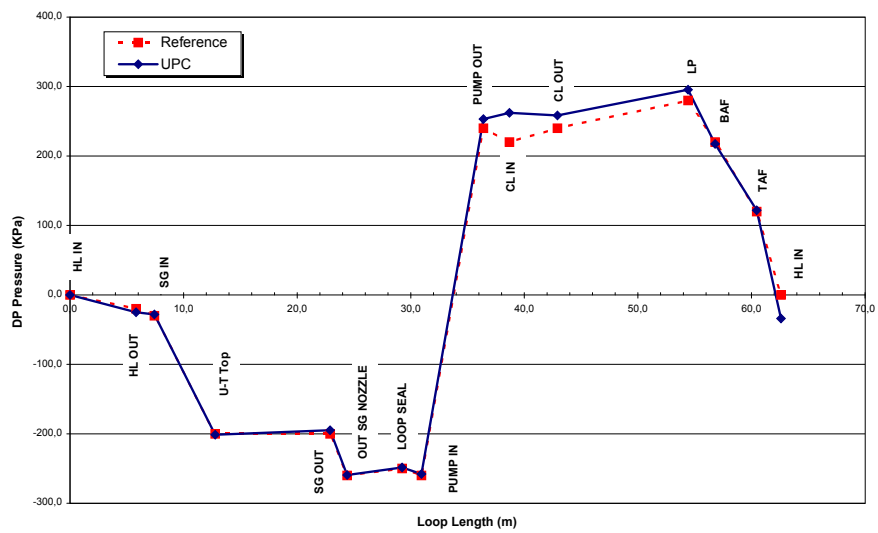


Figure D.15: UPC — Normalized pressure distribution versus loop length

N°		Unit	DATA
<b>Nodalization development</b>			
1	Primary circuit volume (with pressurizer, WITHOUT accumulators) - volume of the pipes	$m^3$	352,7
2	Secondary circuit volume - volume of the pipes	$m^3$	664,7
4	Core heat transfer surface area	$m^2$	4847,60
5	SG U-tubes heat transfer external surface area (without tube sheet)	$m^2$	19134,82
6	Core heat transfer volume (volume surrounding active core)	$m^3$	20,23
7	SG U-tubes heat transfer volume (without tube sheet)	$m^3$	87,86
8	Maximum of the axial power distribution for the average rod in average channel (zone 2)	kW/m	26,94
9	Maximum of the axial power distribution for the hot rod in hot fuel assembly (zone 5)	kW/m	40,42
<b>Steady State</b>			
1	Core power	MW	3250
2	Heat transfer in the steam generators (4 loops)	MW	3255
3	Primary system hot leg pressure	MPa	15,5
4	Pressurizer pressure (top volume)	MPa	15,5
5	Steam generator 1 exit pressure	MPa	6,7
6	Accumulator 1 pressure	MPa	4,1
7	Intact HL 1 temperature (near vessel)	K	601
8	Intact CL 1 temperature (near vessel)	K	570
9	Reactor vessel downcomer temperature	K	570
10	Broken loop HL temperature (near vessel)	K	601
11	Broken loop CL temperature (near vessel)	K	570
12	Pressurizer temperature (lower volume)	K	608
13	Rod surface temperature (hot rod in hot channel , 1.6 - 1.8 m)	K	614
14	Upper header temperature	K	570
15	Reactor coolant pump of loop 1 velocity	rpm	1146,5
16	Reactor pressure vessel pressure loss	kPa	259
17	Core pressure loss	kPa	164
18	Primary system total loop pressure loss	kPa	511
19	Steam generator 1 pressure loss	kPa	167
20	Primary system total mass inventory (with pressurizer, without accumulators)	kg	235276
21	Steam generator 1 total mass inventory	kg	43969
22	Primary system total loop coolant mass flow	kg/s	17437,8
23	Steam generator 1 feedwater mass flow	kg/s	439,2
24	Core coolant mass flow	kg/s	17197,6
25	Core bypass mass flow (LP-UP)	kg/s	240,2
26	Pressurizer level (collapsed)	m	8,8
27	Secondary side downcomer level	m	12,2

Table D.26: UPC — Nodalization and steady state data table